

7.77 — Termodynamika. Wplyw temperatury na materialy.

Andrzej Ziabicki

NUCLEATION OF PHASE TRANSITIONS
IN THE VICINITY OF PHASE BOUNDARY

Part I — Comparison of various isolated mechanisms

Part II — Coupled cluster growth processes

30/1984

P. 269



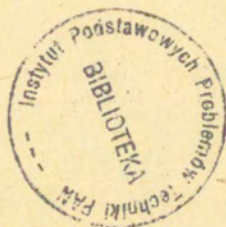
WARSZAWA 1984

<http://rcin.org.pl>

N 0208-5658

Praca wpłynęła do Redakcji dnia 5 czerwca 1984 r.

56978



Na prawach rękopisu

Instytut Podstawowych Problemów Techniki PAN
Nakład 150 egz. Ark.wyd. 5,6. Ark. druk. 8,5
Oddane do drukarni w lipcu 1984 r.
Nr zamówienia 480/84.

Warszawska Drukarnia Naukowa, Warszawa,
ul. Śniadeckich 8.

Andrzej Ziabicki
Pracownia Fizyki Polimerów
IPPT PAN, Warszawa

NUCLEATION OF PHASE TRANSITIONS IN THE
VICINITY OF PHASE BOUNDARY.
I. COMPARISON OF VARIOUS ISOLATED MECHANISMS

INTRODUCTION I

The effect of interfaces leading to so-called "heterogeneous nucleation" has been recognized at the very beginning of the development of nucleation theory (cf. ¹). Later, it has been also recognized that growth of the heterogeneous cluster (nucleus) can proceed according to different mechanisms²⁻⁶ - impingement of single kinetic elements from the bulk phase, and surface diffusion - conditions when one or the other mechanism controls the sum, representing total nucleation rate were discussed. In all these treatments two problems seem to have been overlooked, however

- in many cases of heterogeneous nucleation, growth of a cluster located on the boundary between two phases involves three, rather than two mechanisms: impingement of single kinetic elements (atoms, vacancies, molecules) from the bulk of phase I, impingement from the bulk of phase II, and attachment of elements adsorbed on the interface (adatoms, advacancies,

etc.) (cf. Figure 1 below); typical cases when two bulk impingement processes are provided by liquid/liquid and solid/solid interfaces;

- the individual cluster growth mechanisms are not independent and the resulting nucleation rate is generally different from the sum of contributions from isolated processes. The coupling is due to concentration of single kinetic elements in the bulk phases I and II, as well as surface concentration of adsorbed elements on the interface.

Coupled growth of nuclei adsorbed on a solid boundary (impingement from phase I plus surface addition of elements adsorbed on the interface) has been solved by the present author a few years ago⁷ using continuous cluster distribution functions proposed by Turnbull and Fisher⁸ and applied in earlier papers of the author⁹⁻¹¹. This coupled theory⁷ has recently been applied by Krzeminski to the problem of nucleation of voids from vacancies and advacancies on the boundary of crystal grains in strained metals^{12,13}. In this and the following papers we will present more general solutions based on a more elegant, discrete formalism of the nucleation theory, as used by Frank and Tosi¹⁴, Lauritzen et al.¹⁵ and others.

In the present paper we will compare five different nucleation mechanisms possible in the vicinity of an interface, taking all mechanisms as independent. Another paper will be concerned with heterogeneous nucleation, coupled of three mechanisms discussed in this paper.

We will discuss thermodynamic and kinetic aspects of nucleation in the presence of an interface. In particular, we will analyze critical conditions (temperature, concentration)

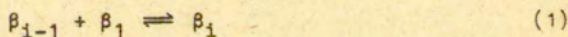
in which thermodynamic equilibrium can be reached (no nucleation), equilibrium and steady-state concentration distributions of cluster sizes, maximum free energy of cluster formation, and nucleation rates.

Our approach will be mostly phenomenological, without entering the atomic (molecular) sources of thermodynamic and transport parameters describing phase transition. A general formal solution of the problem, applicable to liquid/liquid, solid/solid, solid/gas, liquid/gas and liquid/solid interfaces will be given, and some special cases discussed.

BASIC FORMALISM OF THE THEORY

The equations contained in this section are basically equivalent to those of Frank and Tosi¹⁴, with minor modifications.

Consider a system of reversible quasi-chemical reactions between clusters of the new phase composed of "i" single elements each, β_i and single elements (atoms, vacancies, molecules) β_1



It is generally assumed that the molar fraction n_i , of clusters β_i ($i > 1$) is much smaller than that of single elements, n_1 , so that reactions involving clusters β_{i-k} and β_k ($k > 1$) can be neglected, as much less probable. The flux j_i (frequency of formation) of i-size clusters results from eq.(1) in the form

$$J_i = k_{i-1}^+ n_{i-1} n_1 - k_i^- n_i ; \quad i \geq 2 \quad (2)$$

and the rate constants for formation, k_{i-1}^+ and dissociation, k_i^- are assumed in the form

$$k_{i-1}^+ = \nu \varphi_{i-1} \exp(-\varepsilon/kT) \exp[-z \delta f_i/kT] \quad (3)$$

$$k_i^- = \nu \varphi_i \exp(-\varepsilon/kT) \exp[(1-z)\delta f_i/kT] \quad (4)$$

where¹⁶

$$z(i) = \frac{1}{2}[1 + \text{sign}(\delta f_i)] \quad (5)$$

ν is basic frequency of molecular events which can lead to reactions (1), like vibrations of crystal lattice in solids, binary collisions in gas phase etc.; ε is activation energy of transport (self-diffusion) in the system, required for bringing single elements to, and from cluster surface. Functions φ_{i-1} , φ_i indicate the number of sites on the cluster surface accessible to reactions (1). For the sake of simplicity we will assume generally

$$\varphi_{i-1} \approx \varphi_i \quad (6)$$

so that the ratio of reaction rate constants yields the equilibrium constant

$$k_{i-1}^+ / k_i^- = \exp(-\delta f_i / kT) \quad (7)$$

δf_i is free energy of the reaction (1), i.e. the difference between the free energy of cluster β_i , and that of the sum of substrates (β_{i-1}, β_1)

$$\delta f_i = F_i - (F_{i-1} + F_1) = a(\eta_i - \eta_{i-1}) + b \quad (8)$$

Similarly, the total free energy of formation of a cluster β_i from i single elements reads

$$\Delta F_i = \sum_{m=2}^i \delta f_m = F_i - i \cdot F_1 = a \eta_i + (i-1) \cdot b \quad (9)$$

In eqs.(8) and (9) F_i denotes free energy of a cluster β_i , b is size-independent free energy density and $a\eta_i$ is non-linear size-, and shape dependent part of the free energy related to faces (surface), edges, and vertices of the cluster. Generally η_i increases slower than linearly with i , so that

$$\lim_{i \rightarrow \infty} \eta_i / i = 0 \quad (10)$$

In the following considerations we will confine our analysis to surface energy only, assuming

$$\eta_i = i^3 - 1 \quad (11)$$

The form of the non-linear term η_i does not affect considerations of the thermodynamic equilibrium and critical nucleation conditions, but changes (quantitatively rather than qualitatively) the kinetic characteristics.

The fractions of clusters, $n_i = N_i/\mathcal{N}$, where \mathcal{N} is the total number of kinetic elements in the system, satisfy the equation of continuity

$$\partial n_i / \partial t + j_{i+1} - j_i = -n_i (d \ln \mathcal{N} / dt) ; \quad i \geq 1 \quad (12)$$

Generally, aggregation or dispersion affects the total number of kinetic elements, hence \mathcal{N} is not a constant.

What is constant in steady-state, as well as in transient conditions, is the total number of single kinetic elements (atoms, etc.) included in clusters of all sizes up to some limit, i_{\max}

$$\sum_{i=1}^{i_{\max}} i n_i = \text{const.} \quad (13)$$

what converts condition (12) into

$$\sum_{i=1}^{i_{\max}} i (j_{i+1} - j_i) = \sum_{i=2}^{i_{\max}} (j_i - j_{i-1}) = 0 \quad (14)$$

In this paper we will confine our analysis to equilibrium and steady-state conditions, i.e. ones where the distribution of cluster sizes is constant and the number of kinetic elements does not change in time

$$\partial n_i / \partial t = dN / dt = 0 \quad (15)$$

There are two solutions of eqs.(2), which satisfy condition (15)

$$j_i = 0 \quad \text{for all } i \quad (\text{no nucleation})$$

$$j_i = j_{i+1} = j_{st} > 0 \quad \text{for all } i \quad (\text{steady-state nucleation})$$

The first case ($j_i = 0$) for an isolated nucleation process determines thermodynamic equilibrium. We will show in another paper, that it is not necessarily true for coupled processes where disappearance of the total flux of clusters, j_i , can also be due to kinetic factors. Substituting $j_i = 0$ into eqs.(2) yields immediately the zero-nucleation (equilibrium) cluster distribution

$$n_i = (n_1)^i \prod_{m=2}^i (k_{m-1}^+ / k_m^-) \quad (16)$$

which, together with eqs.(7) and (9) yields

$$n_i = (n_1)^i \exp(-\Delta F_i / kT) = n_1 \exp(-\tilde{\Delta F}_i / kT) \quad (17)$$

where

$$\tilde{\Delta F}_i = \Delta F_i - (i-1)kT \ln n_1 \quad (18)$$

is free energy of cluster formation completed with the entropy of mixing (cf. ^{11,17}). In the conditions of undercooling, ΔF_i

provides the driving force for nucleation; in eq.(17) $\Delta\tilde{F}_i$ acts as a total free energy in the equilibrium, Boltzmann distribution.

The necessary condition for the distribution (16) to be physically sensible is convergence, i.e.

$$\lim_{i \rightarrow \infty} n_i = 0. \quad (19)$$

which is equivalent to

$$\lim_{i \rightarrow \infty} \delta\tilde{f}_i = \lim_{i \rightarrow \infty} (\delta f_i - kT \ln n_i) \geq 0 \quad (20)$$

Since the non-linear energy term increment ($\eta_i - \eta_{i-1}$) disappears at large i , the critical condition for convergent distribution of clusters at $j_i = 0$ which determines critical transition conditions (e.g. critical temperature T_c) reduces to

$$T = T_c : \quad b(T_c) - kT_c \ln n_1 = 0 \quad (21)$$

We will use eq.(21) in discussing critical conditions for isolated nucleation processes; a different condition will be derived for coupled processes.

Whereas eqs.(16) - (20) describe real equilibrium systems, the other time-independent solution, one assuming $j_i = j_{st} > 0$, provides a theoretical artefact, nonexisting in real systems. In the subcritical conditions, cluster growth does proceed as

an inherently time-dependent process, until all the material is transformed into a single giant cluster. "Steady-state nucleation" implies that all clusters (nuclei) of size i_{\max} are removed from the system, split into single elements, and refeed into the system as an external flux j_1 . In spite of its artificiality, the steady-state model is often used in the theory, both because of its simplicity, and because at low concentration of clusters, $n_i \ll n_1$, the above assumptions do not introduce major errors.

Assuming non-zero constant flux of clusters, $j_1 = j_{st}$, and requiring convergent steady-state distribution, n_i (cf. eq.19), one obtains from the system of eqs.(2)

$$j_{st} = k_1^+(n_1)^2 / [1 + \sum_{i=2}^{\infty} \prod_{m=2}^i (k_m^- / k_m^+ n_1)] = (n_1)^2 / \sum_{i=1}^{\infty} \frac{1}{k_i^+} \exp(\Delta \tilde{F}_i / kT) \quad (22)$$

and

$$n_i = n_1 \exp(-\Delta \tilde{F}_i / kT) \sum_{m=1}^{\infty} \frac{1}{k_m^+} \exp(\Delta \tilde{F}_m / kT) / \sum_{m=1}^{\infty} \frac{1}{k_m^+} \exp(\Delta \tilde{F}_m / kT) \quad (23)$$

Eqs.(22) and (23) provide exact solutions of eqs.(2) for the second time-independent case, viz. steady-state flux (nucleation frequency), j_{st} , and steady-state cluster distribution function, n_i .

It is often useful to approximate the infinite sum in eqs. (22), (23) by an integral, evaluated by series expansion of the continualized free energy $\Delta \tilde{F}_i \rightarrow \Delta F(i)$ around its maximum at $i = i^*$ (cf.ref.¹⁸)

$$\sum_{i=1}^{\infty} \frac{1}{k_i^+} \exp(\Delta\tilde{F}_i/kT) \cong \frac{1}{k_{i^*}^+} \exp(\Delta\tilde{F}^*/kT) \int_{-\infty}^{\infty} \exp[-C(i-i^*)^2] di \quad (24)$$

where

$$C = \frac{1}{2} \left[\frac{d^2 \Delta\tilde{F}(i)}{di^2} \right]_{i=i^*} / kT, \quad \left. \vphantom{C} \right\} \quad (25)$$

$$\Delta\tilde{F}^* = \Delta\tilde{F}(i=i^*) = \text{maximum}$$

In eq.(24) k_i^+ does not appear under the integral, because its dependence on i , especially in the vicinity of the maximum, is weak¹⁶, and introduces only minor correction to the integral.

Using eqs.(9),(11) and (18) it is easy to find

$$i^* = -[2a/3(b - kT \ln n_1)]^3 \quad (26)$$

$$\Delta\tilde{F}^* = 4a^3/27(b - kT \ln n_1)^2 - (a + b - kT \ln n_1) = \frac{1}{27}a(i^{*3} - 3 + 2i^{*-3}) \quad (27)$$

and the approximate expression for steady-state flux (frequency) j_{st}

$$j_{st} \cong \frac{1}{3} i^{*-3} (a/\pi kT)^{\frac{1}{2}} k_{i^*}^+ (n_1)^2 \exp(-\Delta\tilde{F}^*/kT) \quad (28)$$

Numerical analysis reported in Appendix A shows accuracy of replacing semi-infinite sum by the infinite integral appearing in (eq.24). In the range excluding very small a/kT ratios and small i^* (close to 2), steady-state nucleation frequency can reasonably well be approximated by eq.(28), or, in a transcribed form

$$j_{st} = \text{const. } n_1 \exp(-\epsilon/kT) \exp[-\frac{1}{3} a(i^{*3} - 3)/kT] \quad (28a)$$

When cluster growth is controlled by impingement of single elements on cluster surface, the number of sites accessible to reactions (1) is proportional to i^3

$$\varphi_i = \varphi \cdot i^{\frac{3}{2}}$$

which yields the constant in eq.(28a) as

$$\text{const.} = \frac{1}{3} v\varphi(a/\pi kT)^{\frac{1}{2}} \exp(b/kT) \quad (29a)$$

On the other hand, for surface-diffusion-controlled growth (addition of single elements to the peripheral belt on cluster surface)

$$\varphi_i = \varphi \cdot i^{\frac{3}{2}}$$

and the constant in eq.(28a) results as

$$\text{const.} = \frac{1}{3} v\varphi[(-b + kT \ln n_1)/(\pi a kT)^{\frac{1}{2}}] \exp(b/kT) \quad (29b)$$

It should be noted that in the vicinity of $i = i^*$ the energy partition parameter, z , in eq.(3) is identically equal to zero. We will use eqs.(26) - (29a) for comparison of various nucleation processes.

THERMODYNAMIC AND TRANSPORT CHARACTERISTICS FOR VARIOUS CLUSTER GROWTH MECHANISMS

We will start with classification of cluster growth mechanisms possible in a two-phase system (Figure 1). We will use superscripts to identify the source of single elements active in cluster growth (first superscript), and location of the cluster (second superscript). All physically possible processes are listed in Table I. These include two homogeneous processes (j^{11} and j^{22}) where single elements are supplied from bulk phase I or II, and the clusters are located in the same phase. Three heterogeneous processes, j^{10} , j^{20} , and j^{00} , involve cluster located on the interface (second superscript "0") and the growth controlled either by impingement of single elements from bulk phases I and II (j^{10} and j^{20}), or by elements adsorbed on the interface and transported via surface diffusion to the circumference belt on the cluster surface adjacent to the interface (j^{00}).

Other combinations of superscripts (01, 02, 12, 21) do not describe any real process; cluster located in a bulk phase (I or II) cannot grow by attachment of single elements located in another phase because these are too distant for collision.

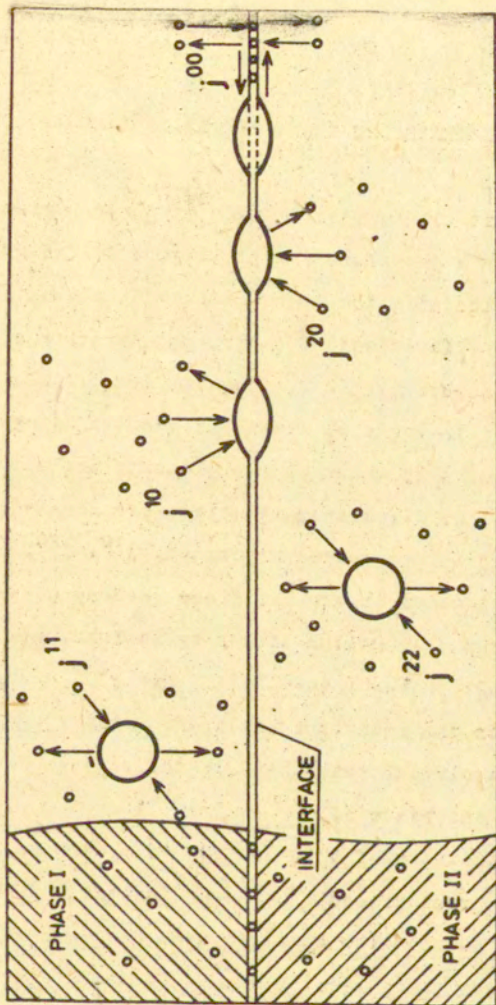


Figure 1. Scheme of various nucleation processes possible in the vicinity of an interface.

Table I.

Cluster growth processes possible in a two-phase system

Source of single elements	Location of the growing cluster		
	phase I	phase II	interface
phase I	j^{11}		j^{10}
phase II		j^{20}	j^{20}
interface			j^{00}

As follows from the general formalism described in the preceding section, the thermodynamic and kinetic characteristics of nucleation can be described by the free energy parameters, a , and b , effective concentration of single elements, n_1 , activation energy for transport of single elements, ϵ , and a factor indicating the number of sites on cluster surface accessible to reaction, ϕ_1 . These parameters assume different values for various growth mechanisms listed in Table I.

An important characteristics is also energy of adsorption of a single element from the bulk phase, E . The important parameters are listed in Table II.

Transport energy, ϵ , is controlled solely by the phase which supplies single elements. ϵ^1 and ϵ^2 are characteristics of bulk phases I and II, while ϵ^0 is activation energy for surface diffusion along the interface. Similarly, E^1 (E^2) denotes adsorption energy of a single element from phase I (phase II) on the interface.

Bulk free energy of transformation per one attached element, b , (cf. eqs. 8, 9) changes from one process to another

only because of different energies of single elements in various phases, F_1 . If b^1 for phase I is taken as a reference (processes j^{11} , and j^{10}), the other parameters can be calculated using adsorption energies E^1 , E^2

$$\left. \begin{aligned} b^0 &= b^1 - E^1 \\ b^2 &= b^1 - E^1 + E^2 = b^1 - \Delta E \end{aligned} \right\} \quad (30)$$

Concentrations of single elements in various phases, n_1 , play important role in the thermodynamics and kinetics of nucleation. In this section, we will discuss only equilibrium values of the three molar fractions, n_1^1 , n_1^2 , and n_1^0 , respectively in phases I and II, and on the interface. It should be noted, that n_1^1 (n_1^2) are fractions of the reacting species β_1 in the bulk of phase I (phase II), while n_1^0 is surface fraction of elements β_1 adsorbed on the interface, i.e. the number of adsorbed β_1 divided by the total number of all kinetic units on the interface.

Assuming that the net fluxes of adsorption from phase I and II are equal to zero, we arrive at the following equilibrium solutions

$$n_1^2/n_1^1 = \exp[(-E^1 + E^2)/kT] / \{1 - n_1^1 + n_1^1 \exp[(-E^1 + E^2)/kT]\} \quad (31)$$

$$n_1^0/n_1^1 = \exp(-E^1/kT) / [1 - n_1^1 + n_1^1 \exp(-E^1/kT)] \quad (32)$$

providing a kind of Langmuir isotherm.

Table II
Basic thermodynamic and transport parameters of nucleation processes

Parameter	Nucleation (cluster growth) mechanism					
	Homogeneous			Heterogeneous		
	j^{11}	j^{22}	j^{10}	j^{20}	j^{00}	
Activation energy of transport (self-diffusion), ϵ	ϵ^1	ϵ^2	ϵ^1	ϵ^2	ϵ^0	
Adsorption energy of single elements on the interface, E			E^1	E^2	0	
Bulk free energy density of transformation per single element, b	b^1	$b^2 = b^1 - E^1 + E^2$	b^1	b^2	$b^0 = b^1 - E^1$	
Equilibrium fraction of single elements, n_1	n_1^1	$n_1^2 = n_1^1 [n_1^1 (E^1 - E^2) / kT]$	n_1^1	n_1^2	$n_1^0 = n_1^1 (n_1^1, E^1 / kT)$	
Surface free energy coefficient, a	a^1	a^2	a^0	a^0	a^0	
Function of sites accessible to attachment or dissociation, ϕ_1	$\phi^{11,3}$	$\phi^{11,3}$	$\phi^{10,3}$	$\phi^{20,3}$	$\phi^{00,3}$	

The coefficient of surface energy density, a , in eqs.(8), (9), depends on the location of the cluster and its shape. For homogeneous nucleation mechanisms, j^{11} and j^{22} , the coefficient a is proportional to interface tension and spherical (or regular) geometry of the cluster immersed in a homogeneous medium with cluster-medium interface tension σ^{c1} , or σ^{c2} . Consequently

$$a^2 = a^1 \sigma^{c2}/\sigma^{c1} \quad (33)$$

Heterogeneous cluster located on the interface assumes a double-lens shape (cf. Figure 1) and the total surface energy is controlled by interface tensions σ^{c1} , σ^{c2} , and angles α_1, α_2 . Assuming minimum surface free energy, and taking into account the interface tension between phases I and II, σ^{12} one can find the equilibrium shape of the lens

$$\cos \alpha_1 = f_1[\sigma^{c2}/\sigma^{c1}, \sigma^{12}/\sigma^{c1}] ; \cos \alpha_2 = f_2[\sigma^{c2}/\sigma^{c1}, \sigma^{12}/\sigma^{c1}]$$

and the corresponding surface energy coefficient for the heterogeneous cluster (applicable for processes j^{10} , j^{20} , j^{00})

$$a^0 = a^1 \cdot f[\cos \alpha_1, \cos \alpha_2] \quad (34)$$

The corresponding relations between equilibrium angles α_1 , α_2 and interface tensions σ^{c1} , σ^{c2} , σ^{12} are given in Appendix B.

Site number functions, φ_i , appearing in the reaction rate constants k_i^+ , k_i^- (eqs.3 and 4) are determined by the shape and

size of that region of the cluster surface which is accessible to the given mechanism of growth. For any homogeneous nucleation process, φ_i^{nm} is proportional to spherical surface of the cluster. Therefore,

$$\varphi_i^{11} = \varphi_i^{22} = \varphi^{11} \cdot i^{\frac{2}{3}} \quad (35)$$

where φ^{11} is a numerical constant dependent only on the shape and dimensions of single elements. For spherical single elements $\varphi^{11} = 4$. For a heterogeneous cluster, functions φ_i are different for different growth mechanism and depend on the region of cluster surface exposed to single elements. For growth mechanisms j^{10} and j^{20} controlled by impingement of single elements on the surface of the lens immersed in phase I (phase II), φ_i^{10} (φ_i^{20}) is proportional to $i^{\frac{2}{3}}$ and depends on the equilibrium shape of the lens, i.e. on the angles α_1, α_2 . Thus

$$\left. \begin{aligned} \varphi_i^{10} &= \varphi^{10} i^{\frac{2}{3}} = \varphi^{10} [\cos \alpha_1, \cos \alpha_2] \cdot i^{\frac{2}{3}} \\ \varphi_i^{20} &= \varphi^{20} i^{\frac{2}{3}} = \varphi^{20} [\cos \alpha_1, \cos \alpha_2] \cdot i^{\frac{2}{3}} \end{aligned} \right\} \quad (36)$$

In the case of attachment of single elements adsorbed on the interface, and surface-diffusing towards the periphery of the cluster, the region accessible to reaction is a monomolecular circumferential belt at the intersection of the lens with the interface plane (cf. Figure 1). The area of such a belt is proportional to $i^{\frac{2}{3}}$ rather than $i^{\frac{3}{3}}$, and the proportionality

coefficient φ^{00} is another function of lens shape (cf. Appendix B), viz.

$$\varphi_i^{00} = \varphi^{00} [\cos \alpha_1, \cos \alpha_2] \cdot i^{\frac{1}{2}} \quad (37)$$

The fact that surface addition mechanisms (j^{10} , j^{20}) contribute to nucleation frequency with a different power of cluster size, i , than the peripheral (circumferential) mechanism j^{00} , has far-going consequences in the thermodynamics and kinetics of coupled heterogeneous nucleation.

COMPARISON OF VARIOUS NUCLEATION MECHANISMS

We will compare now thermodynamic and kinetic characteristics of the five mechanisms of nucleation as if they were acting independently one from another. First, we will analyze critical temperature for a non-zero, steady-state flux T_c ,

nucleation rate parameters i^* , ΔF^* , and steady-state nucleation frequency j_{st} .

Critical Nucleation Temperature, T_c

To find the critical temperature T_c for the transition from thermodynamic equilibrium to non-zero nucleation rate, we will discuss the condition eq.(20) with various parameters b and n_1 from Table II. We will assume linear dependence between the free energy density, b and temperature T

$$b(T) = \Delta h(T - T_0)/T_0 \quad (38)$$

where T_0 is critical temperature of transition (equilibrium temperature) for a pure substance ($n_1 = 1$), and Δh is heat of the transition per one attached element.

For the homogeneous process in phase I (j^{11}) as well as for the heterogeneous process involving single elements from phase I, (j^{10}) the relevant parameters are b^1 and n_1^1 and the critical condition

$$b^1(T) - kT \ln n_1^1 = 0 \quad (39)$$

leads immediately to the critical temperature T_c^{11}

$$T_c^{11} = T_0^{11} / [1 - (kT_0^{11} \ln n_1^1) / \Delta h^1] \quad (40)$$

and

$$T_c^{10} = T_c^{11} \quad (41)$$

It is evident that the critical temperature for a pure system, T_0^{11} , is reduced by dilution, monotonically approaching $T_c^{11} = 0$ at $n_1^1 = 0$. Adsorption of the cluster on the interface does not change the critical temperature, if the effective single elements are supplied from the same phase as in the homogeneous process (process j^{10}).

Change of the parameter b , as well as that of the equilibrium concentration of single elements n_1 due to adsorption on the interface, yields the following critical condition for the surface-diffusion-controlled process, j^{00} :

$$b^0(T) - kT \ln n_1^0 = b^1(T) - kT \ln n_1^1 + \\ + kT \ln[1 - n_1^1 + n_1^1 \exp(-E^1/kT)] = 0 \quad (42)$$

which leads to the transcendental equation for the critical temperature T_c^{00}

$$T_c^{00} = T_o^{11} / \{1 + (kT_o^{11}/\Delta h^1) \ln[1/n_1^1 - 1 + \exp(-E^1/kT_c^{00})]\} \quad (43)$$

which can be rewritten in the form

$$T_c^{00} = T_c^{11} / \{1 + (kT_c^{11}/\Delta h^1) \ln[1 - n_1^1 + n_1^1 \exp(-E^1/kT_c^{00})]\} \quad (44)$$

It can be observed that the ratio T_c^{00}/T_c^{11} can be smaller or greater than unity, dependently on the sign of the adsorption energy, E^1 . Figure 2. presents the logarithm appearing in eq. (44) as a function of molar fraction of single elements, n_1^1 . The logarithm is negative when E^1 is positive (repulsion by the interface) and positive when $E^1 < 0$, i.e. when single elements are attracted and adsorbed on the interface. This leads to the reduction of the critical temperature in case of strong adsorption ($E^1 < 0$), and to the increase of T_c^{00} above the T_c^{11} level in case of repulsion ($E^1 > 0$). This is illustrated in Figure 3 where critical transition temperatures calculated from eq.(44) are plotted vs. reduced critical temperature for the homogeneous process, T_c^{11}/T_o^{11} . For repulsive forces ($E^1 > 0$) critical temperatures for the surface diffusion

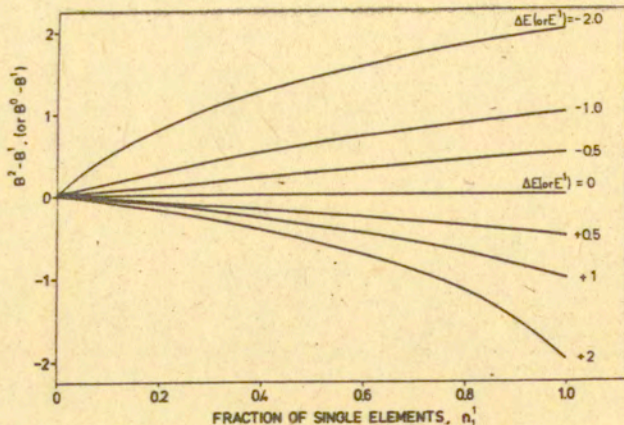


Figure 2. The difference between driving forces for nucleation in phases II and I ($B^2 - B^1$), or between the interface and phase I ($B^0 - B^1$), as functions of molar fraction of single elements in the reference phase I, n_1^1 . Difference between the energy of a single element in phase II (interface) and in the reference phase I, ΔE (E^1) indicated. B^0, B^1, B^2 and $\Delta E, E^1$ expressed in kT units.

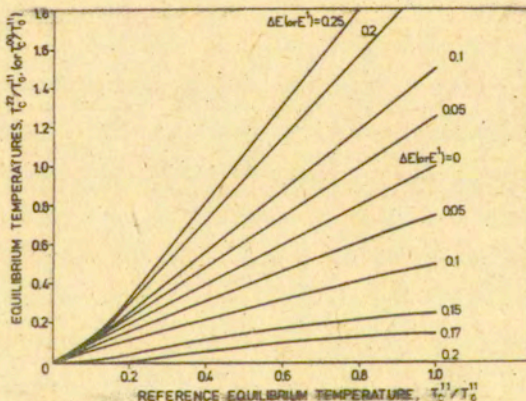


Figure 3. Reduced critical (equilibrium) temperature for a homogeneous process in the bulk phase II, T_c^{22} , and for a heterogeneous process on the interface, T_c^{00} , vs. reduced critical temperature for homogeneous transition in phase I, T_c^{11} . Reference temperature, T_c^1 , concerns transition in phase I at $n_1^1 = 1$. Difference between the energy of a single element in phase II (interface) and phase I (ΔE , or E^1) indicated. ΔE and E^1 expressed in kT units.

process T_c^{00} are higher than those for the reference homogeneous process, T_c^{11} . In the conditions of adsorption ($E^1 < 0$) the reverse is true.

Limiting value of T_c^{00} at $n_1^1 = 1$ can be found directly from eq.(44) as

$$T_c^{00} = T_c^{11} (1 + E^1 / \Delta h^1) \quad (45)$$

The effect of adsorption energy E^1 can be explained as follows. On one hand, E^1 affects concentration of single elements on the interface, n_1^0 , pumping it above the n_1^1 level when $E^1 < 0$; at the same time E^1 modifies the bulk free energy of transition, b^0 , negative E^1 reducing the absolute value of b^0 below that of b^1 . The effect on the bulk free energy b^0 more than compensates the influence on concentration, what leads to stimulation of the interface mechanism in case of repulsion ($E^1 > 0$) and discrimination in case of attraction (adsorption), $E^1 < 0$.

All the above consideration apply also to the second homogeneous nucleation process, j^{22} , when adsorption energy E^1 is replaced by the difference of transition energies in phases II and I, $\Delta E = E^1 - E^2 = b^1 - b^2$. The critical transition temperature, T_c^{22} , calculated from the condition

$$b^2(T) - kT \ln n_1^2 = b^1(T) - kT \ln n_1^1 + kT \ln [1 - n_1^1 + n_1^1 \exp(-\Delta E/kT)] = 0 \quad (46)$$

is a solution of the equation

$$T_c^{22} = T_c^{11} / \left\{ 1 + (kT_c^{11} / \Delta h^1) \ln[1 - n_1^1 + n_1^1 \exp(-\Delta E / kT_c^{22})] \right\} \quad (47)$$

and behaves in exactly the same way as does T_c^{00} for the surface-diffusion-controlled process j^{00} . When ΔE is negative, i.e. when the energy of a single element in phase II is smaller than that in phase I, the equilibrium concentration in phase II is increased ($n_1^2 > n_1^1$), but critical temperature for the homogeneous process j^{22} in phase II is reduced, $T_c^{22} < T_c^{11}$.

The above considerations lead to the following conclusions:

- there is no preference for heterogeneous nucleation compared with the homogeneous process, when critical temperature for the onset of nucleation is concerned. Heterogeneous and homogeneous processes (e.g. j^{11} and j^{10} , or j^{22} and j^{20}) start at the same critical temperature, provided that they are governed by the same concentration of single elements (respectively, n_1^1 and n_1^2).
- surface-diffusion-controlled cluster growth on the interface (j^{00}) starts at a critical temperature lower than that for the homogeneous, or bulk-diffusion-controlled heterogeneous processes (j^{11} , j^{10} , or j^{22} , j^{20}) if energy of adsorption of single elements on the interface E^1 (or E^2) is negative. The reverse is true for positive E^1 (E^2).

Critical Cluster Size, i^*
and Maximum Free Energy $\Delta \tilde{F}^*$

Although heterogeneous nucleation processes are not preferred to homogeneous ones as far as critical transition temperature is concerned, significant changes in the nucleation

kinetics can be due to other factors: surface free energy (coefficient a in eqs.8,9), and mobility of single elements participating in cluster growth, reflected by activation energy of self-diffusion, ϵ .

An important characteristic of the nucleation process is critical cluster size, i^* from eq.(26). Larger i^* contributes to higher maximum free energy of cluster formation, $\Delta\tilde{F}^*$, and to smaller nucleation rate, j_{st} .

Comparing two homogeneous cluster growth processes, j^{22} and j^{11} , we obtain

$$i^{*22}/i^{*11} = [a^2(b^1 - kT \ln n_1^1)/a^1(b^2 - kT \ln n_1^2)]^3 =$$

$$= \left\{ \frac{a^2/a^1}{1 + (kT/B^1) \ln[1 - n_1^1 + n_1^1 \exp(-\Delta E/kT)]} \right\}^3 \quad (48)$$

where

$$B^1 = b^1 - kT \ln n_1^1$$

is negative definite.

The effect of the difference of free energies of a single element in phase I and II

$$\Delta E = E^1 - E^2 = F_1^2 - F_1^1$$

on the ratio of interface tensions σ^{c2}/σ^{c1} (which controls a^2/a^1) is difficult to estimate. One can only argue that

energy of the surface of cluster surrounded by phase with higher energy of single elements F_1 , should be higher than surface energy of the same cluster surrounded by phase with smaller F_1 . Consequently $\sigma^{c2} - \sigma^{c1}$ should be positive for $\Delta E > 0$ and vice-versa. This effect yields for positive ΔE , (a^2/a^1) higher than unity and an increase of the critical cluster size ratio i^{*22}/i^{*11} . At the same time, at $\Delta E > 0$ the nominator in eq.(48) is also greater than unity. The net result is indefinite, and depends on how sensitive are both factors to ΔE ; i^{*22}/i^{*11} can both be smaller or larger than unity.

More clear result is obtained when a homogeneous process is compared with bulk-diffusion-controlled heterogeneous cluster growth (i.e. j^{10} vs. j^{11} , or j^{20} vs. j^{22}). Such processes involve different surface energies, but equal bulk energies, b , and concentrations n_1 , yielding ratios

$$i^{*10}/i^{*11} = (a^0/a^1)^3 \leq 1 \quad (49)$$

and

$$i^{*20}/i^{*22} = (a^0/a^2)^3 \leq 1 \quad (50)$$

generally smaller than unity. The advantage of heterogeneous nucleation compared with a homogeneous process lies in smaller critical cluster size i^* , and smaller thermodynamic barrier for cluster growth, ΔF^* .

Comparing heterogeneous nucleation process involving surface transport on the interface (j^{00}) with any of the heterogeneous processes based on bulk diffusion (j^{10} , or j^{20}) we obtain

$$i^{*00}/i^{*10} = [(b^1 - kT \ln n_1^1)/(b^0 - kT \ln n_1^0)]^3 =$$

$$= \left\{ 1 + (kT/B^1) \ln[1 - n_1^1 + n_1^1 \exp(-E^1/kT)] \right\}^{-3} \quad (51)$$

and

$$i^{*00}/i^{*20} = [(b^2 - kT \ln n_1^2)/(b^0 - kT \ln n_1^0)]^3 =$$

$$= \left\{ \frac{1 + (kT/B^1) \ln[1 - n_1^1 + n_1^1 \exp(-\Delta E/kT)]}{1 + (kT/B^1) \ln[1 - n_1^1 + n_1^1 \exp(-E^1/kT)]} \right\}^3 =$$

$$= \left\{ 1 + (kT/B^2) \ln[1 - n_1^2 + n_1^2 \exp(-E^2/kT)] \right\}^{-3} \quad (52)$$

with

$$B^2 = b^2 - kT \ln n_1^2$$

It can be noted that the ratios (i^{*00}/i^{*10}) , (i^{*00}/i^{*20}) are always smaller than unity for the case of repulsion (positive adsorption energies E^1 , or E^2), and greater than unity for $E^1 < 0$ ($E^2 < 0$), i.e. for true adsorption. Adsorption increases the critical cluster size i^{*00} , and makes surface-diffusion-controlled process j^{00} slower; this corresponds to the reduction of critical transition temperature T_c^{00} discussed in the preceding section.

Although the maximum free energy of cluster formation $\Delta\tilde{F}^*$

$$\Delta\tilde{F}^* = 4(a)^3/27(b - kT \ln n_1)^2 - (a + b - kT \ln n_1) =$$

$$= 4(a)^3/27(B)^2 - (a + B) \quad (53)$$

includes combination of parameters a, b, n, (or a, B) different than the critical cluster size, i^* (eq.26), all the conclusions concerning effect of nucleation mechanism on i^* apply to maximum free energy $\Delta\tilde{F}^*$. In the physically sensible range of parameters ($i^* > 1$) the direction of changes of $\Delta\tilde{F}^*$ with parameters a and B is the same as that of changes of i^* , i.e.

$$\left. \begin{aligned} \text{sign}(\partial\Delta\tilde{F}^*/\partial a) &= \text{sign}(\partial i^*/\partial a) \\ \text{sign}(\partial\Delta\tilde{F}^*/\partial B) &= \text{sign}(\partial i^*/\partial B) \end{aligned} \right\} \quad (54)$$

Consequently, for isolated processes, the maximum free energy of cluster formation $\Delta\tilde{F}^*$ which provides a thermodynamic barrier for nucleation is reduced when bulk-diffusion-controlled heterogeneous process (j^{10} , or j^{20}) is compared with a corresponding homogeneous cluster growth (j^{11} or j^{22})

$$\left. \begin{aligned} \Delta\tilde{F}^{*10}/\Delta\tilde{F}^{*11} &\leq 1 \\ \Delta\tilde{F}^{*20}/\Delta\tilde{F}^{*22} &\leq 1 \end{aligned} \right\} \quad (55)$$

what makes heterogeneous nucleation faster than the homogeneous one. Among the heterogeneous mechanisms, surface-diffusion-controlled process j^{00} is ^{thermodynamically} favored as compared with either bulk-diffusion-controlled process (j^{10} , or j^{20}), only when the adsorption energy (E^1 , or E^2) is positive, i.e. when single elements are repelled from the interface. Adsorption on the interface (negative energy E^1 , or E^2) increases $\Delta\tilde{F}^{*00}$

above $\Delta\tilde{F}^{*10}$ or $\Delta\tilde{F}^{*20}$ and slows down the surface-diffusion process j^{00} .

$$\Delta\tilde{F}^{*00}/\Delta\tilde{F}^{*10} \quad \left\{ \begin{array}{ll} \leq 1 & \text{for } E^1 \geq 0 \\ > 1 & \text{for } E^1 < 0 \end{array} \right. \quad (56)$$

and

$$\Delta\tilde{F}^{*00}/\Delta\tilde{F}^{*20} \quad \left\{ \begin{array}{ll} \leq 1 & \text{for } E^2 \geq 0 \\ > 1 & \text{for } E^2 < 0 \end{array} \right. \quad (57)$$

Like in the case of critical cluster size, i^* , the ratio of maximum free energies for two different homogeneous processes, $\Delta\tilde{F}^{*22}/\Delta\tilde{F}^{*11}$ can be smaller, or greater than unity, dependently on the effect of energy of a single element on interface tensions (σ^{c1} and σ^{c2}).

Steady-State Nucleation Frequency, j_{st}

Eqs.(28,29a-b) provide the basis for comparison of nucleation frequency in various isolated cluster growth, processes.

Comparison of two homogeneous mechanisms in bulk phases I and II

$$j^{22}/j^{11} = \frac{\exp(-\varepsilon^2/kT)(a^2/kT)^{\frac{1}{2}}(n_1^2) \exp[-4(a^2)^3/27kT(B^2)^2 + (a^2 + b^2)/kT]}{\exp(-\varepsilon^1/kT)(a^1/kT)^{\frac{1}{2}}(n_1^1) \exp[-4(a^1)^3/27kT(B^1)^2 + (a^1 + b^1)/kT]}$$

yields a complex picture. All kinetic and thermodynamic parameters involved in nucleation: transport free energy, ϵ , concentration of effective single elements, n_1 , surface-, and bulk free energy coefficients (a,b), are different for homogeneous processes in various phases. Consequently, the ratio of nucleation frequencies in eq.(58) can be smaller or greater than unity, and no general rule can be proposed for its behavior. Obviously, the transport (mobility) term can play the determining role favoring, or discriminating one of the compared mechanisms when the absolute difference of activation energies, $|\epsilon^2 - \epsilon^1|$ is large. The group of thermodynamic factors related to different surface energy, a, bulk energy of transition, b, and concentration of single elements, n_1 , can in some conditions lead to lower nucleation frequency in phase II, higher in others.

An important problem is the behaviour of a heterogeneous, bulk-diffusion-controlled mechanism vs. a corresponding homogeneous one, say j^{10} vs. j^{11} . Both processes involve the same transport activation energy, ϵ^1 , concentration of single elements, n_1^1 , and bulk free energy of transition, b^1 . Consequently, the ratio of nucleation frequencies

$$j^{10}/j^{11} = \frac{\varphi^{10} n_1^0 (a^0)^{\frac{3}{2}}}{\varphi^{11} n_1^1 (a^1)^{\frac{3}{2}}} \exp \left[\frac{-4[(a^0)^3 - (a^1)^3]}{27 kT(B^1)^2} + \frac{(a^0 - a^1)}{kT} \right] \quad (59)$$

includes only three parameters different for the compared mechanisms, the kinetic coefficient, φ , related to the number of sites on cluster surface accessible to growth/dissociation

reactions, surface energy coefficient, a , and concentration of single elements, n_1 .

The ratio $\varphi^{10}/\varphi^{11}$ is a function of shape of the heterogeneous cluster (contact angle cosines x^* , y^* , cf. Appendix B), but, except for extremely flat clusters ($x^*, y^* > 0.95$) it is contained within the range (0.5 - 1.0). The ratio n_1^0/n_1^1 is a constant. We will neglect the first two factors in eq.(59), and analyze the ratio j^{10}/j^{11} as a function of a single variable $\xi = a^0/a^1$, i.e. the ratio of surface energies of a heterogeneous vs. homogeneous cluster. Generally ξ is not greater than unity, because adsorption of the cluster on an interface reduces its surface energy. We will analyze the function equivalent to eq.(59) with $\varphi^{10}/\varphi^{11} = 1$, i.e.

$$(j^{10}/j^{11}) \sim \xi^{\frac{1}{2}} \exp\left\{-\left(a^1/kT\right)\left[\frac{1}{2} i_{11}^* (\xi^3 - 1) + 1 - \xi\right]\right\} \quad (60)$$

The ratio j^{10}/j^{11} from eq.(60) is plotted vs. ξ for a couple of parameters a^1/kT and $i_{11}^* = -(2a^1/3B^1)^3$, in Figure 4. It is evident that reduction of surface energy from a^1 to $a^0 = \xi a^1$ in the range of large a^1/kT stimulates heterogeneous nucleation frequency ($j^{10} > j^{11}$); in the range of very small a^1/kT - heterogeneous nucleation j^{10} is smaller than the corresponding homogeneous process j^{11} . Figure 5. shows the range of conditions (i_{11}^* vs. a^1/kT) where enhancement of heterogeneous nucleation is replaced by reduction, i.e. conditions where

$$d(j^{10}/j^{11})/d\xi = 0 \text{ at } \xi = 1: (a^1/kT)_{\text{crit}} = 1/2(i_{11}^{*3} - 1) \quad (61)$$

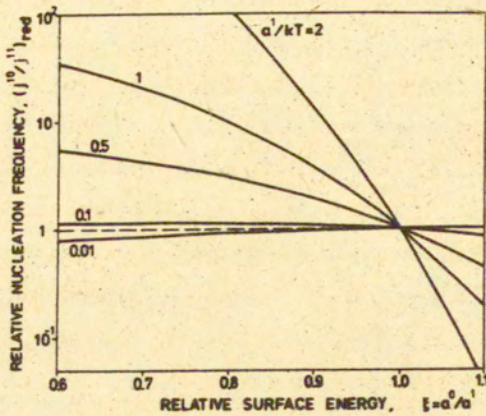


Figure 4. Reduced ratio of steady-state nucleation frequencies for a bulk-diffusion-controlled heterogeneous process, j^{10} , and the corresponding homogeneous process, j^{11} , vs. the ratio of surface energies $\xi = a^0/a^1$. $i_{11}^* = \text{const.} = 64$; $a^1/kT = \text{const.}$, indicated. Ordinate indicates the ratio from eq.(60).

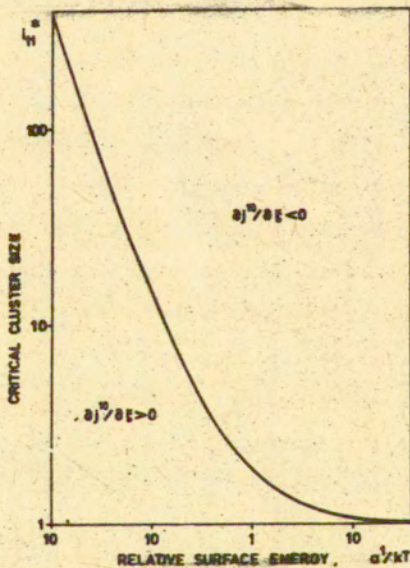


Figure 5. Critical conditions for enhancement vs. reduction of heterogeneous nucleation frequency, j^{10} , compared with the corresponding homogeneous process, j^{11} . $(a^1/kT)_{cr} = 1/2(i_{11}^{*2} - 1)$.

Large surface energies a^1 and small driving forces $|B^1|$ (large i_{11}^*) lead to enhanced heterogeneous nucleation rates. At small a^1 and small i_{11}^* (large $|B^1|$) the reverse is true.

We will compare now two bulk-diffusion-controlled heterogeneous processes, j^{20} and j^{10} . Surface free energy density, $a = a^0$, is identical in both cases, but all other variables, like kinetic factors, φ , transport energies, ε , concentration of single elements, n_1 , and bulk energies of transition, b , are different.

In the ratio

$$j^{20}/j^{10} = \frac{\varphi^{20} \exp(-\varepsilon^2/kT) \exp[-4(a^0)^3/27kT(B^2)^2 + b^2/kT]}{\varphi^{10} \exp(-\varepsilon^1/kT) \exp[-4(a^0)^3/27kT(B^1)^2 + b^1/kT]} \quad (62)$$

surface energy coefficient, a^0 , the same for both processes, appears as a parameter. Here, again, the ratio of kinetic coefficients ($\varphi^{20}/\varphi^{10}$) is a function of cluster shape (cf. Appendix B) but, except for extreme cases, is a factor of the order of unity. Transport energy, determines the ratio j^{20}/j^{10} , switching the nucleation process to either mechanism when the absolute difference $|\varepsilon^2 - \varepsilon^1|$ is large compared with kT . In other conditions the determining role is played by the difference of the energy of a single element in two phases $\Delta E = E_1^2 - E_1^1$ which controls the ratio of equilibrium concentrations of single elements (n_1^2/n_1^1), the difference between bulk free energy of transition, $b^2 - b^1$, and driving forces, $B^2 - B^1$, (cf. eqs. 30-32 above). Neglecting the ratio of kinetic factors ($\varphi^{20}/\varphi^{10}$) and the ratio of transport rates, $\exp[-(\varepsilon^2 - \varepsilon^1)/kT]$,

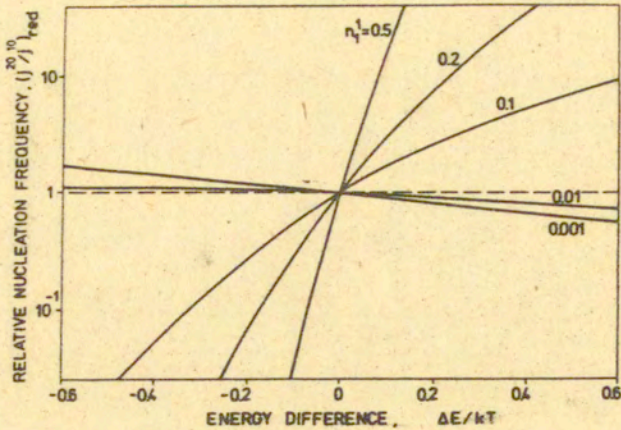


Figure 6. Reduced ratio of steady-state nucleation frequencies for two different bulk-diffusion-controlled heterogeneous processes, j^{20} and j^{10} , vs. energy difference for a single element in the corresponding phases, $\Delta E/kT = (F_1^2 - F_1^1)/kT$. $i_{10}^* = 64$, $B_1^1/kT = -1$. Fraction of single elements in phase I, n_1^I , indicated. Ordinate indicates the ratio from eq.(63).

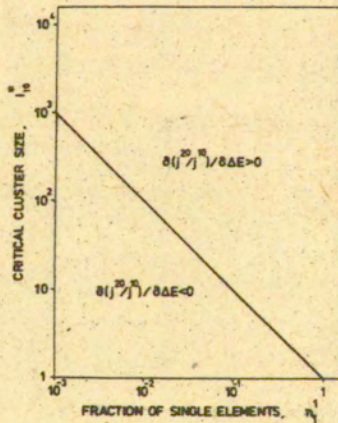


Figure 7. Critical conditions for enhancement vs. reduction of the nucleation frequency ratio (j^{20}/j^{10}). $(n_1^I)_{cr} = 1/i_{10}^*$

we will transcribe the group of thermodynamic factors controlling j^{20}/j^{10} in eq.(62) in the form

$$j^{20}/j^{10} \sim \exp(-\Delta E/kT) \times \exp\left[-\frac{1}{2}(i_{10}^* B^1/kT)\{1 - [1 + (kT/B^1)\ln C]^{-2}\}\right] \quad (63)$$

where

$$C = C(n_1^1, \Delta E) = \exp[(B^2 - B^1)/kT] = 1 - n_1^1 + n_1^1 \exp(-\Delta E/kT)$$

$$i_{10}^* = -(2a^0/3B^1)^3$$

The function from eq.(63) is plotted vs. $\Delta E/kT$ in Figure 6. At large concentrations, j^{20}/j^{10} is an increasing function of ΔE : positive ΔE leads to enhancement of the nucleation frequency j^{20} , negative ΔE reduces j^{20} below the reference level j^{10} . This behavior corresponds with an increase of critical transition temperature (T_c^{20} vs. T_c^{10}) when ΔE is positive (cf. eq.37 and Figure 3) and with the effect of ΔE on the critical cluster size (i_{20}^* vs. i_{10}^*). At very low concentrations of single elements, the effect of ΔE on the frequency ratio (j^{20}/j^{10}) is different. The derivative at $\Delta E = 0$ determines transition from one regime to the other

$$d \ln(j^{20}/j^{10})/d(\Delta E/kT) = 0 \text{ at } \Delta E = 0: (n_1^1)_{cr} = 1/i_{10}^* \quad (64)$$

Figure 7 shows regions in the $i_{10}^* - n_1^1$ plane where positive and negative energy difference stimulates j^{20} compared with j^{10} .

Last, not least we will compare heterogeneous nucleation frequencies related, respectively, to surface-diffusion, and bulk-diffusion-controlled mechanisms of cluster growth. The ratio

$$j^{00}/j^{10} = i_{00}^{*-3/2} \frac{\varphi^{00} \exp(-\epsilon^0/kT) \exp[-4(a^0)^3/27kT(B^0)^2 + b^0/kT]}{\varphi^{10} \exp(-\epsilon^1/kT) \cdot \exp[-4(a^0)^3/27kT(B^1)^2 + b^1/kT]} \quad (65)$$

is similar to (j^{20}/j^{10}) discussed above, but for the additional factor, $i_{00}^{*-3/2} = -3B^0/2a^0$ appearing in the surface-diffusion-controlled mechanism j^{00} as a consequence of the fact, that the number of sites on cluster surface accessible for addition/dissociation reactions (φ_i^{00}) is proportional to $i^{1/2}$ rather than to $i^{3/2}$ as in the bulk-diffusion controlled process j^{10} (cf. Appendix B). The ratio of numerical coefficients $\varphi^{00}/\varphi^{10}$ in most conditions lies within the range 2.0 ± 2.4 and we will replace it by a constant 2. Effect of transport rates discussed above, we will concentrate our attention on the group of thermodynamic factors in eq.(65) controlled by adsorption energy, E^1 . The following expression will thus be analyzed

$$j^{00}/j^{10} \sim 2 \cdot i_{10}^{*-3/2} \exp(-E^1/kT) [1 + (kT/B^1) \ln C] \times \\ \times \exp \left[-\frac{1}{2} (i_{10}^* B^1/kT) \{ 1 - [1 + (kT/B^1) \ln C]^{-2} \} \right] \quad (66)$$

where

$C = C(n_1^1, E^1)$ has the same form as in eq.(63).

Figure 8. presents examples of the function from eq.(66) plotted vs. adsorption energy E^1/kT . The behavior, in the range of not too low concentrations, is similar to that observed for the ratio j^{20}/j^{10} . Positive E^1 (repulsion from the interface) stimulates surface-diffusion-controlled nucleation, negative E^1 (adsorption) reduces j^{00} . There is, however a range of conditions (low concentrations, small cluster sizes) where opposite behavior can be expected. Analysis of the derivative at $E^1 = 0$

$$d \ln(j^{00}/j^{10})/d(E^1/kT) \Big|_{E^1=0} = -1 + n_1^1(i_{10}^* - kT/B^1) \quad (67)$$

equated to zero, yields critical conditions when stimulation of j^{00} by positive energy E^1 is replaced by reduction

$$(n_1^1)_{cr} = 1/(i_{10}^* - kT/B^1) \quad (68)$$

Figure 9, presents region in the $i_{10}^* - n_1^1$ plane corresponding to these two regimes. So, in the range of not too small n_1^1 and not too small i_{10}^* , positive E^1 stimulates surface-diffusion-controlled nucleation, negative E^1 suppresses j^{00} . Such a behavior is consistent with the effect of adsorption energy on critical transition temperature T_c^{00} and on the critical cluster size, i_{10}^* . The range of low n_1^1 and small i_{10}^* admits an opposite behavior.

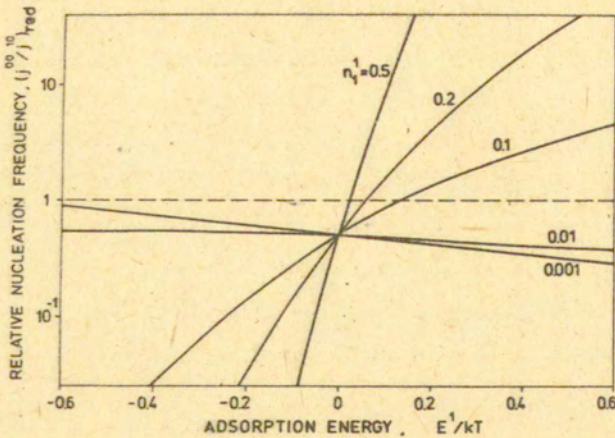


Figure 8. Reduced ratio of steady-state nucleation frequencies for a surface-diffusion-controlled process, j^{00} , and bulk-diffusion-controlled process, j^{10} , vs. energy of adsorption of a single element from phase I onto the interface, $E^1/kT = (F_1^0 - F_1^1)/kT$. $i_{10}^* = 64$, $B^1/kT = -1$, n_1^1 indicated. Ordinate indicates the ratio from eq.(66).

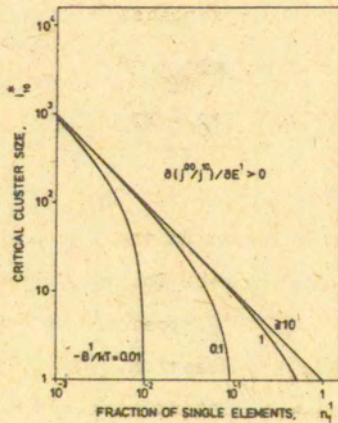


Figure 9. Critical conditions for enhancement vs. reduction of surface nucleation frequency ratio j^{00}/j^{10} . $(n_1^1)_{cr} = 1/(i_{10}^* - kT/B^1)$.

CONCLUSIONS

Validity of our analysis based on the discussion of physical variables (kinetic and thermodynamic) appearing in five nucleation mechanisms possible in a system with interface is subject to some limitations.

Conclusions about the critical conditions (temperature, T_c , fraction of single elements, n_1) for thermodynamic equilibrium, do not include any special assumptions. Those concerned with nucleation kinetics however, based on the assumption of steady-state processes, and "equilibrium" concentration distribution (n_1^2 and n_1^0 vs. n_1) are valid, provided that the system is not far from a true equilibrium. This assumption is widely used in irreversible thermodynamics, but its limiting effect on the predictions should always be remembered.

The role of transport rate, viz. activation energy of diffusion, ϵ , required for a single kinetic element to approach, or to leave the growing cluster, can be determining when processes with very different transport energies are considered. One can expect, comparing two possible mechanisms, that mechanism "1" will be practically discriminated if the ratio $\exp(-\epsilon^1/kT)/\exp(-\epsilon^2/kT)$ is very small, or the difference $(\epsilon^1 - \epsilon^2)/kT$ is large. It seems rather obvious that such a situation exists in systems gas/solid, and liquid/solid, where molecular mobility in the solid phase (II), and reactions controlled by it, are negligibly small compared with those in the liquid, or gas phase "1". Consequently, out of the five nucleation mechanisms possible in the system, mechanisms j^{22} and j^{20} will be practically eliminated. It is not obvious that such

an exclusion would also apply to the surface-diffusion-controlled mechanism, j^{00} . In liquid/liquid, gas/liquid, or solid/solid systems, differences between mobilities can be small or large, and exclusion can take place in some conditions. In a solid-solid system where the boundary between two crystals consists in a layer of defects and dislocations, one can expect increased mobility on the interface, larger than that in the bulk of each crystal. This would stimulate surface diffusion on the interface, and emphasize the role of surface-diffusion-controlled nucleation mechanism, j^{00} . Nucleation of microvoids from vacancies in polycrystalline materials seems to provide a good example, without excluding homogeneous processes j^{22} , j^{11} , and bulk-diffusion-controlled heterogeneous processes j^{20} , j^{10} (cf. refs. 12, 13).

Conclusions following from the thermodynamic considerations predict higher equilibrium (transition) temperatures for processes taking place in the bulk phase, where free energy of a single, uncombined element is higher ($\Delta E = F_1^2 - F_1^1$ positive). This result follows from the combined effect of the energy difference ΔE on the free energy of transition, (b^2 vs. b^1) and on the equilibrium partition of concentration of single elements between two contacting phases (n_1^2 vs. n_1^1). Adsorption of a growing cluster on the interface does not affect critical temperature when single elements are supplied by impingement from the bulk phase (equal critical temperatures for processes j^{11} and j^{10}). On the other hand, critical transition temperature for the surface-diffusion-controlled process j^{00} is reduced when single elements are adsorbed on the interface (i.e. when the adsorption energy $E^1 = F_1^0 - F_1^1$ is negative. This results

from the same source as the effect of ΔE in the comparison of two homogeneous processes j^{22} and j^{11} (cf. Figure 3).

Although heterogeneous nucleation does not offer any advantage over homogeneous processes in critical transition temperature (there is a disadvantage when surface-diffusion mechanism with strong adsorption is considered), thermodynamic and kinetic variables strongly influence critical cluster sizes, i^* , critical nucleation energies, ΔF^* , and nucleation frequencies, j .

Transition from one homogeneous process (say j^{11}) to another one (j^{22}) involves change of all physical variables, including transport energies, ϵ , surface energies, a , bulk energies of transition, b , and equilibrium concentrations, n_1 . Depending on the properties of the two phases compared, process j^{22} can be slower, or faster than j^{11} , in some conditions by many orders of magnitude. Discrimination of one mechanism by very small mobility is one of many possibilities, but no general and exhaustive rules can be put forward for prediction of j^{22}/j^{11} .

Comparison of a bulk-diffusion-controlled process, j^{10} , with the corresponding homogeneous process, j^{11} , involves only the change in the surface free energy; a^0 for the heterogeneous process is always smaller than a^1 for the homogeneous one (cf. Appendix B). This leads to smaller critical cluster sizes, i^* , and smaller critical energies ΔF^* for the heterogeneous process, and in the range of not too small (a/kT) and not too small i^* , makes the heterogeneous process j^{10} faster than j^{11} . More detailed discussion of these conditions is contained in the preceding section (cf. also Figure 5).

Surface-diffusion-controlled process j^{00} when compared with bulk-diffusion-controlled one, j^{11} (or j^{20}) is largely affected by molecular mobility, different for the bulk phase I (energy ϵ^1) and for the interface (energy ϵ^0). It may be expected that in solid/solid systems ϵ^0 for surface diffusion on the grain boundary is considerably smaller than either ϵ^1 or ϵ^2 for the contacting bulk phases, thus stimulating surface diffusion and the related nucleation mechanism. As far as thermodynamic parameters are concerned, negative adsorption energy (negative E^1 , $F_1^0 < F_1^1$) increases critical cluster size, i^* and critical energy $\Delta\bar{F}^*$, and in most conditions (not too small concentrations, not too small i^*) suppresses the surface-diffusion-controlled mechanism compared with bulk-diffusion-controlled one. More details can be found in the text, and in Figures 8 - 9.

Analysis included in this paper concerns nucleation mechanisms acting independently. In fact, all heterogeneous processes j^{10} , j^{20} and j^{00} are coupled, and the resulting thermodynamic and kinetic behavior may be different to that described above. This problem has been already touched⁷ and will be treated more in detail in another paper.

REFERENCES TO PART I

1. M.Volmer, *Kinetik der Phasenbildung*, T.Steinkopff, Dresden-Leipzig, 1939
2. R.A.Sigsbee, *J.Crystal Growth*, 13/14, 135, (1972)
3. R.D.Gretz, *Surface Science*, 6, 468, (1967)
4. B.K.Chakraverty, *J.Phys.Chem.Solids*, 28, 2401, (1967)

5. G.M.Pound, M.T.Simnad and L.Yang, *J.Chem.Phys.*, 22, 1215, (1954)
6. W.K.Burton, N.Cabrera and F.C.Frank, *Proc.Roy.Soc. (London)*, A243, 299, (1951)
7. A.Ziabicki, *Prace IPPT (Inst.Fund.Technological Res. Reports) No 4*, (1977)
8. D.Turnbull and J.C.Fisher, *J.Chem.Phys.*, 17, 71, (1949)
9. A.Ziabicki, *J.Chem.Phys.*, 48, 4368, (1968)
10. A.Ziabicki, *ibid.* 48, 4374, (1968)
11. A.Ziabicki, *ibid.* 66, 1638, (1977)
12. J.Krzemiński, *Prace IPPT (IFTR Reports) No 3*, (1983); *Arch.Mech.*, 35, 639, (1983)
13. J.Krzemiński, *Proc.II Int.Symposium on Defects, Fracture and Fatigue, Mont Gabriel, Que.*, 1982; Nijhoff, The Hague 1983
14. F.C.Frank and M.Tosi, *Proc.Roy.Soc. (London)*, A263, 323, (1961)
15. J.D.Hoffman and J.I.Lauritzen, *J.Res.NBS*, 65A, 297, (1961)
16. A.Ziabicki and L.Jarecki, *J.Chem.Phys.* (in press)
17. W.B.Hillig and B.McCarroll, *J.Chem.Phys.* 45, 3887, (1966)
18. J.Frenkel, *Kinetic Theory of Liquids*, Oxford University Press, London, 1946

APPENDIX A 1

ACCURACY OF THE INTEGRAL APPROXIMATION FOR
STEADY STATE NUCLEATION FREQUENCY

by M.Kość and A.Ziabicki

Exact solution of the steady-state nucleation frequency, j_{st} (eq.22) is inversely proportional to the semi-infinite sum

$$\Sigma = \sum_{i=1}^{\infty} \frac{1}{k_i^+} \exp(\Delta\tilde{F}_i/kT) \quad (A-1)$$

where the rate constant k_i^+ switches from one form to another at some critical value $i = i_0^*$

$$k_i^+ = \begin{cases} k_0 i_0^{3/2} \exp(-\delta f_i/kT) & \text{for } i < i_0^* \\ k_0 i^{3/2} & \text{for } i \geq i_0^* \end{cases} \quad (A-2)$$

δf_i is free energy of transition per one kinetic element, and the total driving force for cluster formation, $\Delta\tilde{F}_i$ is controlled by surface energy density, a , bulk free energy of transition, b , and molar fraction of single kinetic elements which are to be combined to form a cluster, n_1

$$\Delta\tilde{F}_i = a(i^{3/2} - 1) + b(i - 1) - kT(i - 1) \ln n_1 \quad (A-3)$$

The sum Σ , according to the procedure proposed by Frenkel¹⁸ is approximated by the integral

$$\Sigma_0 = (1/k_{i_0}^+) \int_{-\infty}^{\infty} \exp[\Delta\bar{F}^*/kT + \frac{1}{2}(d^2\Delta\bar{F}/di^2kT)_{i_0}(i-i_0)^2] di \quad (A-4)$$

Using three independent parameters, a/kT , $i_0^* = -(2a/3b)^3$, and $i^* = -[2a/3(b - kT \ln n_1)]^3$, one arrives at the following expressions

$$\Sigma = \sum_{i=1}^{\infty} \frac{1}{k_i^+} \exp\left\{ \left(\frac{a}{kT} \right) \left[\left(i^{\frac{3}{2}} - 1 \right) - \frac{2}{3} i^{*\frac{-3}{2}} (i-1) \right] \right\} \quad (A-5)$$

$$\Sigma_0 = (3/k_0) (\pi kT/a)^{\frac{1}{2}} \exp\left[\frac{2}{3} a \left(i_0^{\frac{3}{2}} - 3 - 2i_0^{*\frac{-3}{2}} \right) / kT \right] \quad (A-6)$$

$$\delta f_1 = \frac{2}{3} a \left(i_0^{-\frac{3}{2}} - i_0^{*\frac{-3}{2}} \right) \quad (A-7)$$

The ratio Σ/Σ_0 represents accuracy of the integral approximation. The values $\Sigma/\Sigma_0 = f(i_0^*, i^*, a/kT)$ were calculated numerically. Evaluation of the sum in eq.(A-1) was stopped at the term whose value was smaller than 0.001% of the current value of the sum. Additionally, to avoid the effect of apparent convergence, indices of the neglected terms were required to be greater than $i_0^* + 20$. Results of the calculations are presented as layer lines $\Sigma/\Sigma_0 = \text{const.}$ in the $a/kT - i^*$ plane.

The ratio $i_0^*/i^* = [(1 - kT/b)\ln n_1]^3$ was kept constant at the following levels

$$i_0^*/i^* = 0.01, 0.1, 0.5, 0.9, 1.0$$

The results are shown in Figures A1 - A5. Region between 0.9 and 1.1 lines represents the range of nucleation conditions $(i^*, a/kT)$ where the integral approximation bears an error smaller than $\pm 10\%$ with respect to the directly calculated sum Σ , the range between $\Sigma/\Sigma_0 = 0.8$ and 1.2 - an error smaller than $\pm 20\%$, etc. Figure A 6 presents layer lines $\Sigma/\Sigma_0 = 0.9$, $\Sigma/\Sigma_0 = 1.1$ calculated for different values of the ratio i_0^*/i^* and thus allows to notice how the region of good accuracy of the integral approximation changes with i_0^* .

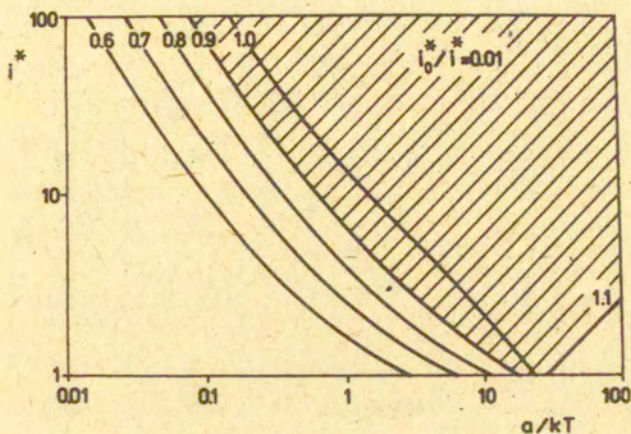


Fig.A1. Layer lines $\Sigma/\Sigma_0 = \text{const.}$, representing accuracy of the integral approximation in the $a/kT - i^*$ plane. Results calculated for $i_0^*/i^* = 0.01$.

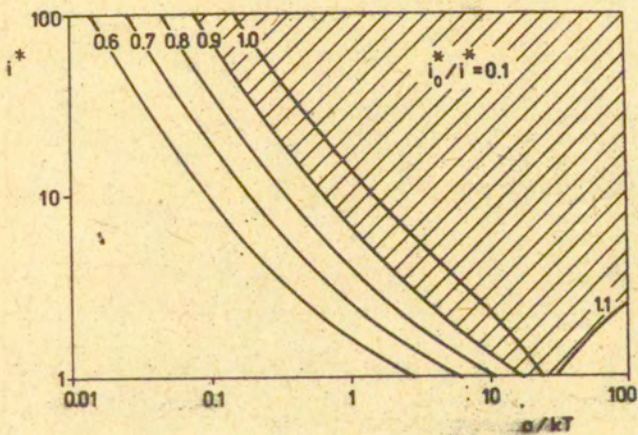


Fig.A2. Layer lines $\Sigma/\Sigma_0 = \text{const.}$, representing accuracy of the integral approximation in the $a/kT - i^*$ plane. Results calculated for $i_0^*/i^* = 0.1$.

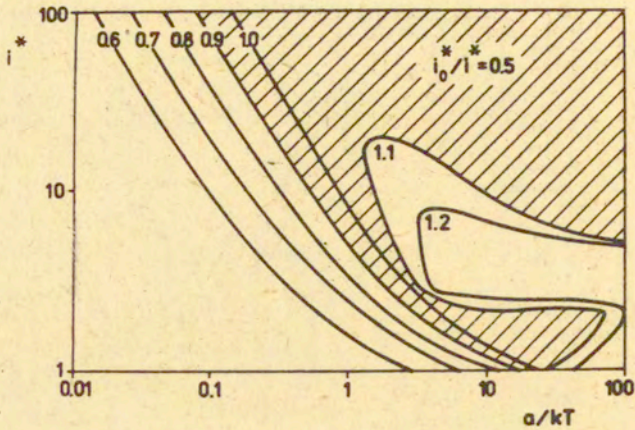


Fig.A3. Layer lines $\Sigma/\Sigma_0 = \text{const.}$, representing accuracy of the integral approximation in the a/kT - i^* plane. Results calculated for $i_0^*/i^* = 0.5$.

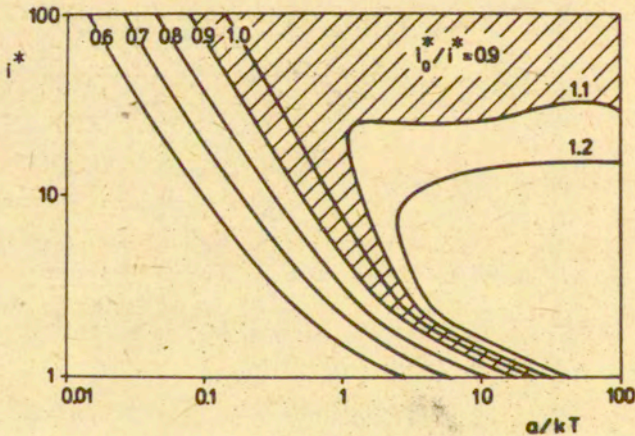


Fig.A4. Layer lines $\Sigma/\Sigma_0 = \text{const.}$, representing accuracy of the integral approximation in the a/kT - i^* plane. Results calculated for $i_0^*/i^* = 0.9$.

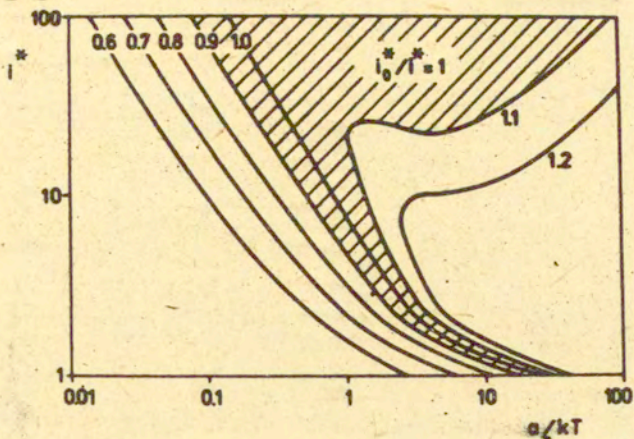


Fig.A5. Layer lines $\Sigma/\Sigma_0 = \text{const.}$, representing accuracy of the integral approximation in the $a/kT - i^*$ plane. Results calculated for $i_0^*/i^* = 1$.

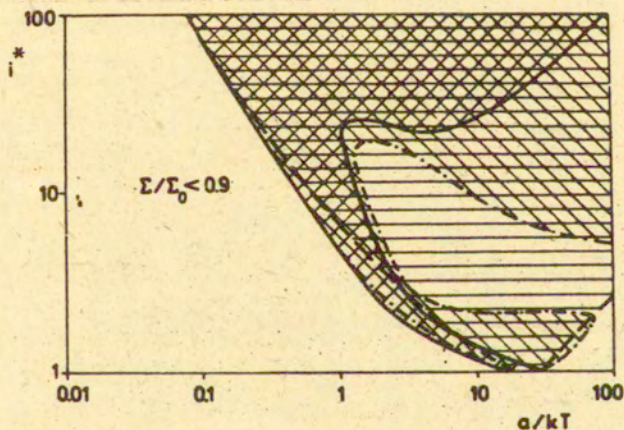


Fig.A6. Regions on the $a/kT - i^*$ plane where the integral approximation bears an error smaller than $\pm 10\%$, i.e. $0.5 < \Sigma/\Sigma_0 < 1.1$. Results calculated for $i_0^*/i^* = 1.0$ (—), 0.5 (---), 1.0 (- - -)

APPENDIX B 1

GEOMETRY OF CLUSTERS AND RELATED NUCLEATION CHARACTERISTICS

by M.Kość and A.Ziabicki

Two parameters in the nucleation theory, viz. surface energy coefficient, a , in eqs.(8-9), and the number of sites accessible to addition/dissociation reactions, φ_i , in eqs. (3-4), are controlled by geometry of clusters, different for individual nucleation mechanisms. We will derive here the appropriate characteristics for spherical, homogeneous clusters, and spherical-cap, and double-lens (heterogeneous) clusters located on the interface between two mother phases I and II.

Spherical Clusters (Homogeneous Nucleation)

Consider a spherical cluster of volume V , composed of i single kinetic elements, each of volume v_0

$$V = v_0 i = 4\pi R^3/3 \quad (B-1)$$

The total surface of the cluster, S reads thus

$$S = 4\pi R^2 = (36\pi v_0^2)^{\frac{1}{3}} i^{\frac{2}{3}} \quad (B-2)$$

which yields the surface energy coefficient, for homogeneous nucleation, a^1

$$a^1 = S\sigma/i^{\frac{2}{3}} = (36\pi v_0^2)^{\frac{1}{3}} \sigma \quad (\text{B-3})$$

and the corresponding coefficient $\varphi^{11} = S/i^{\frac{2}{3}} s_0$

$$\varphi^{11} = S/s_0 i^{\frac{2}{3}} = (36\pi v_0^2)^{\frac{1}{3}} / s_0 \quad (\text{B-4})$$

where σ is interface tension between cluster and the mother phase and s_0 is area of the projection of a single element on cluster surface. Assuming spherical single elements with radius r_0 , $v_0 = 4\pi r_0^3/3$, $s_0 = \pi r_0^2$, one arrives at the following results

$$\begin{aligned} a^1 &= 4\pi r_0^2 \sigma \\ \varphi^{11} &= 4 \end{aligned} \quad (\text{B-5})$$

Spherical-Cap Cluster on a Solid, Undeformable Interface

We will briefly review well known results for a spherical cap located on a solid interface (Figure B1). The cosine of the "contact angle", $x = \cos\alpha$, and the radius R of the base circle, R , determine volume of the cluster

$$V = v_0 i = \frac{1}{3}\pi R^3(2+x)(1-x)^{\frac{3}{2}}/(1+x)^{\frac{1}{2}}, \quad (\text{B-6})$$

the surface area exposed to addition/dissociation reactions,

S_1 ,

$$S_1 = 2\pi R^2/(1+x) \quad (B-7)$$

and area of the base circle

$$S_2 = \pi R^2 \quad (B-8)$$

If σ^{c1} , and σ^{c2} are interface tensions between the cluster "c" and mother phases I, II, and σ^{12} is interface tension between phases I and II, the total surface energy difference due to formation of the cluster reads

$$A = S_1\sigma^{c1} + S_2(\sigma^{c2} - \sigma^{12}) \quad (B-9)$$

The equilibrium shape of the cluster characterized by parameters x^* , R^* , can be found either by minimization of the function A with respect to the parameters x , R , at constant cluster volume, or from the balance of forces. The forces of interface tension are shown in Fig.B1. In the case of undeformable interface, the necessary condition for equilibrium is the balance of forces along the direction parallel to the interface. Thus one obtains

$$\sigma^{12} = \sigma^{c1}x^* + \sigma^{c2} \quad (B-10)$$

or

$$x^* = (\sigma^{12} - \sigma^{c2})/\sigma^{c1} \quad (B-11)$$

Of course, since $x = \cos\alpha$, eq.(B-10) can be satisfied, provided that

$$\sigma^{c2} - \sigma^{c1} \leq \sigma^{12} \leq \sigma^{c1} + \sigma^{c2} \quad (\text{B-12})$$

If $\sigma^{12} \leq \sigma^{c1} - \sigma^{c2}$, there is no wetting and the cluster assumes spherical shape. For $\sigma^{12} > \sigma^{c1} + \sigma^{c2}$, cluster tends to be infinitely flat, and the equilibrium does not exist.

The radius of the base circle of the equilibrium cluster can be determined from eq.(B-6) with $x = x^*$. Then, one can express the surface energy coefficient, and kinetic coefficients as functions of the interface tension. The surface energy coefficient $a^0 = A(x^*, R^*)/i^{\frac{3}{2}}$ reads

$$a^0 = a^1 \left[\frac{(\sigma^{c1} + \sigma^{c2} - \sigma^{12})^2 (2\sigma^{c1} - \sigma^{c2} + \sigma^{12})}{4(\sigma^{c1})^3} \right]^{\frac{1}{2}} \quad (\text{B-13})$$

where $a^1 = 4\pi r_0^2 \sigma^{c1}$ is the surface energy coefficient for homogeneous nucleation.

The kinetic coefficient for surface S_1 , exposed to impingement of single elements from the bulk phase I (mechanism j^{10})

$$\phi^{10} = S_1/s_0 i^{\frac{3}{2}} = 4 \frac{2^{\frac{1}{2}} \sigma^{c1}}{[(\sigma^{c1} + \sigma^{c2} - \sigma^{12})(2\sigma^{c1} - \sigma^{c2} + \sigma^{12})]^{\frac{1}{2}}} \quad (\text{B-14})$$

In the case of surface-diffusion-controlled cluster growth (mechanism j^{00}) surface exposed to reactions of growth/dissociation, S_{00} , is a monomolecular circumferential belt with width $2r_0$ (diameter of a single element); hence the kinetic coefficient

$$\phi^{00} = S_{00}/s_0 i^{\frac{1}{2}} = 8 \frac{2^{-\frac{1}{2}}(\sigma^{12} + \sigma^{c1} - \sigma^{c2})^{\frac{1}{2}}}{[(\sigma^{c1} + \sigma^{c2} - \sigma^{12})(2\sigma^{c1} - \sigma^{c2} + \sigma^{12})]^{\frac{1}{2}}} \quad (\text{B-15})$$

It can be easily noticed that for $\sigma^{12} = \sigma^{c2} - \sigma^{c1}$, eqs. (B-13, B-14) reduce to the results of the preceding section since, as mentioned before, for $\sigma^{12} \leq \sigma^{c1} - \sigma^{c2}$ the equilibrium cluster assumes spherical shape.

Double-Lens Cluster on a Deformable Interface

More complex case exists when both phases, on the boundary of which the cluster is located, are deformable. The resulting equilibrium cluster exhibits double-lens shape with base circle of radius R , and two "contact angles" α_1 (to phase I), and α_2 (to phase II). The contact angles and the forces of interface tensions are shown in Fig. B2. Since the interface is deformable, in equilibrium one has to require balance of forces both in the direction parallel, and perpendicular to the interface plane. Denoting cosines of the angles α_1 and α_2 by x and y , respectively, the equations for the balance of forces read

$$\sigma^{12} = \sigma^{c1}x + \sigma^{c2}y \quad (\text{B-16})$$

and

$$\sigma^{c1} \sqrt{1-x^2} = \sigma^{c2} \sqrt{1-y^2} \quad (\text{B-17})$$

The solutions of eqs.(B-16,B-17) exist, provided that

$$|\sigma^{c1} - \sigma^{c2}| \leq \sigma^{12} \leq \sigma^{c1} + \sigma^{c2} \quad (\text{B-18})$$

and are given by

$$x^* = \frac{(\sigma^{12})^2 + (\sigma^{c1})^2 - (\sigma^{c2})^2}{2\sigma^{c1}\sigma^{12}} \quad (\text{B-19})$$

$$y^* = \frac{(\sigma^{12})^2 + (\sigma^{c2})^2 - (\sigma^{c1})^2}{2\sigma^{c2}\sigma^{12}} \quad (\text{B-20})$$

If $\sigma^{12} \leq |\sigma^{c1} - \sigma^{c2}|$ the equilibrium cluster does not cross the interface plane and must be of spherical shape (one or two spheres). Let us assume from now on that the tension σ^{c1} is greater than σ^{c2} . In such a case a spherical equilibrium cluster should be immersed in phase II since then its energy is the lowest.

For $\sigma^{12} > \sigma^{c1} + \sigma^{c2}$, like in the case of undeformable interface, the equilibrium cluster cannot exist.

The results given by eqs.(B-19,B-20) can be also obtained by minimization of surface energy with respect to R, x, y , keeping constant volume of the cluster. This procedure is not simple, however.

Proceeding to calculations of kinetic coefficients we will define new variables

$$u = \tan \frac{\alpha_1}{2} ; \quad v = \tan \frac{\alpha_2}{2} \quad (\text{B-21})$$

Then, one can express the total surface energy difference due to formation of the cluster, and its volume as functions of R, u, v

$$A(R, u, v) = \pi R^2 [\sigma^{c1}(u^2 + 1) + \sigma^{c2}(v^2 + 1) - \sigma^{12}] \quad (\text{B-22})$$

$$V(R, u, v) = \frac{\pi}{6} R^3 [u(u^2 + 3) + v(v^2 + 3)] \quad (\text{B-23})$$

The equilibrium values of u and v read

$$u^* = \frac{\sigma^{12} - \sigma^{c1} + \sigma^{c2}}{\sigma^{12} + \sigma^{c1} - \sigma^{c2}} \quad \frac{\sigma^{c1} + \sigma^{c2} - \sigma^{12}}{\sigma^{c1} + \sigma^{c2} + \sigma^{12}} \quad (\text{B-24})$$

$$v^* = \frac{\sigma^{12} + \sigma^{c1} - \sigma^{c2}}{\sigma^{12} + \sigma^{c1} - \sigma^{c2}} \quad \frac{\sigma^{c1} + \sigma^{c2} - \sigma^{12}}{\sigma^{c1} + \sigma^{c2} + \sigma^{12}} \quad (\text{B-25})$$

Using eq.(B-23), the radius R can be eliminated from eq. (B-22) giving the surface energy A as a function of two variables u, and v. The value of A(u, v) in equilibrium yields the surface energy coefficient for heterogeneous cluster growth mechanisms (j^{10} , j^{20} , j^{00})

$$a^0 = a^1 \frac{(u^*)^2 + 1 + \frac{\sigma^{c2}}{\sigma^{c1}}[(v^*)^2 + 1] - \frac{\sigma^{12}}{\sigma^{c1}}}{\{u^*[(u^*)^2 + 3] + v^*[(v^*)^2 + 3]\}^{\frac{2}{3}}} \quad (\text{B-26})$$

where a^1 is surface energy coefficient for homogeneous nucleation in phase I (eq.B-5).

The kinetic coefficients φ^{kj} , for processes j^{10} , j^{20} , and j^{00} , are given by

$$\varphi^{10} = \varphi^{11} \frac{(u^*)^2 + 1}{\{u^*[(u^*)^2 + 3] + v^*[(v^*)^2 + 3]\}^{\frac{2}{3}}} \quad (\text{B-27})$$

$$\varphi^{20} = \varphi^{22} \frac{(v^*)^2 + 1}{\{u^*[(u^*)^2 + 3] + v^*[(v^*)^2 + 3]\}^{\frac{2}{3}}} \quad (\text{B-28})$$

$$\varphi^{00} = (\varphi^{11} + \varphi^{22}) \frac{1}{\{u^*[(u^*)^2 + 3] + v^*[(v^*)^2 + 3]\}^{\frac{2}{3}}} \quad (\text{B-29})$$

where $\varphi^{11} = \varphi^{22} = 4$, is the kinetic coefficient for homogeneous nucleation.

For $\sigma^{12} \rightarrow \sigma^{c1} - \sigma^{c2}$ ($\sigma^{12} > \sigma^{c1} - \sigma^{c2}$) parameters u^* , v^* approach their limits, $u^* \rightarrow 0$, $v^* \rightarrow \infty$, and the coefficients given by eqs.(B-26 - B-29) reduce to

$$a^0 = a^1(\sigma^{c2}/\sigma^{c1}) = a^2 \quad (\text{B-30})$$

$$\varphi^{10} = 0 \quad (\text{B-31})$$

$$\varphi^{20} = \varphi^{22} \quad (\text{B-32})$$

$$\varphi^{00} = 0 \quad (\text{B-33})$$

The above coefficients characterize homogeneous nucleation in phase II. They remain unchanged also for $\sigma^{12} < \sigma^{c1} - \sigma^{c2}$ since, according to the discussion presented before, in this regime a spherical cluster immersed in phase II is the most stable one.

To illustrate properties of the obtained solutions, numerical calculations were performed. The results are presented in the form of three-dimensional plots of functions depending on the ratios of interface tensions, σ^{12}/σ^{c1} and σ^{c2}/σ^{c1} (assumed: $\sigma^{c1} > \sigma^{c2}$). The functions shown in Figs. B3 - B8 are, respectively:

- cosines of contact angles, $x^* = \cos \alpha_1$, and $y^* = \cos \alpha_2$ (Figs. B3 - B4),
- surface energy coefficient for heterogeneous nucleation normalized by the value of corresponding coefficient for homogeneous nucleation, in phase I, a^0/a^1 (Fig. B5),
- kinetic coefficients for processes controlled by j^{10} , and j^{20} normalized by the value of corresponding coefficient for homogeneous nucleation, $\varphi^{10}/\varphi^{11}$ and $\varphi^{20}/\varphi^{22}$ (Figs. B6 - B7),
- normalized kinetic coefficient for the process controlled by j^{00} , $\varphi^{00}/(\varphi^{11} + \varphi^{22})$ (Fig. B8).

Since the equilibrium cluster exists only for $\sigma^{12} < \sigma^{c1} + \sigma^{c2}$ the above functions are properly determined if $\sigma^{12}/\sigma^{c1} < 1 + \sigma^{c2}/\sigma^{c1}$; cosines x^* , y^* of the contact angles

were assumed equal to unity in the instability region
($\sigma^{12} > \sigma^{c1} + \sigma^{c2}$) to visualize that the cluster tends to be infinitely flat.

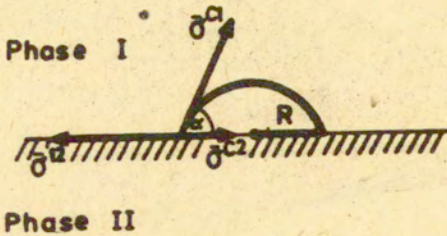


Fig.B1. Spherical cap cluster located on an undeformable interface. α contact angle to phase I (wetting angle); $\vec{\sigma}^{c1}$, $\vec{\sigma}^{c2}$ forces of interface tension between the cluster and phases I, II; $\vec{\sigma}^{12}$ force of interface tension between phases I and II.

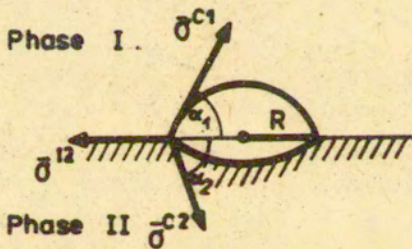


Fig.B2. Double-lens cluster located on a deformable interface. α_1 , α_2 contact angles to phase I, and II; $\vec{\sigma}^{c1}$, $\vec{\sigma}^{c2}$, $\vec{\sigma}^{12}$ forces of interface tension (cf. caption to Fig.B1).

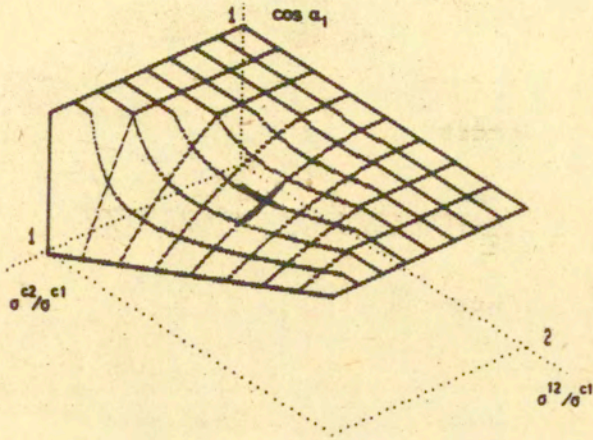


Fig.B3. Cosine of equilibrium contact angle of a double-lens cluster to phase I, $x^* = \cos \alpha_1$, as a function of two ratios of interface tensions σ^{c2}/σ^{c1} and σ^{12}/σ^{c1} (assumed: $\sigma^{c1} > \sigma^{c2}$).

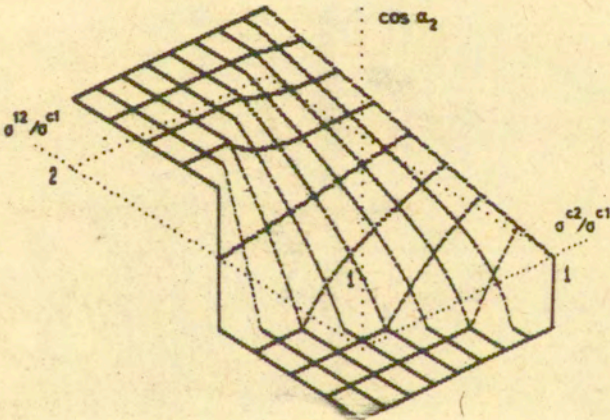


Fig.B4. Cosine of equilibrium contact angle of a double-lens cluster to phase II, $y^* = \cos \alpha_2$, as a function of two ratios of interface tensions σ^{c2}/σ^{c1} and σ^{12}/σ^{c1} (assumed: $\sigma^{c1} > \sigma^{c2}$).

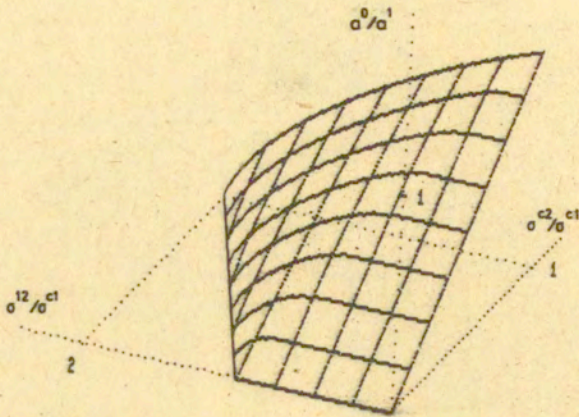


Fig.B5. Normalized surface energy coefficient for heterogeneous nucleation, a^0/a^1 , as a function of two ratios of interface tensions σ^{c2}/σ^{c1} and σ^{12}/σ^{c1} (assumed: $\sigma^{c1} > \sigma^{c2}$).

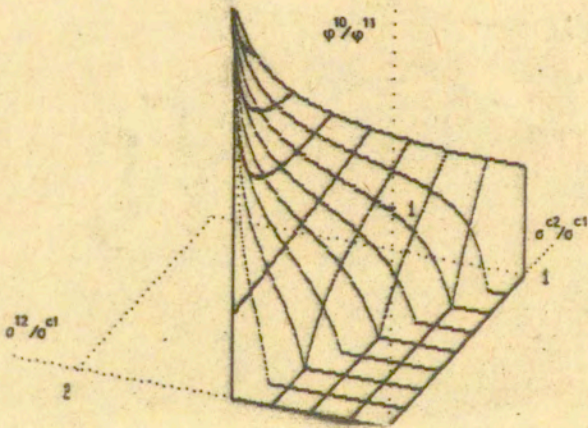


Fig.B6. Normalized kinetic coefficient for process controlled by $j^{10}, \varphi^{10}/\varphi^{11}$, as a function of two ratios of interface tensions σ^{c2}/σ^{c1} and σ^{12}/σ^{c1} (assumed: $\sigma^{c1} > \sigma^{c2}$).

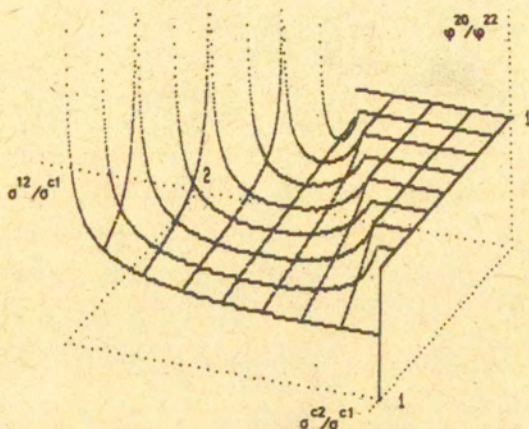


Fig. B7. Normalized kinetic coefficient for process controlled by j^{20} , $\frac{\varphi^{20, 22}}{\varphi}$ as a function of two ratios of interface tensions $\frac{\sigma^{c2}}{\sigma^{c1}}$ and $\frac{\sigma^{12}}{\sigma^{c1}}$ (assumed: $\sigma^{c1} > \sigma^{c2}$).

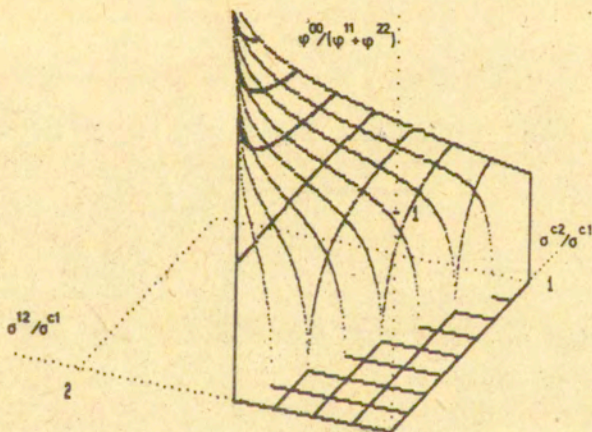


Fig. B8. Normalized kinetic coefficient for process controlled by j^{00} , $\frac{\varphi^{00}}{\varphi + \varphi}$ as a function of two ratios of interface tensions $\frac{\sigma^{c2}}{\sigma^{c1}}$ and $\frac{\sigma^{12}}{\sigma^{c1}}$ (assumed: $\sigma^{c1} > \sigma^{c2}$).

SUMMARY I

Phase transitions in the vicinity of a boundary between two regions (solid-solid, solid-liquid, liquid-liquid, etc.) can involve several different mechanisms, j^{pq} , according to where the cluster of the new phase is located (superscript "q") and which region supplies reacting elements for its growth (superscript "p"). p and q can assume three different values corresponding, respectively, to bulk regions (p,q = 1, or 2) and the monomolecular interface layer (p,q = 0). The thermodynamics and kinetics for various j^{pq} mechanisms differ from one mechanism j^{pq} to another. In this paper we have analyzed all five mechanisms of nucleation possible in the vicinity of an interface: two homogeneous processes, j^{11} and j^{22} proceeding within the bulk regions "1" and "2", respectively, and three heterogeneous mechanisms, j^{10} , j^{20} , j^{00} , where the growing cluster is always located on the interface (q = 0) and single kinetic elements are supplied from bulk regions (p = 1, or 2) or from the monomolecular interface region (p = 0). Kinetics and thermodynamics of the five processes were analyzed as if they acted independently one from the other. Effects of interface energy density, σ , adsorption energy from the two bulk regions, E^1 , E^2 , as well as mobilities in individual regions, ε^1 , ε^2 , ε^0 , were analyzed and discussed.

Andrzej Ziabicki
Pracownia Fizyki Polimerów
IPPT PAN, Warszawa

NUCLEATION OF PHASE TRANSITIONS IN THE VICINITY
OF PHASE BOUNDARY.

II. COUPLED CLUSTER GROWTH PROCESSES

INTRODUCTION II

In the preceding paper¹ we have analyzed various mechanisms of cluster growth, possible in the vicinity of a boundary. They include two homogeneous processes, labelled j^{11} and j^{22} occurring, respectively, in the bulk of phases I and II, and three heterogeneous processes, where cluster of the new phase is located on the interface (second superscript "0") and single elements for cluster growth are supplied from phase I or II by impingement on the respective cluster surface (processes j^{10} , j^{20}), or by surface diffusion along the interface and peripheral addition of single elements adsorbed in a monomolecular layer (process j^{00}). We have discussed differences between the five individual processes as if they were acting independently, and analyzed effects of kinetic and thermodynamic material parameters on the state of equilibrium and nucleation rates.

In fact, the three heterogeneous processes are not independent. Sorption-desorption on the interface makes possible migration of single elements from bulk phase I to the

monomolecular layer on the interface, and to the other bulk phase. This leads to a number of new phenomena, new critical conditions, and nucleation rates which are not a linear superposition of the isolated mechanisms.

We will complete now our discussion of heterogeneous nucleation in the vicinity of an interface, by discussing critical conditions of nucleation, conditions of thermodynamic equilibrium (which appear to be different from the above mentioned), and nucleation rate kinetics. Analysis of a few cases of special interest will suggest possible non-trivial applications of the theory.

FORMAL EQUATIONS OF COUPLED NUCLEATION PROCESSES

As discussed in the former paper¹, and earlier works in the field of nucleation (e.g. refs.^{2,3}) the thermodynamic and kinetic characteristics of an isolated nucleation mechanism, j_i^{pq} (subscript "p" refers to the region from which originate single elements participating in cluster growth, "q" - to localization of the growing cluster) can be described by a set of kinetic equations

$$\left. \begin{aligned} j_2^{pq} &= k_1^{+pq} n_1^q n_1^p - k_2^{-pq} n_2 & \text{for } i = 2 \\ j_i^{pq} &= k_{i-1}^{+pq} n_{i-1} n_1^p - k_i^{-pq} n_i & \text{for } i > 2 \end{aligned} \right\} \quad (1)$$

k_{i-1}^{+pq} , k_i^{-pq} are addition and dissociation rate constants

assumed to obey the condition (strictly satisfied in thermodynamic equilibrium)

$$k_{i-1}^{+pq}/k_i^{-pq} = \exp(-\delta f_i^{pq}/kT) \quad (2)$$

and the free energy of transition for a single step (energy of addition one single element to an "i-1" cluster) consists of a surface, and a bulk term

$$\delta f_i^{pq} = \frac{2}{3} a^q i^{-\frac{2}{3}} + b^p \quad (3)$$

Free energy of formation of an i-size cluster from "i" single elements results in the form

$$\Delta F_i^{pq} = \sum_{m=2}^i \delta f_m^{pq} = a^q (i^{\frac{2}{3}} - 1) + b^p (i - 1) \quad (4)$$

and the total driving force for the reaction of addition

$$\left. \begin{aligned} k_{i-1}^{+pq} n_1^p / k_i^{-pq} &\rightarrow \exp(-\delta f_i^{pq}/kT) \\ \delta f_i^{pq} = \delta f_i^{pq} - kT \ln n_1^p ; \quad \Delta F_i^{pq} = \Delta F_i^{pq} - kT(i-1) \ln n_1^p \end{aligned} \right\} \quad (5)$$

The superscripts (p,q) in eqs.(1-5) assume values 0, 1, and 2. p = 1 or 2 denotes single elements supplied by the bulk phase I or II; p = 0 refers to single elements adsorbed on the

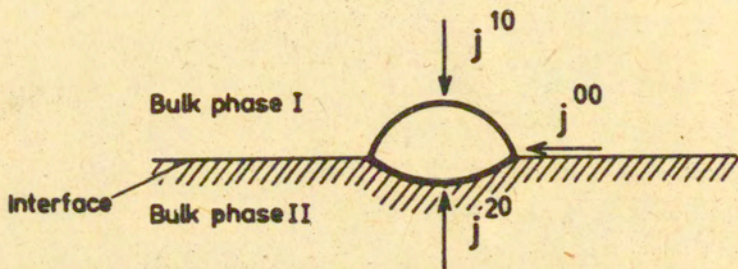


Figure 1. Scheme of a heterogeneous cluster located on the interface between phases I and II. j^{10} , j^{20} and j^{00} - three component fluxes of growth.

interface and transported by surface diffusion along the interface to the circumferential belt on cluster surface. Similarly, $q = 1$ or 2 denotes homogeneous cluster within phase I or II, $q = 0$ - heterogeneous cluster located on the interface between phases I and II (Figure 1).

For any isolated nucleation process j^{pq} , one can find critical transition conditions (temperature, T , fraction of single elements, n_1) beyond which no transition is ever possible

$$(T, n_1)_{crit}^{pq}: \lim_{i \rightarrow \infty} \Delta \tilde{F}_i^{pq} = 0 \Leftrightarrow b^p(T) - kT \ln n_1^p = 0 \quad (6)$$

and steady-state nucleation rate

$$j_{st}^{pq} = n_1^p n_1^q / \sum_{i=1}^{\infty} [\exp(\Delta \tilde{F}_i^{pq}/kT) / k_i^{+pq}] \quad (7)$$

In the former work¹ we have discussed and compared five nucleation mechanisms possible in the vicinity of an interface. Three heterogeneous mechanisms, j^{10} , j^{20} and j^{00} , concern the same cluster located on the interface (cf. Fig. 1) and can be coupled.

How do the above solutions change when an isolated process j^{pq} is replaced by three coupled processes? If j_i denotes coupled flux of clusters of the i -size, n_i is global fraction of clusters "i", and all other characteristics retain their former meanings, the fundamental kinetic equations replacing eqs. (1) result as

$$\begin{aligned} \hat{j}_2 &= (k_1^{+10} n_1^1 + k_1^{+20} n_1^2 + k_1^{+00} n_1^0) n_1^0 - (k_2^{-10} + k_2^{-20} + k_2^{-00}) \hat{n}_2 \\ \hat{j}_i &= (k_{i-1}^{+10} n_1^1 + k_{i-1}^{+20} n_1^2 + k_{i-1}^{+00} n_1^0) \hat{n}_{i-1} - (k_i^{-10} + k_i^{-20} + k_i^{-00}) \hat{n}_i \end{aligned} \quad \left. \vphantom{\hat{j}_2} \right\} (8)$$

for $i > 2$

Introducing "effective" rate constants \hat{k}_{i-1}^+ , \hat{k}_i^-

$$\begin{aligned} \hat{k}_{i-1}^+ &= (k_{i-1}^{+10} n_1^1 + k_{i-1}^{+20} n_1^2 + k_{i-1}^{+00} n_1^0) / n_1^1 \\ \hat{k}_i^- &= k_i^{-10} + k_i^{-20} + k_i^{-00} \end{aligned} \quad \left. \vphantom{\hat{k}_{i-1}^+} \right\} (9)$$

from which follows "effective" driving force for the transition

$$\hat{\delta f}_i = kT \ln(\hat{k}_i^- / \hat{k}_{i-1}^+ n_1^1) \quad (10)$$

one arrives at kinetic equations identical with (1) which yield formal solution for the critical conditions of the transition

$$(T, n_1)_{\text{crit}}: \lim_{i \rightarrow \infty} \hat{\delta f}_i = 0 \quad (11)$$

and steady-state nucleation frequency

$$\hat{j}_{\text{st}} = n_1^1 n_1^0 / \sum_{i=1}^{\infty} [\exp(\hat{\Delta F}_i / kT) / \hat{k}_i^+] \quad (12)$$

Solutions for a coupled process, \hat{j} , are formally identical with those for any isolated process, j^{pq} (eqs.6,7). The difference lies in the nature of the effective driving force, $\hat{\delta f}_i$. Substituting effective rate constants \hat{k}_i^- , \hat{k}_{i-1}^+ from eqs.(9) into eq.(10) one obtains

$$\hat{\delta f}_i = \tilde{\delta f}_i^{10} - kT \ln(1 + K_i^2 \eta + K_i^0 \xi) + kT \ln(1 + K_i^2 + K_i^0) \quad (13)$$

where η , and ξ are reduced concentration ratios multiplied by respective energy terms

$$\eta = (n_1^2/n_1^1) e^{-p(\Delta E/kT)} ; \quad \xi = (n_1^0/n_1^1) \exp(E^1/kT) \quad (14)$$

and K_i^2 , K_i^0 are ratios of dissociation rate constants

$$K_i^2 = k_i^{-20}/k_i^{-10} ; \quad K_i^0 = k_i^{-00}/k_i^{-10} \quad (15)$$

As evident from eq.(13), $\hat{\delta f}_i$, unlike $\tilde{\delta f}_i^{pq}$ for any isolated process, is not a purely thermodynamic characteristic, but depends on the mobility of single elements in various phases, as characterized by the ratios K_i^2 and K_i^0 .

K_i^2 and K_i^0 are functions of cluster size, i. K_i^2 , comparing dissociation rates in two different bulk phases (II vs. I)

$$K_i^2 = \frac{\text{const. exp}(-\varepsilon^2/kT)\varphi^{20}i^{\frac{2}{3}} \text{exp}(y_2 \delta f_i^{20}/kT)}{\text{const. exp}(-\varepsilon^1/kT)\varphi^{10}i^{\frac{1}{3}} \text{exp}(y_1 \delta f_i^{10}/kT)} =$$

$$= K_0^2 \text{exp}(-y_2 \Delta E/kT) \text{exp}[(y_2 - y_1)\delta f_i^{10}/kT] \quad (16)$$

where the characteristic functions $y_1(\delta f_i^{10})$ and $y_2(\delta f_i^{20})$ determine cluster size at which the potential barrier for dissociation switches from transition-independent, into a transition-dependent form (cf.ref.⁴)

$$y_1 = \begin{cases} 1 & \text{for } \delta f_i^{10} < 0, \text{ or } i > i_0^{*10} \\ 0 & \text{for } \delta f_i^{10} \geq 0, \text{ or } i \leq i_0^{*10} \end{cases} \quad (17)$$

$$y_2 = \begin{cases} 1 & \text{for } \delta f_i^{20} < 0, \text{ or } i > i_0^{*20} \\ 0 & \text{for } \delta f_i^{20} \geq 0, \text{ or } i \leq i_0^{*20} \end{cases} \quad (18)$$

In eq.(16) both compared processes (j^{20} and j^{10}) are based on surface-impingement growth and kinetic functions, $\varphi_i^{10}, \varphi_i^{20}$ are both proportional to $i^{\frac{2}{3}}$. In the other ratio, K_1^0 , surface-diffusion-controlled process, j^{00} , with peripheral growth proportional to $i^{\frac{1}{3}}$ is compared with a bulk-diffusion-controlled process, j^{10} , whose frequency is proportional to $i^{\frac{2}{3}}$. Consequently, the ratio of dissociation rates

$$\begin{aligned}
 K_1^0 &= \frac{\text{const. exp}(-\epsilon^0/kT) \varphi^{00} i^{\frac{3}{2}} \exp(y_0 \delta f_1^{00}/kT)}{\text{const. exp}(-\epsilon^1/kT) \varphi^{10} i^{\frac{3}{2}} \exp(y_1 \delta f_1^{10}/kT)} = \\
 &= K_0^0 i^{-\frac{1}{2}} \exp(-y_0 E^1/kT) \exp[(y_0 - y_1) \delta f_1^{10}/kT] \quad (19)
 \end{aligned}$$

is a strongly decreasing function of i . The characteristic function is

$$y_0(\delta f_1^{00}) = \begin{cases} 1 & \text{for } \delta f_1^{00} < 0, \text{ or } i > i_0^{*00} \\ 0 & \text{for } \delta f_1^{00} > 0, \text{ or } i \leq i_0^{*00} \end{cases} \quad (20)$$

In eqs.(17,18,20) a^q and b^p denote surface, and bulk energy coefficients for individual nucleation mechanisms described in ref.¹. In this paper we are interested in heterogeneous clusters ($q=0$) and bulk energy densities for three considered processes, viz.

$$\begin{aligned}
 b^1 & \quad \text{for } j^{10}; \quad i_0^{*10} = -(2a^0/3b^1)^3 \\
 b^2 = b^1 - \Delta E & \quad \text{for } j^{20}; \quad i_0^{*20} = -(2a^0/3b^2)^3 \\
 b^0 = b^1 - E^1 & \quad \text{for } j^{00}; \quad i_0^{*00} = -(2a^0/3b^0)^3
 \end{aligned} \quad (21)$$

The characteristic parameters of the coupled process, K_1^2 and K_1^0 , assume different values in various ranges of cluster size, i , dependently on the relative energies E^1 and ΔE . We

Table I.
Parameters of coupled heterogeneous nucleation in various ranges of cluster size i .

	Case 1. $\Delta E < E^1 < 0$ K_i^2/K_0^2 K_i^0/K_0^0 $i^{-\frac{1}{3}}$	Case 11. $\Delta E > E^1 > 0$ K_i^2/K_0^2 K_i^0/K_0^0 $i^{-\frac{1}{3}}$	Case 111. $\Delta E = 0$; $E^1 < 0$ K_i^2/K_0^2 K_i^0/K_0^0 $i^{-\frac{1}{3}}$
First range	$i < i_0^{*10}$	$i < i_0^{*20}$	$i < i_0^{*10}$
	1	1	1
Second range	$i_0^{*10} < i < i_0^{*00}$	$i_0^{*20} < i < i_0^{*00}$	$i_0^{*10} < i < i_0^{*00}$
	$e^{-\delta f_i^{10}/kT}$	$e^{-(\Delta E - \delta f_i^{10})/kT}$	$e^{-\delta f_i^{10}/kT}$
Third range	$i_0^{*00} < i < i_0^{*20}$	$i_0^{*00} < i < i_0^{*10}$	$i > i_0^{*00}$
	$e^{-\delta f_i^{10}/kT}$ $e^{-E^1/kT}$	$e^{-(\Delta E - \delta f_i^{10})/kT}$ $e^{-(E^1 - \delta f_i^{10})/kT}$	1 $e^{-E^1/kT}$
Fourth range	$i > i_0^{*20}$	$i > i_0^{*10}$	
	$e^{-\Delta E/kT}$ $e^{-E^1/kT}$	$e^{-\Delta E/kT}$ $e^{-E^1/kT}$	1 $e^{-E^1/kT}$
Adsorption rate ratio C/C_0	$e^{-E^1/kT}$	$e^{E^2/kT}$	1

will consider three special situations which seem to cover most physically sensible situations.

- i. $\Delta E < 0$; $E^1 < 0$; $|E^1| < |\Delta E|$
- ii. $\Delta E > 0$; $E^1 > 0$; $|E^1| < |\Delta E|$
- iii. $\Delta E = 0$; $E^1 < 0$

In both cases i. and ii., energy at the interface is considered intermediate between that in phases I and II, either smaller (case i.), or greater (case ii.) than in phase I. Case iii. refers to two phases with the same energy separated by defective interface with reduced energy ($E^1 < 0$). Table I presents relations between critical cluster sizes $i_0^{*p0} = -(2a^0/3b^p)^3$ which determine characteristic functions y_1, y_2, y_0 , the resulting ratios K_1^2, K_1^0 in various cluster size ranges, and the ratio of adsorption rates from phase II and from phase I, $C = C_2/C_1$ to be discussed below. As evident from Table I, in the range of very small i , K_1^2 and K_1^0 in all cases reduce to forms independent of any transition energy δf_i^{pq}

$$\begin{array}{l}
 K_1^2 = K_0^2 \\
 \text{at small } i: \\
 K_1^0 = K_0 i^{-\frac{1}{3}}
 \end{array}
 \left. \vphantom{\begin{array}{l} K_1^2 = K_0^2 \\ K_1^0 = K_0 i^{-\frac{1}{3}} \end{array}} \right\} \quad (22a)$$

and in the range of high i are controlled by the respective energy difference between phase I and other phases

$$K_{\infty}^2 = K_0^2 \exp(-\Delta E/kT)$$

at large i :

$$K_{\infty}^0 = K_0^0 i^{-\frac{1}{2}} \exp(-E^1/kT) \xrightarrow{i \rightarrow \infty} 0 \quad \} \quad (22b)$$

Concentration of single elements in various phases (n_1^1 , n_1^2 , n_1^0) and the related parameters η , ξ , are not independent but result from additional balance conditions to be discussed below.

PARTITION OF SINGLE ELEMENTS AMONG THE BULK PHASES AND THE INTERFACE

Fractions of single elements in individual regions, n_1^p must satisfy the equations of conservation

$$\begin{aligned} \frac{dn_1^1}{dt} + j_a^1 + \sum_2^{\infty} j_i^{10} &= j_{ex}^1 && \text{for bulk phase I} \\ \frac{dn_1^2}{dt} + j_a^2 + \sum_2^{\infty} j_i^{20} &= j_{ex}^2 && \text{for bulk phase II} \\ \frac{dn_1^0}{dt} - j_a^1 - j_a^2 + \sum_2^{\infty} j_i^{00} &= j_{ex}^0 && \text{for the interface} \\ j_a^1 + j_a^2 + j_a^0 &= 0 && \text{adsorption balance} \end{aligned} \quad (23)$$

j_a^1 and j_a^2 are net fluxes of adsorption on the interface from bulk phase I and II, respectively, and j_{ex}^1 , j_{ex}^2 , j_{ex}^0 are fluxes of single elements supplied from outside if steady-state processes are to be realized. $\sum j_i^{10}$, $\sum j_i^{20}$ and $\sum j_i^{00}$ denote sums of nucleation frequencies according to various mechanisms which account for consumption of single elements,

respectively, in regions "1", "2" and "0". The adsorption fluxes for a monomolecular layer can be written in the form

$$j_a^1 = C_1 [n_1^1(1 - n_1^0) e^{-E^1/kT} - n_1^0(1 - n_1^1)] = C_1 n_1^0 [1/\xi - 1/\xi_0] \quad (24)$$

$$j_a^2 = C_2 [n_1^2(1 - n_1^0) e^{-E^2/kT} - n_1^0(1 - n_1^2)] = C_2 n_1^0 [\eta/\xi - \eta_0/\xi_0]$$

E^1 and E^2 denote energies of adsorption on the interface from bulk phases I and II. Adsorption rate constants, C_1 , C_2 are controlled by the same fundamental frequency, and the same activation energies (self-diffusion barriers) as the respective reaction rate constants in phase I (k_i^{-1q} , k_i^{+1q}) or phase II (k_i^{-2q} , k_i^{+2q}). C_1 and C_2 depend on the adsorption energies E^1 , E^2 in the same way as do reaction rates k_i^{-pq} on the transition energies δf_i^{pq}

$$C_1 = \text{const.} \exp(-\epsilon^1/kT) \exp(z_1 E^1/kT)$$

$$C_2 = \text{const.} \exp(-\epsilon^2/kT) \exp(z_2 E^2/kT) \quad (25)$$

$$C = C_2/C_1 = C_0 \exp[(z_2 E^2 - z_1 E^1)/kT]$$

where the characteristic functions (cf.ref.⁴) read

$$z_1(E^1) = \begin{cases} 0 & \text{for } E^1 > 0 \\ 1 & \text{for } E^1 < 0 \end{cases}$$

$$z_2(E^2) = \begin{cases} 0 & \text{for } E^2 > 0 \\ 1 & \text{for } E^2 < 0 \end{cases} \quad (26)$$

In the conditions of thermodynamic equilibrium, $dn_1^p/dt = 0$, $j_a^p = 0$, $j_{ex}^p = 0$ in all three regions, and equations (23) reduce to

$$j_a^1 = j_a^2 = 0 \quad (27)$$

which yields relative equilibrium concentrations of single elements in regions "1", "2" and "0":

$$\xi = (n_1^0/n_1^1) \exp(E^1/kT) = [1 - n_1^1 + n_1^1 \exp(-E^1/kT)]^{-1} = \xi_0 \quad (28)$$

$$\eta = (n_1^2/n_1^1) \exp(\Delta E/kT) = [1 - n_1^1 + n_1^1 \exp(-\Delta E/kT)]^{-1} = \eta_0$$

$\Delta E = E^1 - E^2 = F_1^2 - F_1^1 = b^1 - b^2$ is the difference between free energies of a single, uncombined element in phases II and I. Eqs. (28) provide an example of a Langmuir adsorption isotherm.

Another solution of eqs. (23) which will appear useful for our further considerations, is one corresponding to circulation of single elements between phases I and II, i.e. for $dn_1^1/dt = dn_1^2/dt = 0$, $j_{ex}^1 = j_{ex}^2 = 0$, and $\Sigma j_i^{10} + \Sigma j_i^{20} = 0$. These conditions yield

$$j_a^1 + j_a^2 = 0 \quad (29)$$

and the following relation between concentrations in phase II and on the interface

$$\xi/\xi_0 = (1 + C\eta)/(1 + C\eta_0) \quad (30)$$

CRITICAL CONDITIONS FOR COUPLED NUCLEATION

Formal application of eq.(11) to the effective driving force $\widehat{\delta f}_i$ derived for the coupled process, \widehat{j} (eq.13), indicates conditions in which the total flux of clusters $\widehat{j}_i = j_i^{10} + j_i^{20} + j_i^{00}$ disappears, and a convergent, Boltzmann-type global distribution of cluster sizes, \widehat{n}_i , is established. Requiring that

$$\lim_{i \rightarrow \infty} [\widehat{\delta f}_i^{10} - kT \ln(1 + K_i^2 \eta + K_i^0 \xi) + kT \ln(1 + K_i^2 + K_i^0)] = 0 \quad (31)$$

one realizes that terms with K_i^0 disappear, K_i^2 reduces to its asymptotic form (eqs.22b), and disappears surface energy term ($\frac{2}{3} a i^{-\frac{1}{3}}$) in $\widehat{\delta f}_i^{10}$. Consequently, the condition of zero global flux ($\widehat{j}_i = 0$) results, after simple rearrangements, in the form

$$1 + K_0^2 \exp(-\Delta E/k\widehat{T})\widehat{\eta} = [1 + K_0^2 \exp(-\Delta E/k\widehat{T})] \exp[(b^1 - kT \ln n_i^1)/k\widehat{T}] = [1 + K_0^2 \exp(-\Delta E/k\widehat{T})] \exp[\Delta h(\widehat{T} - T_C^1)/kT \widehat{T}_C^1] \quad (32)$$

where Δh is heat of transition for the reference mechanism, j_i^{10} , and T_C^1 is equilibrium temperature for the isolated process j_i^{10} . Eq.(32) provides one equation for determination of two (or three) conditions at which the global flux disappears: temperature, \widehat{T} , concentration in phase II, $\widehat{\eta}$, and concentration on the interface, $\widehat{\xi}$. It is evident from eq.(32) that the critical temperature, \widehat{T} is contained between two asymptotic limits. When $K_0^2 = 0$ (no mobility in, and no supply of single

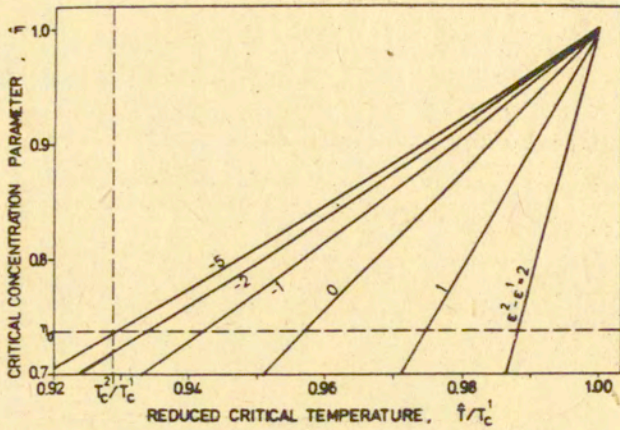


Figure 2. Relation between the critical temperature, \hat{T} , and critical value of the concentration parameter, $\hat{\eta}$ for different mobility ratios (cf. eq. 32) $\Delta E/kT_c^1 = -0.5$.

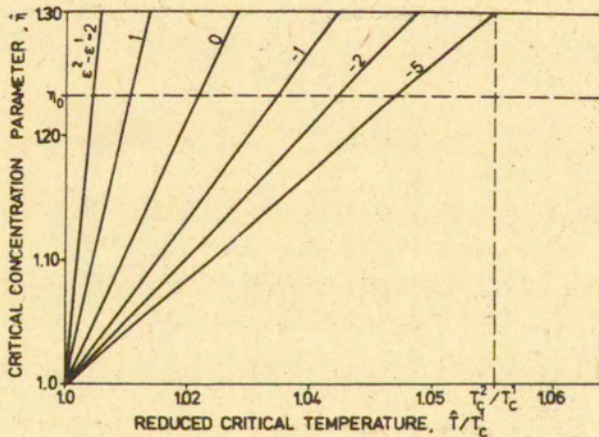


Figure 3. Relation between the critical temperature, \hat{T} , and critical value of the concentration parameter, $\hat{\eta}$. $\Delta E/kT_c^1 = +0.5$.

elements from, phase II)

$$K_0^2 = 0 \implies \hat{T} = T_c^1 \quad (32a)$$

the critical temperature reduces to equilibrium temperature for isolated process j^{10} . On the other hand, when $K_0^2 \rightarrow \infty$ (no mobility in phase I):

$$K_0^2 \rightarrow \infty \implies \hat{\eta} = \exp[\Delta h(\hat{T} - T_c^1)/k\hat{T} T_c^1] \iff \hat{T} = T_c^2 \quad (32b)$$

and the critical temperature \hat{T} assumes the limit for the isolated process j^{20} . Figures 2 and 3 present relations between critical temperature \hat{T} and critical concentration parameter $\hat{\eta}$ for various transport energy differences, $\Delta \varepsilon/kT_c^1$, and two free energy differences: $\Delta E/kT_c^1 = -0.5$, $E^1/kT_c^1 = -0.25$ (case i.), and $\Delta E/kT_c^1 = 0.5$, $E^1/kT_c^1 = 0.25$ (case ii.). For case iii. ($\Delta E = 0$) all critical temperatures converge

$$\Delta E = 0 : \hat{T} = T_c^1 = T_c^2 ; \hat{\eta} = 1 \quad (32c)$$

To find the critical conditions for zero global flux (\hat{T} , $\hat{\eta}$, $\hat{\xi}$) one has to solve simultaneously eq.(32) with eqs.(23) putting $dn_i^p/dt = 0$, $j_{ex}^p = 0$ for $p = 0, 1, 2$.

Although the global flux $\hat{j}_i = j_i^{10} + j_i^{20} + j_i^{00}$ disappears, separately j_i^{10} , j_i^{20} , and j_i^{00} are functions of cluster size, i . Generally, the kinetic equations (8) yield for three nucleation fluxes

$$\begin{aligned}
 j_i^{10} &= k_i^{-10} \hat{n}_i \frac{K_i^2(1-\eta) + K_i^0(1-\xi)}{1 + K_i^2\eta + K_i^0\xi} + \hat{j}_{st}/(1 + K_i^2\eta + K_i^0\xi) \\
 j_i^{20} &= k_i^{-10} \hat{n}_i \frac{K_i^2[\eta - 1 + K_i^0(\eta - \xi)]}{1 + K_i^2\eta + K_i^0\xi} + \hat{j}_{st} K_i^2\eta / (1 + K_i^2\eta + K_i^0\xi) \quad (33) \\
 j_i^{00} &= k_i^{-10} \hat{n}_i \frac{K_i^0[\xi - 1 + K_i^2(\xi - \eta)]}{1 + K_i^2\eta + K_i^0\xi} + \hat{j}_{st} K_i^0\xi / (1 + K_i^2\eta + K_i^0\xi)
 \end{aligned}$$

It is evident that first i -dependent parts compensate to zero, while the second parts sum to the constant, steady-state global flux \hat{j}_{st} . \hat{n}_i in eqs.(33) denotes global distribution of cluster sizes. Eqs.(33) hold true for any steady-state, or zero-flux conditions. To find critical conditions of coupled nucleation, we must put $\hat{j}_{st} = 0$, and assume reduced form of the distribution function \hat{n}_i

$$\hat{j}_{st} = 0 \quad : \quad \hat{n}_i = n_i^0 \exp(-\hat{F}_i/kT) \quad (34)$$

Equations (23), (24) and (33) are strongly coupled, and general solutions are difficult to obtain. Instead, we will solve several special cases for which decoupling is possible, and discuss qualitatively more general cases.

1. Zero Surface Mobility on the Interface, $K_i^0 = 0$.

Putting $K_i^0 = 0$ we obtain from eqs.(33) $j_i^{00} = 0$, and from eq.(23.3)

$$j_a^1 + j_a^2 = 0$$

which yields relation between ξ and η indicated in eq.(30). At the same time, eq.(23.1) yields

$$C_1(\xi_0/\xi - 1) + \xi_0 \sum k_i^{-20} (\hat{n}_i/n_1^0) (1 + K_i^2 \eta)^{-1} (1 - \eta) = 0 \quad (35)$$

Eqs.(30), (32) and (35) yield a single equation for the critical temperature \hat{T}

$$\frac{1 + K_\infty^2 \eta_0 - (1 + K_\infty^2) \exp(B^1/k\hat{T})}{1 - (C/K_\infty^2)[1 - (1 + K_\infty^2) \exp(B^1/k\hat{T})]} + \xi_0 (1 + K_\infty^2) [1 - \exp(B^1/k\hat{T})] \sum_{i=2}^{\infty} \frac{(k_i^{-20}/C_2) \exp(-\hat{\Delta F}_i/k\hat{T})}{1 - (K_i^2/K_\infty^2)[1 - (1 + K_\infty^2) \exp(B^1/k\hat{T})]} = 0 \quad (36)$$

where $B^1/k\hat{T} = \Delta h(\hat{T} - T_c^1)/k\hat{T} T_c^1$.

For numerical evaluation of eq.(36) we have made the following simplifications

$$K_i^2 = K_\infty^2 = \exp[-(\varepsilon^2 - \varepsilon^1)/kT] \exp(-\Delta E/kT) ;$$

$$k_i^{-20} = \text{const.} \exp(-\varepsilon^2/kT) i^{\frac{3}{2}}$$

which reduce eq.(36) to the form

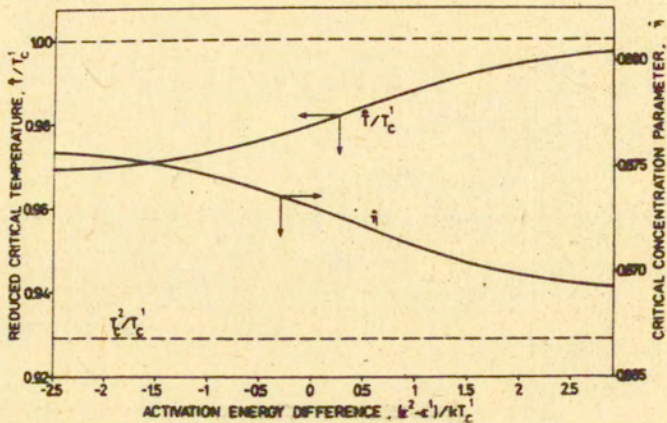


Figure 4. Critical temperature, \hat{T} , and critical concentration parameter, $\hat{\eta}$ for the coupled process, plotted vs. reduced difference of transport energies, $\Delta\epsilon/kT_c^1$. $\Delta E/kT_c^1 = -0.5$, $E^1/kT_c^1 = -0.25$, $a^0/kT_c^1 = 2$, $\Delta h/kT_c^1 = 4$, $n_1^1 = 0.5$, $K_1^0 = 0$.

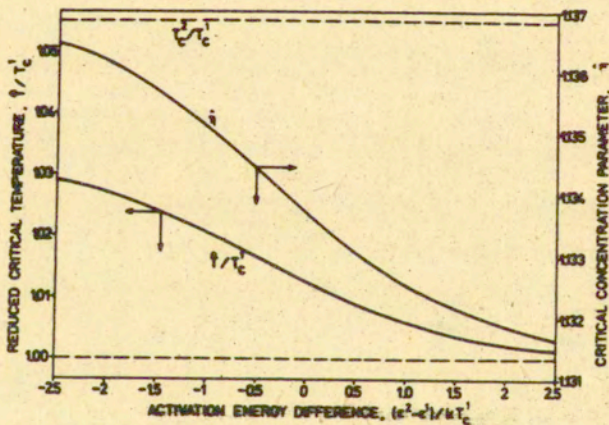


Figure 5. Critical temperature, T , and critical concentration parameter, $\hat{\eta}$ of the coupled process, vs. reduced difference of transport energies, $\Delta\epsilon/kT_c^1$. $\Delta E/kT_c^1 = 0.5$, $E^1/kT_c^1 = 0.25$. Other parameters as in Figure 4.

$$\frac{1 + K_{\infty}^2 \eta_0 - (1 + K_{\infty}^2) \exp(B^1/k\hat{T})}{1 - \alpha [1 - (1 + K_{\infty}^2) \exp(B^1/k\hat{T})]} + \frac{\beta \xi_0 (1 + K_{\infty}^2) [1 - \exp(B^1/k\hat{T})]}{(1 + K_{\infty}^2) \exp(B^1/k\hat{T})} \times$$

$$\times \sum_{i=2}^{\infty} i^{\frac{2}{3}} \exp[-a(i^{\frac{2}{3}} - 1)/k\hat{T}] = 0 \quad (36a)$$

α and β depend on the adsorption energies E^1 , E^2 , and amount to

$$\alpha = \begin{cases} \exp(-E^2/kT) & \text{for } E^1 < 0, E^2 > 0 \quad (\text{case i.}) \\ \exp(E^1/kT) & \text{for } E^1 > 0, E^2 < 0 \quad (\text{case ii.}) \end{cases} \quad (37)$$

$$\beta = \begin{cases} 1 & \text{for } E^2 > 0 \quad (\text{case i.}) \\ \exp(-E^2/kT) & \text{for } E^2 < 0 \quad (\text{case ii.}) \end{cases} \quad (38)$$

Figures 4 and 5 present solutions of eqs.(32) and (36a) for critical temperature \hat{T} and critical concentration parameter $\hat{\eta}$, plotted vs. transport energy difference $\Delta\varepsilon = \varepsilon^2 - \varepsilon^1$, for two values of $\Delta E = \mp 0.5 kT^1$, $E^1 = \Delta E/2$. It is evident that the resulting critical temperature for the coupled process changes from T_c^1 (isolated process j^{10}) to T_c^2 (isolated process j^{20}). At $\Delta E < 0$, T_c^2 being lower than T_c^1 , the critical temperature \hat{T} monotonically increases with $\Delta\varepsilon$ (Figure 4.); at $\Delta E > 0$, T_c^2 is higher than T_c^1 , and \hat{T} decreases with increasing $\Delta\varepsilon$ (Figure 5.). Critical concentration parameter $\hat{\eta}$ in both cases decreases with increasing $\Delta\varepsilon$, what reflects "pumping" effect of reduced mobility in phase I (negative $\Delta\varepsilon$). Naturally,

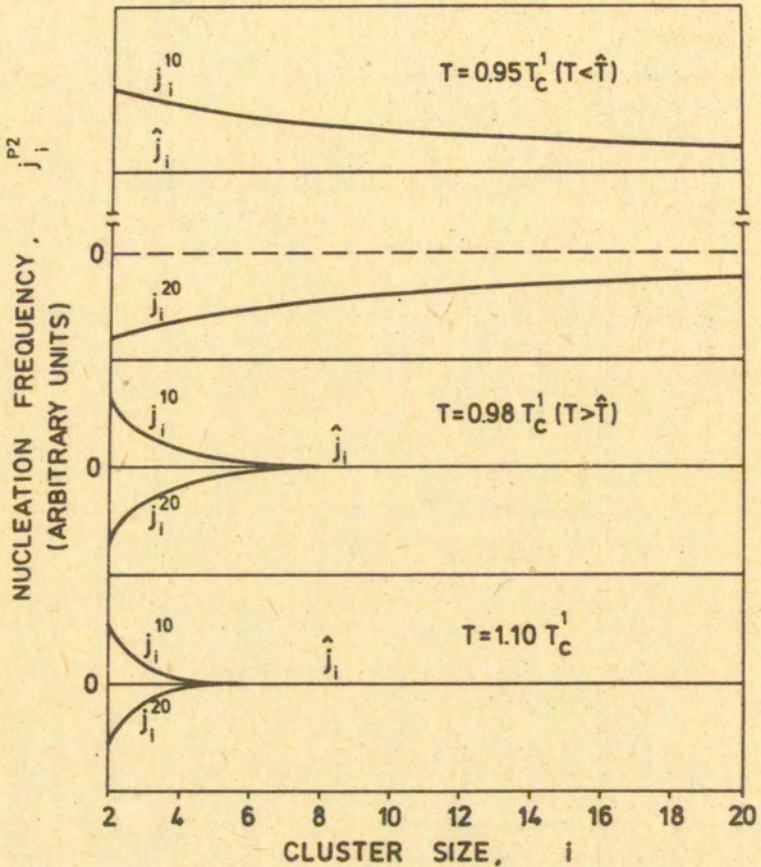


Figure 6. Size-dependent component fluxes, j_i^{10} , and j_i^{20} for a coupled process at different temperatures

- a. $T/T_C^1 = 0.95$; $\hat{T} < T$
- b. $T/T_C^1 = 0.98$; $\hat{T} < T < T_C^1$
- c. $T/T_C^1 = 1.10$

$\Delta E/kT_C^1 = -0.5$, $E^1/kT_C^1 = -0.25$, $\Delta \epsilon = 0$, $K_i^0 = 0$.
Other parameters as in Figures 4 and 5.

critical $\hat{\eta}$, like equilibrium values η_0 , are smaller than unity at $\Delta E < 0$ (Fig.4.) and larger than unity at $\Delta E > 0$ (Fig.5.).

Figure 6 shows example i-dependent component fluxes, j_i^{10} , j_i^{20} , for a coupled nucleation process at three different temperatures. The fluxes have been calculated from eqs.(33) at $K_i^0 = 0$, $\Delta E = -0.5 kT_c^1$ and $\Delta \varepsilon = 0$. Since energy difference ΔE is negative, the critical temperatures for isolated processes (T_c^1 , T_c^2) and for the coupled process (T) are ordered as follows

$$T_c^2 < T < T_c^1 ; \quad \text{for the example considered:}$$

$$T_c^2 = 0.9219 T_c^1 \quad \hat{T} = 0.97976 T_c^1$$

At a temperature lower than the critical temperature \hat{T} , but higher than T_c^2 ($T/T_c^1 = 0.95$) positive contribution of the component with higher critical temperature, j^{10} , is only partially compensated by negative component j^{20} , to produce a positive, steady-state flux $\hat{j}_i = j_i^{10} + j_i^{20} = \hat{j}_{st}$ (Figure 6a). When T is higher than \hat{T} , but lower than the critical temperature for isolated process j^{10} ($T/T_c^1 = 0.98$) the total flux \hat{j}_i disappears, and positive j_i^{10} are exactly compensated by negative j_i^{20} (Fig.6b). Non-zero component fluxes (positive j_i^{10} and negative j_i^{20}) appear at any temperatures above \hat{T} , and only asymptotically tend to zero at either $T \rightarrow \infty$, or $i \rightarrow \infty$. This means that no thermodynamic equilibrium can be reached.

Analysis of eqs.(23) and (33) shows that for $\Delta E > 0$ similar solutions occur, with $\eta > 1$, $T_c^2 > T_c^1$, positive j_i^{20} , and negative j_i^{10} component fluxes.

These two solutions (for $\Delta E < 0$ and $\Delta E > 0$) are illustrated

on a graph of fluxes in Figures 7a and 7b. The net of component fluxes of clusters and adsorption/desorption fluxes of single elements corresponds to the system of eqs.(23) at $dn_i^p/dt = 0$ and $j_{ex}^p = 0$. Naturally, the system of fluxes satisfies Kirchhoff rules.

2. Thermodynamically Equivalent Bulk Phases, $\Delta E = 0$.

Assuming that energy of a single element is identical in both bulk phases ($\Delta E = 0$), with mobility equal, or different ($K_i^2 \neq 1$) we find immediately that the critical temperature for an isolated process, j^{20} , reduces to that for isolated process j^{10}

$$\Delta E = 0 ; \quad \eta_0 = 1 ; \quad T_c^2 = T_c^1$$

One might guess that for $\Delta E = 0$ also in the coupled process the concentration parameter η should be equal to unity (i.e. $n_1^2 = n_1^1$). Substituting $\eta = 1$ to eqs.(23) and (33) one finds that it does present an exact solution to the problem, provided that the ratio of adsorption rate constants $C = (C_2/C_1)$ is equal to the ratio of dissociation rate constants $K_i^2 = k_i^{-20}/k_i^{-10}$. Inspecting eqs.(16),(25) and Table I one finds that for $\Delta E = 0$, C reduces to the ratio of mobilities $C = \exp[-(\epsilon^2 - \epsilon^1)/kT]$, and K_i^2 for all i reduces to the same ratio, multiplied by the ratio of kinetic factors $K_i^2 = \exp[-(\epsilon^2 - \epsilon^1)/kT](\phi^{20}/\phi^{10})$. For $\eta = 1$ and $\Delta E = 0$ it is natural to expect that the double-lens cluster is symmetrical, and $\phi^{20}/\phi^{10} = 1$. Thus the solutions of the symmetrical problem are

$$\begin{aligned} \eta &= \eta_0 = 1 ; & \hat{T} &= T_c^1 \\ j_i^{10} &= k_i^{-10} \hat{n}_i K_i^0 (1 - \xi) / (1 + K_i^2 + K_i^0 \xi) \\ j_i^{20} &= K_i^2 j_i^{10} \\ j_i^{00} &= -(1 + K_i^2) j_i^{10} \\ j_a^2 &= K_i^2 ; & j_a^1 &= K_i^2 C_1 (1/\xi - 1/\xi_0) \end{aligned} \quad (39)$$

It is evident that at negative adsorption energy, $E^1 < 0$, the solution of eq.(23.1) provides $\xi_0 < \xi < 1$, positive (but not necessarily identical) fluxes j_i^{10} and j_i^{20} , compensated by a negative flux j_i^{00} , and negative adsorption fluxes j_a^1, j_a^2 . At positive adsorption energy $E^1 > 0$, $1 < \xi_0 < \xi$, j_i^{10} and j_i^{20} are negative, j_i^{00} , j_a^1 , and j_a^2 positive. Intuitively, it may seem strange that negative adsorption energy leads to desorption in dynamic conditions of self-compensating fluxes, and vice versa. As shown in the first part of this work¹, negative adsorption energy discriminates, rather than stimulates nucleation on the interface and thus provides excess adsorbed kinetic elements which must be disposed of via desorption. The graphs of fluxes for $\Delta E = 0$, are shown in Figures 7c and 7d, respectively for $E^1 < 0$ and $E^1 > 0$.

3. Zero Mobility in Phase II, $K_1^2 = 0$.

Assuming zero mobility in phase II and, consequently, absence of effective reactions involving single elements from that phase, (e.g. in a system gas-solid, or liquid-solid) one

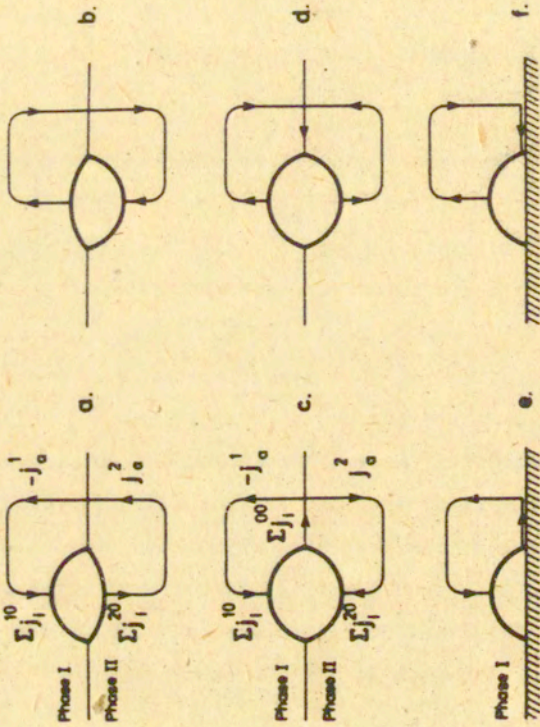


Figure 7. Graphs representing fluxes of single elements in the conditions of internal compensation ($\hat{T} > T$, $\hat{j}_i = 0$).

- a. $K_i^0 = 0$, $\Delta E < 0$; b. $K_i^0 = 0$, $\Delta E > 0$; c. $\Delta E = 0$, $E^1 < 0$;
 d. $\Delta E = 0$, $E^1 > 0$; e. $K_i^2 = 0$, $E^1 < 0$; f. $K_i^2 = 0$, $E^1 > 0$.

finds immediately from eq.(32)

$$\hat{T} = -T_c^1$$

and the following fluxes

$$\begin{aligned} j_i^{10} &= k_i^{-10} \hat{n}_i K_i^0 (1 - \xi) / (1 + K_i^0 \xi) \\ j_i^{20} &= 0 \\ j_i^{00} &= -j_i^{10} \\ j_a^1 &= C_1 (1/\xi - 1/\xi_0) = -\sum_i j_i^{10} \\ j_a^2 &= 0 \end{aligned} \tag{40}$$

Like in the preceding case, negative E^1 yields solutions in the range $\xi_0 < \xi < 1$, positive flux j^{10} , and negative fluxes j^{00} and j_a^1 . Positive E^1 , associated with ξ from the range $1 < \xi_0 < \xi_1$, yields negative j^{10} , positive j^{00} , and positive adsorption flux j_a^1 . These examples are illustrated in graphs presented in Figures 7e, 7f.

4. All Regions Thermodynamically Equivalent, $\Delta E = E^1 = 0$.

We will consider an apparently trivial case when all regions are thermodynamically equivalent (energy of a single element is identical in bulk phases I, II and on the interface), but mobilities in individual regions are different ($K_i^2 \neq 1, K_i^0 \neq 1$). It can be shown, that such a

problem provides an obvious solution for critical conditions

$$\Delta E = E^1 = 0 ; \quad \eta = \eta_0 = 1 ; \quad \xi = \xi_0 = 1 ; \quad T_c^2 = T_c^0 = \hat{T} = T_c^1$$

and all fluxes from eqs.(33) reduce to fractions of the global steady-state flux, \hat{j}_{st} .

$$\begin{aligned} j_i^{10} &= \hat{j}_{st} / (1 + K_i^2 + K_i^0) \\ j_i^{20} &= K_i^2 \hat{j}_{st} / (1 + K_i^2 + K_i^0) \\ j_i^{00} &= K_i^0 \hat{j}_{st} / (1 + K_i^2 + K_i^0) \end{aligned} \quad (41)$$

These solutions predict zero fluxes (equilibrium) at $T \geq \hat{T}$ where $\hat{j}_{st} = 0$, and three positive, i -dependent steady-state fluxes at temperatures lower than the critical temperature T . The i -dependence of component fluxes results from i -dependent ratios $K_i^0 \sim i^{-3}$.

5. General Case.

In the most general case, internal compensation of fluxes requires solution of the equations resulting from combination of eqs.(23),(24) and (33) at $\hat{j}_i = 0$, $dn_i^p/dt = 0$, and $j_{ex}^p = 0$, for $p = 1, 2, 0$

$$\begin{aligned} C_1(\xi_0 - \xi) / \xi \xi_0 + \sum_2 k_i^{-10} \hat{n}_i(\xi, \eta) [K_i^2(1 - \eta) + \\ + K_i^0(1 - \xi)] / (1 + K_i^2 \eta + K_i^0 \xi) = 0 \end{aligned} \quad (42)$$

$$\begin{aligned} C_2(\eta \xi_0 - \xi \eta_0) / \xi \xi_0 + \sum_2 k_i^{-10} \hat{n}_i(\xi, \eta) K_i^2 [\eta - 1 + \\ + K_i^0(\eta - \xi)] / (1 + K_i^2 \eta + K_i^0 \xi) = 0 \end{aligned} \quad (43)$$

Solutions, whenever exist, determine direction of fluxes j_i^{10} , j_i^{20} , j_i^{00} and j_a^1 , j_2^2 . In any case, the solutions would admit non-zero component fluxes (dependently on the resultant values of η and ξ) in the entire range of temperatures above \hat{T} . This means that eqs.(42,43) do not admit isothermal thermodynamic equilibrium which requires that all fluxes disappear simultaneously. The critical temperature \hat{T} at which non-zero component fluxes j_i^{10} , j_i^{20} , j_i^{00} compensate to zero total flux \hat{j}_i is determined by eq.(32) discussed above. This temperature depends on the mobilities in all three regions (bulk phases I and II, interface 0) and is controlled by relative mobility parameters, K_1^2 , K_1^0 , and resultant concentrations of single elements in various regions - variables η and ξ . Although K_1^0 and ξ do not appear explicitly in eq.(32) they affect the critical temperature through the solutions of eqs.(42,43) which determine ξ and η .

Figures 7a- 7f present graphs of fluxes of single elements in systems with internal compensation ($\hat{j}_i = 0$) for special cases when decoupling of eqs.(42,43) is possible. A general case would also admit other combinations not indicated in Figure 7.

STEADY STATE, INTERNAL COMPENSATION OF FLUXES, AND THERMODYNAMIC EQUILIBRIUM

In an isolated nucleation process involving only one mechanism, j^{pq} , the system of fluxes of clusters of various sizes can be represented as a single line (Figure 8a). Junctions indicate cluster sizes, i . In such a system there exist only two

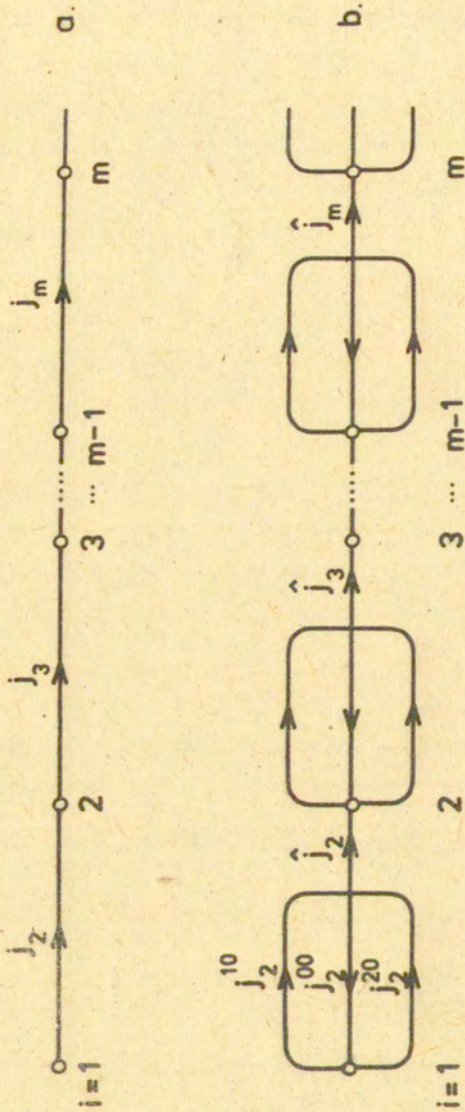


Figure 8. Graphs representing fluxes of clusters of various sizes, i.

a. isolated nucleation mechanism

b. coupled nucleation, composed of three mechanisms

$$\hat{j}_1 = j_1^{10} + j_1^{20} + j_1^{00}$$

Directions of component fluxes correspond to $\Delta E = 0, E^1 < 0$.

time-independent situations:

$$\text{steady-state flux: } j_i = j_{i+1} = j_{st} > 0 \quad \text{at } T < T_c \quad (44a)$$

$$\text{equilibrium: } j_i = 0 \text{ for all } i \quad \text{at } T \geq T_c \quad (44b)$$

Critical temperature, T_c , and concentration of single elements in the system n_{1c} determine conditions when steady state is replaced by equilibrium.

A system of fluxes in a coupled process, admitting three different ways in which an $(i-1)$ -cluster can grow to size "i" corresponds to a graph (Figure 8b) consisting of a chain of loops. Transition from one junction "i" to $(i+1)$ involves a global flux \hat{j}_i , which is a sum of component fluxes j_i^{p0} . $\hat{j}_i = j_i^{10} + j_i^{20} + j_i^{00}$. Directions of component fluxes in Figure 8b correspond to the special case described as $\Delta E = 0, E^1 < 0$ (cf. eqs. 39, Fig. 7c.) but other combinations are possible.

It has been shown in this paper that coupled systems admit two temperature regimes:

$$\text{steady-state global flux: } \hat{j}_i = \hat{j}_{i+1} = \hat{j}_{st} > 0 \quad \text{at } T < \hat{T} \quad (45a)$$

$$\text{with } j_i^{10} \neq j_{i+1}^{10}; \quad j_i^{20} \neq j_{i+1}^{20}; \quad j_i^{00} \neq j_{i+1}^{00}$$

$$\text{internally compensated global flux: } \hat{j}_i = 0 \text{ for all } i \quad \text{at } T \geq \hat{T} \quad (45b)$$

$$\text{with } j_i^{10} \neq j_{i+1}^{10}; \quad j_i^{20} \neq j_{i+1}^{20}; \quad j_i^{00} \neq j_{i+1}^{00}$$

It is important to note that the component fluxes j_i^{10} ,

j_i^{20}, j_i^{00} do not disappear at any finite temperature or any finite cluster size, i .

The steady-state global regime for a coupled process ($T < \hat{T}$) corresponds to steady-state regime for an isolated process, with the difference, that size independent global flux j_i is composed of several i -dependent contributions.

An important difference exists between thermodynamic equilibrium and internally compensated flux, $\hat{j}_i = 0$. It follows from the present work that disappearance of the global flux at $T = \hat{T}$ does not admit zero component fluxes. This means that isothermal thermodynamic equilibrium is not possible in a system of coupled cluster growth processes if individual regions are thermodynamically different ($\Delta E \neq 0$, or $E^1 \neq 0$). One could ask whether a true equilibrium, i.e. $j_i^{10} = j_i^{20} = j_i^{00} = j_i = 0$ would be possible at different temperatures in various regions, say $T^I \neq T^{II} \neq T^0$. The condition for such an equilibrium would require equal Boltzmann-type distributions in various regions, i.e.

$$\begin{aligned} n_1^0 \exp[-\Delta\tilde{F}_1^1(T^I)/kT^I] &= n_1^0 \exp[-\Delta\tilde{F}_1^2(T^{II})/kT^{II}] = \\ &= n_1^0 \exp[-\Delta F_1^0(T^0)/kT^0] \end{aligned} \quad (46)$$

Such distributions, with local temperatures (T^I, T^{II}, T^0) higher than critical temperatures for the corresponding isolated processes

$$T^I > T_c^1; \quad T^{II} \geq T_c^2; \quad T^0 \geq T_c^0$$

would satisfy the requirement of equilibrium

$$j_i^{10}(T^I) = j_i^{20}(T^{II}) = j_i^{00}(T^0) = \hat{j}_i = 0 \quad \text{for all } i$$

We will show that no solution of eq.(46) exists. Free energy of cluster formation, and the corresponding driving force ΔF_i^{pq} is composed of at least two terms with different dependence on cluster size i . In the simplest case,

$$\Delta F_i^{pq}(T) = a^q(i^{\frac{2}{3}} - 1) + [b^p(T^p) - kT^p \ln n_1^p](i - 1) \quad (47)$$

For a heterogeneous process, index $q=0$ determines the same surface energy $a = a^0$ for all growth mechanisms, $p=0,1,2$. Solution of eq.(46) to be valid for any cluster size, "i", is equivalent to requiring simulatenously

$$\begin{aligned} a^0/kT^I &= a^0/kT^{II} = a^0/kT^0 \\ b^1/kT^I - \ln n_1^1 &= b^2/kT^{II} - \ln n_1^2 = b^0/kT^0 - \ln n_1^0 \end{aligned} \quad (48)$$

which obviously cannot be satisfied for different temperatures T^I, T^{II}, T^0 .

The only conclusion which can be drawn from these considerations is that heterogeneous clusters in thermodynamically different phases are thermodynamically unstable. If such a cluster appears on the interface as a result of thermal fluctuations, below the critical temperature \hat{T} it will grow,

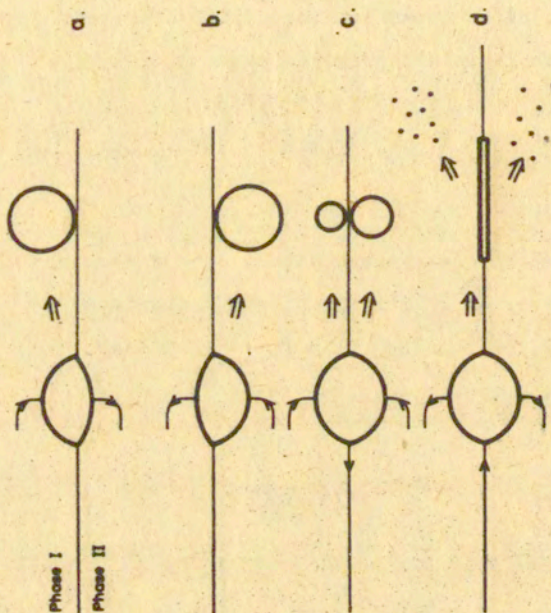


Figure 9. Conversion of heterogeneous clusters with internally compensated fluxes into homogeneous equilibrium clusters (schematic).

- a. $\Delta E < 0$;
- b. $\Delta E > 0$;
- c. $\Delta E = 0$, $E^1 < 0$: different sizes of the resulting spheres correspond to higher mobility in phase II, $K_1^2 > 1$;
- d. $\Delta E = 0$, $E^1 > 0$ - heterogeneous cluster splits into single elements.

accordingly to the rules predicted by the coupled process. Above \hat{T} however, unbalanced growth (growth on one face, melting on the other one) will ultimately eliminate heterogeneous cluster from the interface and convert it into a homogeneous cluster in one of the bulk phases where further growth, and ultimately true equilibrium can be realized.

Special case when energy difference between individual regions are equal to zero, is the only example of an equilibrium heterogeneous cluster which needs not be converted into a homogeneous one. Figure 9 shows how such a conversion proceeds in other cases. If $\Delta E < 0$, what corresponds to positive j_i^{10} , and negative j_i^{20} flux, or at $K_i^2 = 0$ and $E^1 < 0$, heterogeneous cluster will ultimately convert into a homogeneous one in phase I (Figure 9a). Positive ΔE yields, naturally, transformation into homogeneous cluster in phase II (Fig. 9b). At $\Delta E = 0$ and $E^1 < 0$ the resulting homogeneous cluster can appear in both phases (I, and II) and the ratio of mobilities K_i^2 can play some role (Fig. 9c). An interesting case is provided by positive adsorption energy $E^1 > 0$. Bulk fluxes j_i^{10} and j_i^{20} are both negative, and surface-diffusion-controlled growth is stimulated (positive j_i^{00}). Conversion of such a heterogeneous cluster into a cluster in region "0" (monomolecular surface cluster on the interface) does not satisfy the conditions of equilibrium, because such a surface cluster still remains in contact with other phases. In addition to that, surface-impingement-controlled fluxes j_i^{10} , j_i^{20} , proportional to $i^{\frac{2}{3}}$ are of a different measure than peripheral growth according to surface-diffusion-controlled mechanism, j_i^{00} ($\sim i^{\frac{1}{3}}$). Therefore, melting of the cluster according to j_i^{10} and j_i^{20} will be much

faster than additional growth on the surface due to positive j_i^{00} . The consequence of this will be complete disappearance of the heterogeneous cluster, and dispersion of the splitted single elements in phases I and II (Figure 9d).

Conversion of heterogeneous clusters above the critical temperature, \hat{T} , consists in their disappearance from the interface and formation of equivalent clusters within one (or both) bulk phase(s) (Fig.9.). Speaking in terms of distribution functions, coupled distribution $\hat{n}_i = n_i^0 \exp(-\Delta\hat{F}_i/kT)$ will be replaced by equilibrium distribution in phase "q", $n_i^q = n_i^0 \exp(-\Delta\hat{F}_i^{pq}/kT)$, which reduces all fluxes to zero. This process requires some time dependent on the mobility parameters K_0^2 , K_0^0 , and on the superheating above the critical temperature \hat{T} . If the heating temperature, T , lies below equilibrium temperature for one of the component processes, T_c^1 or T_c^2 , the homogeneous cluster removed from the interface will continue to grow as a homogeneous cluster according to the process j^{11} (or j^{22}) (cf. Figures 9a and 9b). Thermodynamic equilibrium in the bulk phase will be established in temperatures higher than T_c^1 (or T_c^2).

The process of equilibration above T_c^1 (or T_c^2) requires some time. This can explain "memory effects" often observed in the crystallization of polymers, and interpreted as due to heterogeneous clusters preserved in the melt above crystal melting temperature, and gradually disappearing with prolonged superheating. This memory depends on the temperature, and time of heating, required for complete conversion of the unstable heterogeneous cluster into an equilibrium, homogeneous one.

KINETICS OF COUPLED NUCLEATION

Although heterogeneous clusters appear to be thermodynamically unstable in temperatures exceeding some critical temperature, coupled cluster growth processes can occur at lower temperatures to produce steady-state flux \hat{j}_{st} . In subcritical conditions, conservation of single elements in all regions requires that external fluxes j_{ex}^1 , j_{ex}^2 , j_{ex}^0 are added to assure non-zero steady-state flux. These external fluxes must satisfy the condition

$$j_{ex}^1 + j_{ex}^2 + j_{ex}^0 = \hat{j}_{st} \quad (49)$$

but no information about their distribution is available. Most simple, though quite arbitrary assumption is to put into eqs. (23)

$$\begin{aligned} j_{ex}^1 &= \Sigma j_i^{10} \\ j_{ex}^2 &= \Sigma j_i^{20} \\ j_{ex}^0 &= \Sigma j_i^{00} \end{aligned} \quad (50)$$

i.e. to compensate consumption of single elements in each region (1,2,0) by appropriate external supply. This converts eqs. (23) into

$$j_a^1 = j_a^2 = 0$$

and yields concentration parameters

$$\xi = \xi_0 ; \quad \eta = \eta_0 \quad (51)$$

Steady-state global flux, \hat{j}_{st} can be obtained from the kinetic equations for a coupled process (eqs.8) in the same form as for any isolated process

$$\hat{j}_{st} = n_1 n_1^0 / \sum_{i=1}^{\infty} [\exp(\hat{\Delta F}_i / kT) / k_i^+] \quad (52)$$

The problem consists in finding the total driving force $\hat{\Delta F}_i$ for the coupled process. By definition

$$\hat{\Delta F}_i = \sum_{i'=2}^i \delta f_{i'} \quad (53)$$

where $\delta f_i = k_i^- / k_{i-1}^+ n_1^1$ is given by eq.(13).

In principle, $\hat{\Delta F}_i$ can be obtained by direct summation of eq.(53) to yield

$$\hat{\Delta F}_i = \hat{\Delta F}_i^{10} - kT \sum_{i'=2}^i \ln \frac{1 + K_{i'}^2 \eta + K_{i'}^0 \xi}{1 + K_{i'}^2 + K_{i'}^0} \quad (54)$$

and the critical cluster size i^* can be found from the equation

$$i^*: \quad \hat{\delta f}_i = 0 \iff \hat{\delta f}_i^{10} - kT \ln \frac{1 + K_i^2 \eta + K_i^0 \xi}{1 + K_i^2 + K_i^0} = 0 \quad (55)$$

Eq.(54) can be evaluated numerically, and used in the exact calculation of the steady-state flux \hat{j}_{st} from eq.(52). Another solution is discussed in Appendix A. Here we will confine ourselves to the approximation valid when mobility on the interface is small compared with each of the mobilities in the bulk phases, i.e. when

$$\left. \begin{aligned} K_i^0 &\ll 1 + K_i^2 \\ \text{and } K_i^0 \xi &\ll 1 + K_i^2 \eta \end{aligned} \right\} \quad (56)$$

which converts eqs.(54-55) into linear forms of K_i^0 , because

$$\ln \frac{1 + K_i^2 \eta + K_i^0 \xi}{1 + K_i^2 + K_i^0} \cong \ln \frac{1 + K_i^2 \eta}{1 + K_i^2} + \frac{K_i^0 [K_i^2 (\xi - \eta) + \xi - 1]}{(1 + K_i^2 \eta)(1 + K_i^2)} \quad (57)$$

In further evaluation of eq.(56a) we will assume K_i^2 , K_i^0 ratios for large i from eq.(22b), i.e. $K_i^2 = K_\infty^2$ independent of i , and $K_i^0 = K_\infty^0 i^{-\frac{1}{2}}$.

This reduces the thermodynamic driving force for the coupled process to the form typical for any isolated process

$$\left. \begin{aligned} \hat{\delta f}_i &= \hat{a} i^{\frac{2}{3}} + \hat{B} \\ \hat{\Delta F}_i &= \hat{a}(i^{\frac{2}{3}} - 1) + \hat{B}(i - 1) \end{aligned} \right\} \quad (58)$$

with the related kinetic characteristics

$$\hat{i}^* = -(2\hat{a}/3\hat{B})^3 \quad (59)$$

$$\hat{\Delta F}^* = \hat{\Delta F}_{\max} = 4(\hat{a})^3/27(\hat{B})^2 - \hat{a} - \hat{B} \quad (60)$$

$$\hat{j}_{st} = \frac{1}{2}(\hat{a}/\pi kT)^{\frac{1}{2}} (\hat{i}^*)^{-\frac{3}{2}} k_{i^*}^+ n_1 n_1^0 \exp(-\hat{\Delta F}^*/kT) \quad (61)$$

$$\begin{aligned} \hat{j}_{st}/j_{st}^{10} &= (\hat{a}/a^0) (1 + K_0^2 n_1^2/n_1^0 + K_0^0 n_1^0 \hat{i}^*^{-\frac{1}{2}}/n_1^0) \times \\ &\times \exp[(\hat{\Delta F}^{*10} - \hat{\Delta F}^*)/kT] \end{aligned} \quad (62)$$

Eqs.(61,62) make use of the approximate evaluation of the semi-infinite sum, suggested by Frenkel⁴

$$\sum_{i=1}^{\infty} [\exp(\hat{\Delta F}_i/kT)/k_i^+] \cong \int_{-\infty}^{+\infty} \exp(\hat{\Delta F}_i/kT) di \cdot \frac{1}{k_{i^*}^+}$$

Substituting to (56a) $K_i^2 = K_0^2 \exp(-\Delta E/kT)$, and $K_i^0 = K_0^0 \exp(-E^1/kT) i^{-\frac{1}{2}}$, one obtains the "effective" parameters in eqs.(57-62)

$$\begin{aligned} \hat{a} &= a^0 - (3kT/2)K_0^0 \exp(-E^1/kT)[K_0^2(\xi - \eta) + \\ &+ (\xi - 1) \exp(\Delta E/kT)] / [(1 + K_0^2 n_1^2/n_1^0)(K_0^2 + \exp(\Delta E/kT))] \end{aligned} \quad (63)$$

$$\hat{B} = B^1 - kT \ln[(1 + K_0^2 n_1^2/n_1^0)/(1 + K_0^2 \exp(-\Delta E/kT))] \quad (64)$$

In the conditions of large mobility in the interface, inequalities (56) are not satisfied and an alternative non-linear approximation described in Appendix A should be used.

It can be seen from eqs.(58) - (62) that coupling of cluster growth mechanisms changes simultaneously the apparent surface energy, \hat{a} , bulk free energy density, \hat{B} , and, consequently, critical cluster size, \hat{i}^* and maximum free energy, $\hat{\Delta F}^*$. In addition to that, in the global nucleation rate \hat{j} there appears the factor $(1 + K_{0n_1}^2/n_1^1 + K_{0n_1}^0 \hat{i}^{*-1/2}/n_1^1)$ accounting for superposition of three nucleation rates effective in growing of a single heterogeneous cluster. This factor naturally increases \hat{j} compared with any single growth mechanism. Changes of the parameters \hat{a} and \hat{B} can lead to an increase, or reduction of the resultant nucleation rate and its temperature dependence.

At unchanged parameters of the reference proces, j^{10} , (a^0 , B^1 , n_1^1 , ϵ^1) kinetics of the coupled nucleation is controlled by four variables: energy differences ΔE and E^1 , which determine concentrations in regions II and 0 (parameters η_0 and ξ_0) and activation energies for transport in regions II and 0 (respectively ϵ^2 and ϵ^0) responsible for the constants K_0^2 and K_0^0 .

When energy difference between phases II and I, ΔE , is negative, $\eta < 1$ and the driving force for the coupled process, \hat{B} , is reduced compared with B^1 for the reference process j^{10} . The reverse is true for positive ΔE , and $\Delta E = 0$ yield unchanged \hat{B} :

$$\text{sign}(\hat{B}/B^1 - 1) = \text{sign}(\Delta E) \quad (65)$$

The change of the apparent surface energy, $(\hat{a} - a^0)$ can be positive, or negative, dependently on the values of ΔE , E^1 , and transport activation energies, ϵ^2 , and ϵ^0 (alternatively

variables η , ξ , K_0^2 , K_0^0). At $\Delta E = 0$, the extra characteristics of the coupled process reduce to:

$$\Delta E = 0: \quad \eta = 1; \quad \hat{B} = B^1; \quad \hat{a} = a^0 - (3kT/2)K_0^0 \times \\ \times \exp(-E^1/kT)(\xi - 1) / [1 + K_0^2 \exp(-\Delta E/kT)] \quad (66)$$

and the sign of the adsorption energy E^1 becomes opposite to that of the difference $(a - a^0)$

$$\text{sign}(a/a^0 - 1) = -\text{sign}(\xi - 1) = -\text{sign}(E^1) \quad (67)$$

Our numerical analysis of coupled nucleation kinetics will be based on the approximations (58 - 64). The approximation evidently fails when \hat{a} from eq.(63) drops to too small a value. In such conditions non-linear approximation from Appendix A is recommended. The following analysis will concern three special groups of conditions classified in the Section PARTITION OF SINGLE ELEMENTS....

group i/ii. assumes that properties of the interface (interaction energy, E^1 , transport energy ϵ^0), is average between those of the bulk phases I and II. This yields

$$\left. \begin{aligned} \Delta E &= 2E^1 \\ \epsilon^2 - \epsilon^1 &= 2(\epsilon^0 - \epsilon^1), \quad \text{or } K_0^2 = (K_0^0)^2 \end{aligned} \right\} \quad (68a)$$

At $\Delta E < 0$ this corresponds to case i., at $\Delta E > 0$ to case ii. discussed above.

group iii. corresponding to case iii. above, assumes two identical bulk phases and an interface with different properties

$$\left. \begin{aligned} \Delta E = 0 ; \quad \epsilon^2 = \epsilon^1 ; \quad K_0^2 = 1 \\ E^1 \neq 0 ; \quad \epsilon^0 \neq \epsilon^1 ; \quad K_0^0 \in (0, \infty) \end{aligned} \right\} \quad (68b)$$

group iv. no mobility in phase II.

$$\left. \begin{aligned} K_0^2 = 0 ; \quad \Delta E \text{ immaterial} \\ E^1 \neq 0 ; \quad \epsilon^0 \neq \epsilon^1 ; \quad K_0^0 \in (0, \infty) \end{aligned} \right\} \quad (68c)$$

Generally, for all groups we have

$$\begin{aligned} \eta = \eta_0 &= [1 - n_1^1 + n_1^1 \exp(-\Delta E/kT)]^{-1} \\ \xi = \xi_0 &= [1 - n_1^1 + n_1^1 \exp(-E^1/kT)]^{-1} \\ K_1^2 = K_\infty^2 &= \exp[-(\epsilon^2 - \epsilon^1)/kT] \exp(-\Delta E/kT) \\ K_1^0 = K_\infty^0 i^{-\frac{1}{3}} &= \exp[-(\epsilon^0 - \epsilon^1)/kT] \exp(-E^1/kT) i^{-\frac{1}{3}} \end{aligned} \quad (69)$$

For each of the three groups, characteristics of the coupled process become functions of two, rather than four, variables: ΔE and $(\epsilon^2 - \epsilon^1)$, for group i/ii; E^1 and $(\epsilon^0 - \epsilon^1)$, for groups iii and iv. For each group we will analyze effective characteristics for coupled nucleation, \hat{a}/a^0 , \hat{B}/B^1 (reduced by

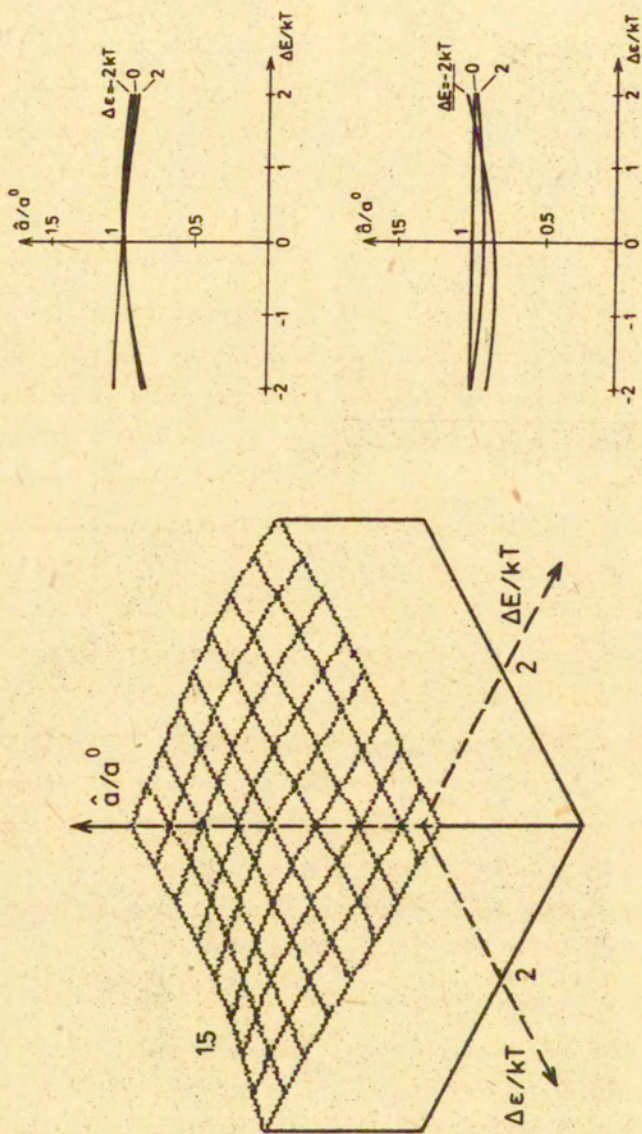


Figure 10. Reduced surface energy density, \hat{a}/a^0 for coupled nucleation. Group i/11, eqs. (68a). a) three-dimensional plot vs. energy difference $\Delta \epsilon$ and transport activation energy difference $\Delta \hat{\epsilon} = \epsilon^2 - \epsilon^1$. b) \hat{a}/a^0 vs. $\Delta \epsilon$ at $\Delta \hat{\epsilon} = \text{constant}$, c) \hat{a}/a^0 vs. $\Delta \hat{\epsilon}$ at $\Delta \epsilon = \text{const}$. Constant parameters indicated.

corresponding characteristics of the reference process, j^{10} , reduced critical cluster size (\hat{i}^*/i_{10}^*), and the reduced steady-state nucleation rates based on Frenkel approximation, \hat{j}_{st}/j_{st}^{10} , $\hat{j}_{st}/\sum_p j_{st}^{p0}$.

Group i/ii. Interface Intermediate Between Two Bulk Phases.

Figures 10 - 12 present reduced characteristics of the coupled process, \hat{a}/a^0 , \hat{B}/B^1 and \hat{i}^*/i_{10}^* as functions of the energy difference between phases I and II, ΔE , and relative mobility parameter ($\epsilon^2 - \epsilon^1$). Although ratios of the effective surface energy \hat{a}/a^0 , and driving force \hat{B}/B^1 always intersect level 1 at $\Delta E = 0$, in other regions they exhibit extrema and assume values higher, or lower than unity. In the range of parameters considered, the critical cluster size \hat{i}^* behaves monotonically, and assumes values larger than unity at $\Delta E < 0$ and smaller than unity at $\Delta E > 0$. This means, that the critical cluster size (and the related maximum driving force $\hat{\Delta F}^*$ which provides potential barrier for nucleation) is higher, and suppresses the coupled process, compared with isolated process controlled by phase I, whenever free energy of phase II is lower than that of phase I ($\Delta E < 0$), and vice versa. This is evident also in Figure 13 which presents the ratio of fluxes \hat{j}_{st}/j_{st}^{10} .

In the vicinity of $\Delta E = 0$, the flux ratio is higher than unity because of the preexponential factor $(1 + K_0^2 n_1^2/n_1^1 + K_0^0 n_1^0 \hat{i}^{*-3/2}/n_1^1)$, but for well negative ΔE the resultant nucleation rate is reduced below that for an isolated process j_{st}^{10} , and in the range of positive

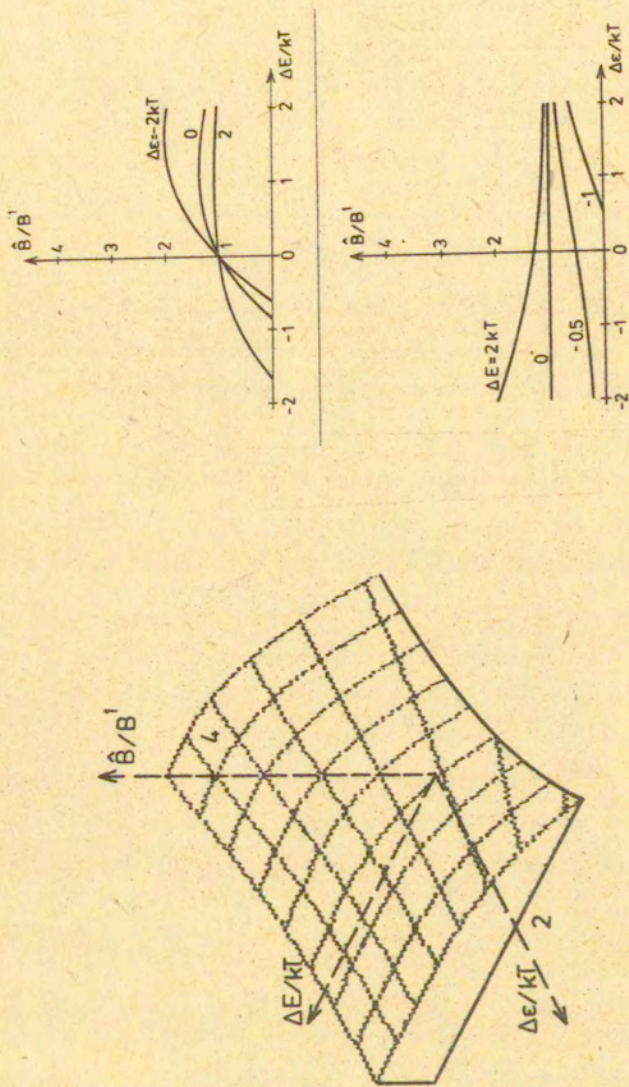


Figure 11. Reduced bulk energy density \hat{E}/B^1 for coupled nucleation. Group 1/11, eqs. (68a).
 a) three-dimensional plot vs. energy difference $\Delta\epsilon$ and transport activation energy difference $\Delta\epsilon = \epsilon^2 - \epsilon^1$, b) \hat{E}/B^1 vs. $\Delta\epsilon$ at $\Delta\epsilon = \text{const.}$, c) \hat{E}/B^1 vs. $\Delta\epsilon$ at $\Delta\epsilon = \text{const.}$. Constant parameters indicated.

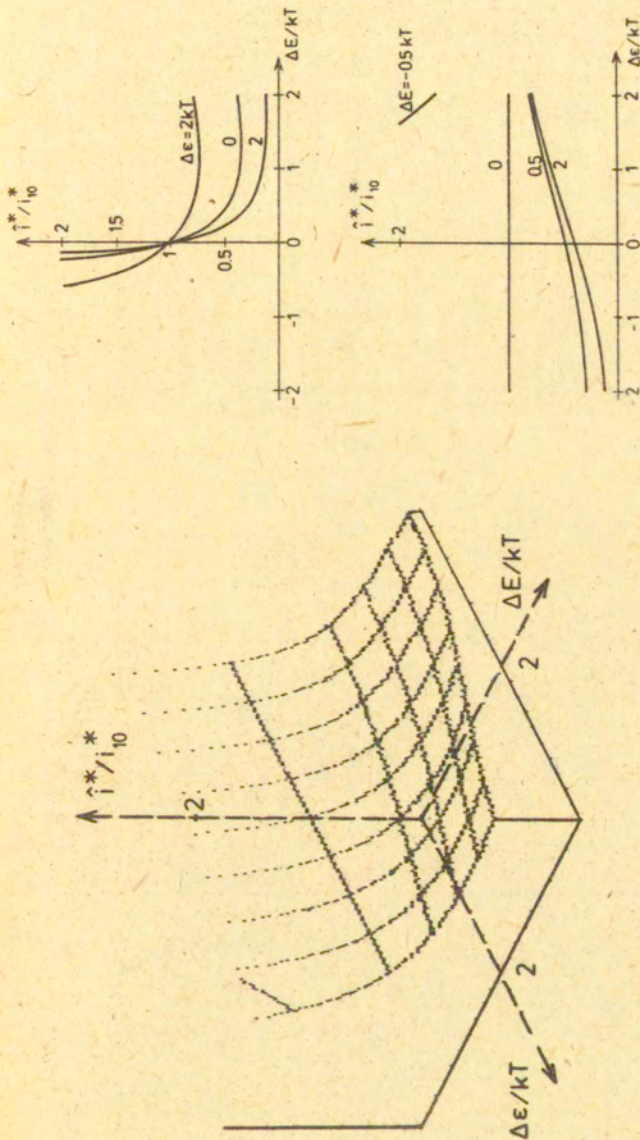


Figure 12. Reduced critical cluster size, \hat{i}^*/i_{10}^* for coupled nucleation. Group i/ii, eqs. (68a). a) three-dimensional plot vs. energy difference ΔE and transport activation energy difference, $\Delta\epsilon = \epsilon_2^* - \epsilon_1^*$, b) \hat{i}^*/i_{10}^* vs. ΔE at $\Delta\epsilon = \text{const.}$, c) \hat{i}^*/i_{10}^* vs. $\Delta\epsilon$ at $\Delta E = \text{const.}$ Constant parameters indicated.

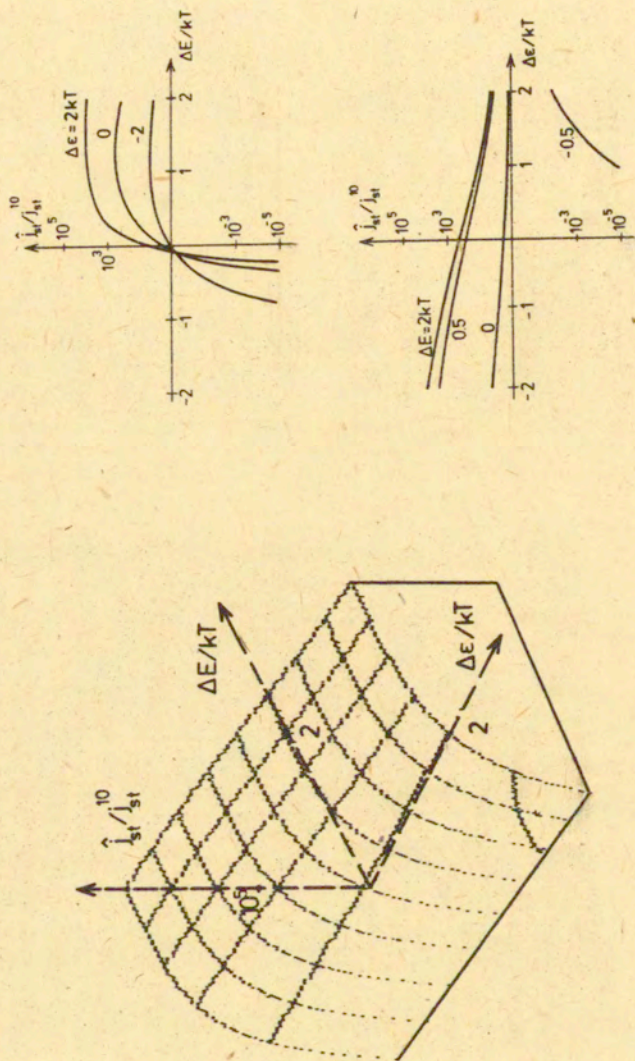


Figure 13. Reduced steady-state nucleation rate for coupled process, \hat{j}/j^{10} . Group 1/11, eqs. (68a). a) three-dimensional plot vs. energy difference $\Delta\epsilon$ and transport activation energy difference, $\Delta\epsilon = \epsilon^2 - \epsilon^1$, b) \hat{j}/j^{10} vs. $\Delta\epsilon$ at $\Delta\epsilon = \text{const}$, c) \hat{j}/j^{10} vs. ΔE at $\Delta E = \text{const}$. Constant parameters indicated.

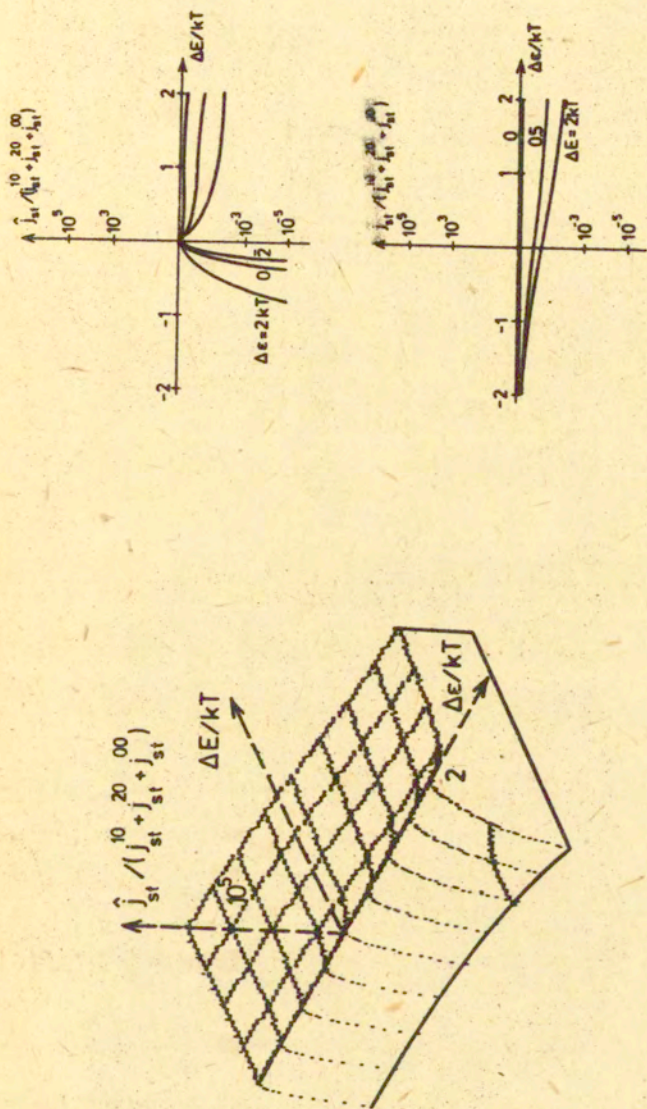


Figure 14. Normalized steady-state nucleation rate for coupled process, $\hat{j} / \Sigma j^0$, Group 1/11, eqs. (68a). a) three-dimensional plot vs. energy difference ΔE and transport activation energy difference $\Delta \epsilon = \epsilon^2 - \epsilon^1$, b) $\hat{j} / \Sigma j^0$ vs. ΔE at $\Delta \epsilon = \text{constant}$, c) $\hat{j} / \Sigma j^0$ vs. $\Delta \epsilon$ at $\Delta E = \text{constant}$. Constant parameters indicated.

energies ΔE , pumped above that level. Sensitivity of the ratios \hat{a}/a^0 , (\hat{i}^*/i_{10}^*) , etc. to the energy difference is the higher, the higher is mobility in the added phase II, i.e. the higher is K_o^2 , or the smaller transport energy difference $(\epsilon^2 - \epsilon^1)$.

It seems more fair, however, to compare coupled nucleation rate \hat{j}_{st} with a sum of isolated steady-state fluxes as if they acted independently. The ratio

$$\begin{aligned} & \hat{j}_{st} / (j_{st}^{10} + j_{st}^{20} + j_{st}^{00}) = \\ & = (\hat{a}/a^0)^{\frac{1}{2}} (1 + K_o^2 n_1^2 / n_1^1 + K_o^0 n_1^0 \hat{i}^{*- \frac{1}{2}} / n_1^1) \exp(\hat{\Delta F}^* / kT) \times \\ & \times [\exp(-\Delta \tilde{F}^{*10} / kT) + K_o^2 (n_1^2 / n_1^1) \exp(-\Delta \tilde{F}^{*20} / kT) + \\ & + K_o^0 (n_1^0 / n_1^1) \hat{i}_{o0}^{*- \frac{1}{2}} / n_1^1] \exp(-\Delta \tilde{F}^{*00} / kT)]^{-1} \end{aligned} \quad (70)$$

is plotted vs. ΔE and $(\epsilon^2 - \epsilon^1)$ in Figure 14.

It is evident that this ratio assumes maximum value 1 at $\Delta E = 0$, but in other regions, both for positive, and negative ΔE , coupled nucleation rate is smaller than the sum of isolated processes. This leads to the conclusion that coupling of various mechanisms reduces, rather than enhances rate of the nucleation process.

Group iii. Identical Bulk Phases, Different Interface.

Solutions in group iii. are simpler, but similar to those discussed above. The driving force \hat{B} is always constant and

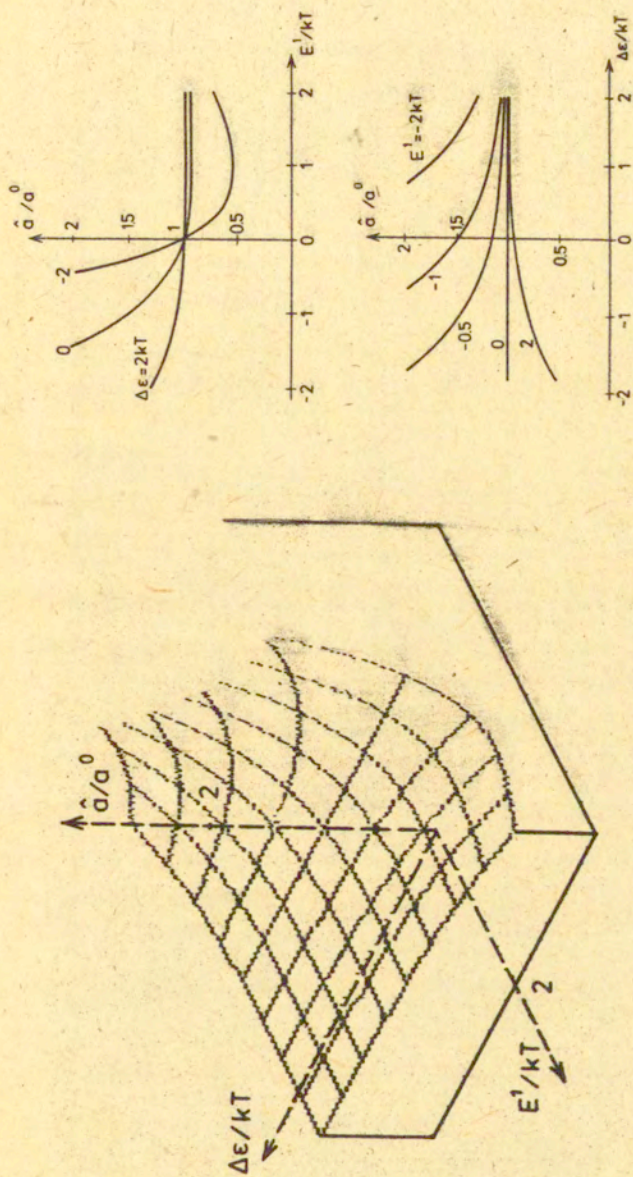


Figure 15. Reduced surface energy density, \hat{a}/a^0 for coupled nucleation. Group iii, eqs. (68b).
 a) three-dimensional plot vs. adsorption energy E^1 and transport activation energy difference $\Delta\epsilon = \epsilon^0 - \epsilon^1$, b) \hat{a}/a^0 vs. E^1 at $\Delta\epsilon = \text{const}$. c) \hat{a}/a^0 vs. $\Delta\epsilon$ at $E^1 = \text{const}$. Constant parameters indicated.

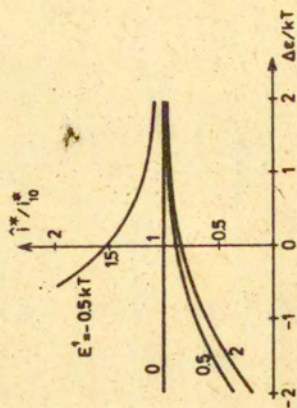
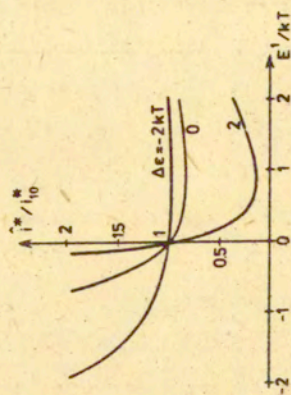
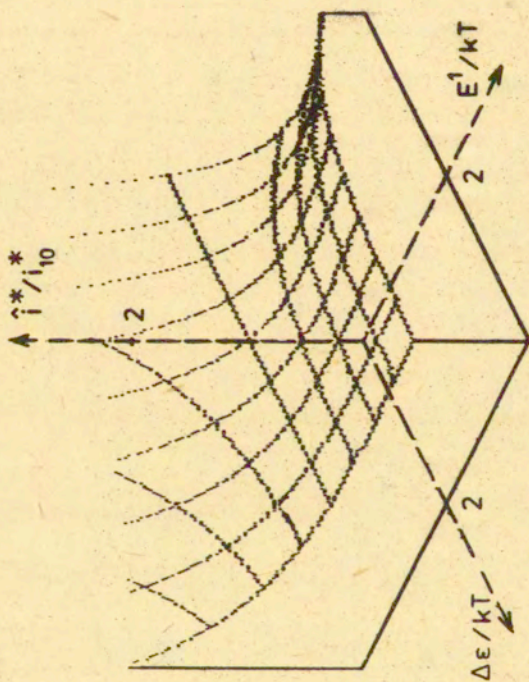


Figure 16. Reduced critical cluster size \hat{i}^*/i_{10}^* for coupled nucleation. Group III, eqs. (68b).
 a) three-dimensional plot vs. adsorption energy E^1 and transport activation energy difference $\Delta\epsilon = \epsilon^0 - \epsilon^1$, b) \hat{i}^*/i_{10}^* vs. E^1 at $\Delta\epsilon = \text{const}$, c) \hat{i}^*/i_{10}^* vs. $\Delta\epsilon$ at $E = \text{const}$. Constant parameters indicated.

equal to that in an isolated j^{10} process, and all other characteristics change monotonically with adsorption energy, E^1 and activation energy difference, $(\varepsilon^0 - \varepsilon^1)$. As evident in Figure 15 the reduced effective surface energy, \hat{a}/a^0 , is higher than unity in the range of negative E^1 ; so is critical cluster size (\hat{i}^*/i_{10}^*) (Figure 16) and maximum driving force $(\hat{\Delta F}^*/\Delta F^{*10})$. The ratios (\hat{a}/a^0) , (\hat{i}^*/i_{10}^*) and $(\hat{\Delta F}^*/\Delta F^{*10})$ monotonically decrease with increasing adsorption energy, pass the unit level at $E^1 = 0$, and drop below it for positive E^1 . The range of positive adsorption energy between two identical bulk phases seems to have little physical significance, though. Relatively small changes of \hat{a} , \hat{i}^* and $\hat{\Delta F}^*$, induce large changes in the steady-state flux, either reducing it to a small fraction of j_{st}^{10} (strongly negative E^1) or pumping it far above the level of unity (Figure 17). At $E^1 = 0$, the steady-state flux \hat{j}_{st} is always higher than isolated value j^{10} , but smaller than the ratio normalized like in eq.(70). Sensitivity of variation of the ratios \hat{a}/a^0 , \hat{i}^*/i_{10}^* , and $\hat{j}_{st} / \sum_p j_{st}^{p0}$ with adsorption energy E^1 is the higher, the higher is relative mobility on the interface, K_0^0 .

Group iv. No Mobility in Phase II.

Group iv. is qualitatively equivalent to group iii. Like in group iii, $\hat{B} = B^1$, but \hat{a} differs by a constant factor $(1 + K_\infty^2)$ from that in case iii.

$$\left. \begin{aligned} \hat{B} &= B^1 \\ \hat{a} - a^0 &= -(3kT/2)K_0^0 \exp(-E^1/kT)(\xi - 1) \end{aligned} \right\} \quad (71)$$

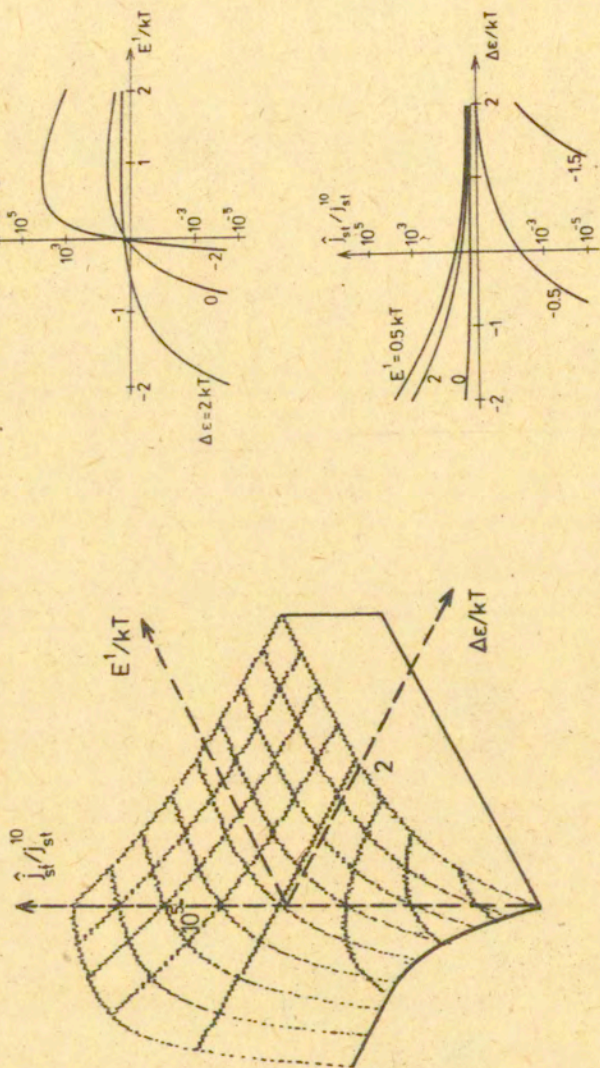


Figure 17. Reduced steady-state nucleation rate for coupled process, \hat{j}/j^{10} . Group III, eqs. (68b). a) three-dimensional plot vs. adsorption energy, E' , and transport activation energy difference, $\Delta E = \epsilon^0 - \epsilon^1$, b) \hat{j}/j^{10} vs. E' at $\Delta E = \text{constant}$, c) \hat{j}/j^{10} vs. ΔE at $E' = \text{const}$. Constant parameters indicated.

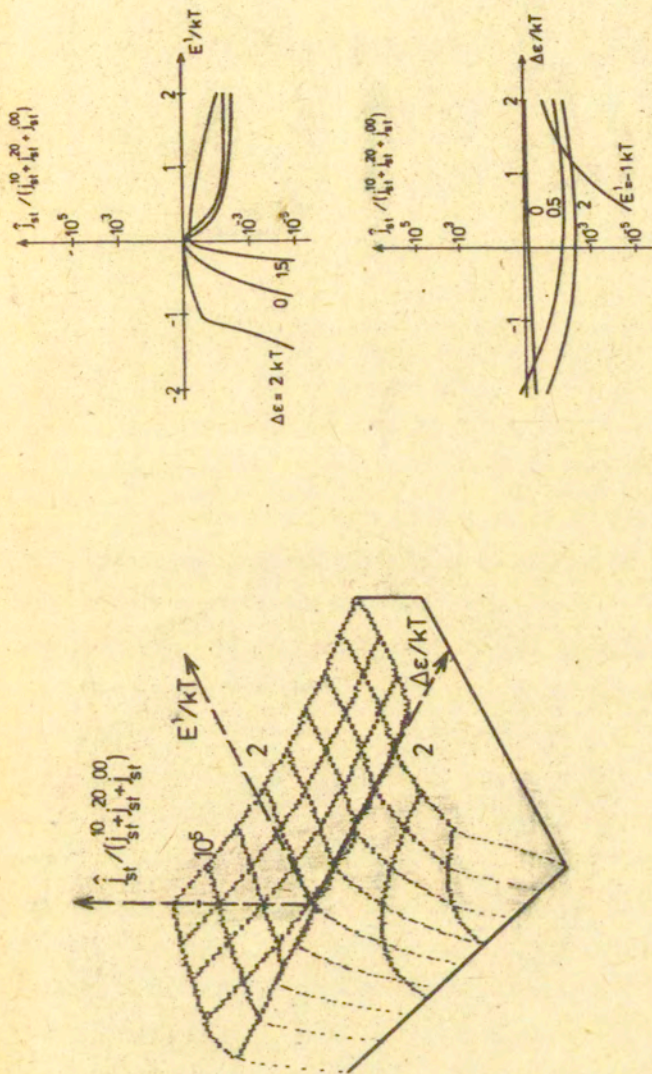


Figure 18. Normalized steady-state nucleation rate for the coupled process, $\hat{j}/\Sigma j^0$; Group III, eqs. (49b). a) three-dimensional plot vs. adsorption energy E' and transport activation energy difference; $\Delta\epsilon = \epsilon^0 - \epsilon'$, b) $\hat{j}/\Sigma j^0$ vs. E' at $\Delta\epsilon = \text{const.}$, c) $\hat{j}/\Sigma j^0$ vs. $\Delta\epsilon$ at $E' = \text{const.}$ Constant parameters indicated.

The ratios \hat{a}/a^0 , \hat{i}^*/i_{10}^* , $\hat{\Delta F}^*/\Delta F^*10$ are similar to those discussed above. The coupled flux \hat{j} reduced by the sum of all non-zero isolated fluxes possible in the system

$$\hat{j}_{st}/(j_{st}^{10} + j_{st}^{00})$$

behaves in the same way as similar ratios in cases i/ii and iii.

DISCUSSION

Considerations included in this, and in the preceding paper¹ throw new light on heterogeneous nucleation.

Our conclusions are based on the analysis of the coupled heterogeneous process, which provides a more general and more realistic model than any isolated mechanism, j^{PQ} . In fact, any heterogeneous cluster is subjected to impingement of single elements from all three regions (coupled growth) and isolated heterogeneous models provide only asymptotic cases.

Unlike for isolated heterogeneous, or homogeneous nucleation, where thermodynamic equilibrium can be established¹ consideration of a coupled process indicates that heterogeneous clusters become unstable in some conditions. Kinetic equations of the coupled process admit steady-state nucleation ($\hat{j}_1 = \text{const.} > 0$) below, and zero global flux ($\hat{j}_1 = 0$) above, some critical temperature \hat{T} dependent on the thermodynamic characteristics of the component processes and relative mobility in various regions supplying single elements. However, zero global flux does not imply that component fluxes are all equal

to zero. Consequently, the state characterized as $\hat{j}_i = j_i^{10} + j_i^{20} + j_i^{00} = 0$ corresponds to internal compensation of fluxes, rather than to thermodynamic equilibrium. Kinetic equations do not admit any true equilibrium (i.e. simultaneously: $j_i^{10} = j_i^{20} = j_i^{00} = 0$) in a system of clusters which can grow in two, or more different ways.

We will analyse the coupled heterogeneous nucleation more in detail. For the sake of simplicity we will confine our considerations to the combination of two, rather than three component fluxes putting K_i^0 and, consequently, j_i^{00} equal to zero.

$$\hat{j}_i = j_i^{10} + j_i^{20} \quad (72)$$

We will assume also that critical temperatures for the isolated processes (T_c^1 and T_c^2) and the zero-global-flux temperature \hat{T} are ordered as follows

$$T_c^1 > \hat{T} > T_c^2 \quad (73)$$

which places the concentration parameter η and interaction energy difference, ΔE in the range

$$\begin{aligned} \eta &< 1 \\ \Delta E &< 1 \end{aligned} \quad (74)$$

From eqs.(33) above one can see that with the conditions

(72 - 74) the flux j_i^{10} corresponding to the mechanism with higher critical temperature T_c^p is always positive. The other component flux, j_i^{20} can be positive or negative. When both fluxes are positive, unlimited growth of all clusters takes place. Instability appears when j_i^{20} becomes negative. The temperature T_{in} and concentration parameter η_{in} for the onset of instability of the smallest clusters

$$(\eta_{in}, T_{in}) : j_i^{20}(i=2) = 0 \quad (75)$$

is equivalent to

$$k_2^{-10} \hat{n}_1 \exp(-\delta \tilde{f}_2^{10})(\eta - 1) + \hat{j}_{st} = 0 \quad (76)$$

Analyzing eqs.(75 - 76) one can separate four different temperature regions.

$T < T_{in}$: j_i^{10} , j_i^{20} , and $\hat{j}_i = j_i^{10} + j_i^{20}$ positive for all i . Unlimited cluster growth.

$T_{in} < T < \hat{T}$: j_i^{10} positive, j_i^{20} negative for small, positive for large i ; $\hat{j}_i > 0$. Small clusters become unstable and can be moved to phase I. Larger cluster still grow.

$\hat{T} < T < T_c^1$: j_i^{10} positive, j_i^{20} negative for all i . $\hat{j}_i = 0$. All heterogeneous clusters unstable, tend to be moved to phase I. Thus formed homogeneous clusters continue to grow ($j_i^{11} > 0$).

$T_c^1 < T$: All heterogeneous clusters unstable. Homogeneous clusters in equilibrium with single elements ($j_i^{11} = 0$).

One can see that in low temperatures (especially below T_{in}) nucleation can effectively proceed according to the heterogeneous mechanism. Instability at higher temperatures stimulates removal of clusters from the interface and their transformation into homogeneous clusters in the phase with higher energy (for $\Delta E < 0$: in phase I). Consequently, near the highest critical temperature of the component processes (for $\Delta E < 0$: near T_c^1) homogeneous nucleation is preferred. This fact, observed also experimentally, does not follow from the theory of single-growth-mechanism heterogeneous nucleation. As shown in ref.¹ isolated processes j^{11} and j^{10} exhibit the same critical temperature, and formation of heterogeneous clusters is favored kinetically because of smaller ^{effective} surface energy. The exclusiveness of homogeneous nucleation in temperature range $\hat{T} < T < T_c^1$, and preference for j^{11} at lower temperatures, $T_{in} < T < \hat{T}$ follow from the coupling of various growth mechanisms and related instability of heterogeneous clusters.

Kinetic parameters for the coupled process (apparent surface energy \hat{a} , and bulk free energy density \hat{B}) are complicated functions of the properties of individual phases. Coupled nucleation rate in the subcritical temperature range, $T < \hat{T}$, can be lower, or higher than for individual isolated nucleation processes. When the coupled process, \hat{j}_{st} , is compared with the sum of component processes as if they acted independently, one finds that coupling generally reduces nucleation rate. The gain in nucleation rate which might be predicted for a simple superposition of isolated mechanisms is actually smaller because of coupling. This reduction is most strongly expressed for a system of thermodynamically very different phases (large

absolute ΔE , and/or E^1), having similar mobilities [small absolute transport energy differences ($\epsilon^2 - \epsilon^1$) and/or ($\epsilon^0 - \epsilon^1$)]. Nevertheless, heterogeneous nucleation, seen as a coupled process offers in many physical situations kinetic advantage over homogeneous processes. Stimulated condensation of vapors on solid interfaces, or crystallization of liquids in the presence of solid particles seem to provide physically sensible examples of such effects. Special cases discussed in this paper can be applied to various real situations. Table II indicates simplified and asymptotic cases of the coupled nucleation theory and the corresponding real systems.

REFERENCES TO PART II

1. A. Ziabicki, Nucleation of Phase Transitions in the Vicinity of Phase Boundary. I. Prace IPPT (IFTR Reports), 1984
2. F.C. Frank and M. Tosi, Proc. Roy. Soc. (London), A263, 323, (1961)
3. J.D. Hoffman and J.I. Lauritzen, J. Res. NBS, 65A, 297, (1961)
4. A. Ziabicki and L. Jarecki, J. Chem. Phys., (in press, 1984)
5. S. Frenkel, Kinetic Theory of Liquids, Oxford University Press, London, 1946

Table II.
Assignment of the parameters of coupled heterogeneous nucleation to various systems

Phase I	Phase II	Relative Mobilities	Energy Differences	Remarks and example solutions
Gas	Liquid	$K_0^2 = 0, K_0^0 < 1$	$E^1 \leq 0$	No mobility in Phase II.
Gas	Solid	$K_0^2 = 0, K_0^0 < 1$	$E^1 \leq 0$	group iv.,
Liquid	Solid	$K_0^2 = 0, K_0^0 < 1$	$E^1 \leq 0$	eqs. (67c), and (71)
Liquid 1	Liquid 2	$K_0^2 \leq K_0^0 \leq 1$	$ \Delta E > E^1 > 0$	Properties of the interface intermediate between those of phases I and II.
Solid 1	Solid 2	$K_0^2 \leq K_0^0 \leq 1$	$ \Delta E > E^1 > 0$	group i/ii., eqs. (58-64), (68a) or (A-4, A-7)
Solid 1	Solid 1	$K_0^2 = 1, K_0^0 > 1$	$\Delta E = 0, E^1 < 0$	Identical phases separated by defective interface group iii., eqs. (68b) or (A-4, A-7)

APPENDIX A 2

KINETIC CHARACTERISTICS OF COUPLED HETEROGENEOUS NUCLEATION
AT HIGH MOBILITY ON THE INTERFACE

Numerical examples included in Section KINETICS ... were based on the assumption that mobility in the interface was small compared with that in phase I and/or in phase II (eqs. 56). When the above conditions are satisfied, kinetic characteristics of the coupled process reduce to the same shape as for any isolated process with modified parameters \hat{a} , and \hat{B} . If one of the bulk phases exhibits high mobility, the other low (like in a solid-gas, or liquid-gas system) and mobility in the interface is intermediate between those in bulk phases, such assumptions are justified. On the other hand, two solid bulk phases separated by a defective interface can deviate from such situation, and simplified solutions for a coupled process given by eqs.(57-64) do not provide any reasonable approximation.

We shall present a non-linear, continualized solution of the problem, starting with the driving force from eq.(13)

$$\hat{\delta f}_i = \delta f_i^{10} + kT \ln \frac{1 + K_i^2 + K_i^0}{1 + K_i^2 \eta + K_i^0 \xi} \quad (A-1)$$

The total driving force, $\hat{\Delta F}_i$ is obtained from (A-1) by integration, rather than summation:

$$\widehat{\Delta F}_1 \cong \int_1^i \widehat{\delta f}(i') di' \quad (A-2)$$

Using asymptotic values of the ratios K_1^2 , K_1^0 from eqs.(22b),
i.e.

$$\left. \begin{aligned} K_1^2 &= K_0^2 \exp(-\Delta E/kT) \\ K_1^0 &= K_0^0 \exp(-E^1/kT) i^{-\frac{1}{3}} \end{aligned} \right\} \quad (A-3)$$

we arrive at the following result

$$\begin{aligned} \widehat{\Delta F}_1 &= \widetilde{\Delta F}_1^{10} + kT \ln \int_1^i \ln \frac{A+B i'^{-\frac{1}{3}}}{C+D i'^{-\frac{1}{3}}} di' = \\ &= \widetilde{\Delta F}_1^{10} + kT \left[i \ln \frac{A+B i^{-\frac{1}{3}}}{C+D i^{-\frac{1}{3}}} - \ln \frac{A+B}{C+D} + \frac{B^3}{A^3} \ln \frac{A i^{\frac{1}{3}} + B}{A+B} - \right. \\ &\left. - \frac{D^3}{C^3} \ln \frac{C i^{\frac{1}{3}} + D}{C+D} + \frac{1}{2} (i^{\frac{2}{3}} - 1) (B/A - D/C) - (i^{\frac{1}{3}} - 1) (B^2/A^2 - D^2/C^2) \right] \end{aligned} \quad (A-4)$$

where:

$$\begin{aligned} A &= 1 + K_0^2 \exp(-\Delta E/kT) \\ B &= K_0^0 \exp(-E^1/kT) \\ C &= 1 + K_0^2 n_1^2/n_1^1 \\ D &= K_0^0 n_1^0/n_1^1 \end{aligned} \quad (A-5)$$

Critical cluster size, i^* found from the transcendental equation

$$\widehat{\delta F}_i = \frac{2}{3} a^0 i^{-\frac{1}{3}} + B^1 + kT \ln \frac{A + B i^{-\frac{1}{3}}}{C + D i^{-\frac{1}{3}}} = 0 \quad (\text{A-6})$$

when substituted to eq.(A-4) yields maximum driving force, $\widehat{\Delta F}^*$.
 Finally, steady-state coupled flux, \widehat{j}_{st} is found from the Frenkel expansion (cf.p.42 above).

$$\widehat{j}_{st} = \frac{1}{3} (\widehat{i}^{*\frac{2}{3}} \widehat{k}_{i^*}^+) (Z/\pi kT)^{\frac{1}{2}} \exp(-\widehat{\Delta F}^*/kT) \quad (\text{A-7})$$

where

$$\begin{aligned} Z = & a^0 + \frac{1}{6} kT K_0^0 [(1 - \xi) \exp(\Delta E/kT) + (\eta - \xi) K_0^2] / [\exp(\frac{E^1 + \Delta E}{kT}) + \\ & + K_0^2 (1 + \eta) \exp(E^1/kT) + K_0^0 (1 + \xi) \exp(\Delta E/kT) \widehat{i}^{*- \frac{1}{3}} + \\ & + K_0^0 K_0^0 (\xi + \eta) \widehat{i}^{*- \frac{1}{3}} + (K_0^2)^2 \exp(E^1/kT) (n_1^0/n_1^1) + \\ & + (K_0^0)^2 \exp(\Delta E/kT) (n_1^0/n_1^1) \widehat{i}^{*- \frac{2}{3}}] \end{aligned} \quad (\text{A-8})$$

SUMMARY II

Out of the five nucleation mechanisms, j^{pq} , discussed in ref.¹, and possible in a system in the vicinity of an interface (boundary), three are heterogeneous, j^{10} , j^{20} , j^{00} , where cluster is located on the interface (superscript $q = 0$) and single kinetic elements participating in cluster growth are supplied from bulk regions ($p = 1$, or 2) or from the monomolecular interface layer ($p = 0$). These three processes are coupled, because the same cluster can simultaneously grow by addition of single elements from all three regions (1,2,0) which surround it. A theory of coupled nucleation was developed, leading to a common steady-state cluster-size distribution function, \hat{n}_1 , overall steady-state flux, \hat{j}_{st} , and critical conditions (temperature, \hat{T} , concentrations of single elements in the surrounding regions, $\hat{n}_1^1, \hat{n}_1^2, \hat{n}_1^0$) at which the net overall flux \hat{j}_{st} reaches zero. It has been shown that, unlike in the theory of simple nucleation processes, such critical conditions do not describe a true thermodynamic equilibrium: component fluxes in the zero-flux, or steady-flux states are different from zero functions of cluster size i . This leads to the conclusion that heterogeneous clusters are inherently unstable above some temperature, and unlike in a simple system, do not approach a Boltzmann distribution in equilibrium but gradually disappear from the interface. Some implications, including so-called "memory effects" in polymer crystallization are discussed.

CONTENTS

	page
PART I. COMPARISON OF VARIOUS ISOLATED MECHANISMS	3
INTRODUCTION I	3
BASIC FORMALISM OF THE THEORY	5
THERMODYNAMIC AND TRANSPORT CHARACTERISTICS FOR VARIOUS CLUSTER GROWTH MECHANISMS	14
COMPARISON OF VARIOUS NUCLEATION MECHANISMS	21
Critical Nucleation Temperature, T_c	21
Critical Cluster size, i^* , and Maximum Free Energy, ΔF^* .26	
Steady-State Nucleation Frequency, j_{st}	31
CONCLUSIONS	41
REFERENCES TO PART I	44
APPENDIX A 1. ACCURACY OF THE INTEGRAL APPROXIMATION FOR STEADY-STATE NUCLEATION FREQUENCY (by M.Kość and A.Ziabicki)	46
APPENDIX B 1. GEOMETRY OF CLUSTERS AND RELATED NUCLEATION CHARACTERISTICS (by M.Kość and A.Ziabicki)	52
SUMMARY I.	66
PART II. COUPLED CLUSTER GROWTH PROCESSES	67
INTRODUCTION II.	67
FORMAL EQUATIONS OF COUPLED NUCLEATION EQUATIONS	68
PARTION OF SINGLE ELEMENTS AMONG THE BULK PHASES AND THE INTERFACE	78
CRITICAL CONDITIONS FOR COUPLED NUCLEATION	81
1. Zero Surface Mobility on the Interface, $K_1^0 = 0$	84
2. Thermodynamically Equivalent Bulk Phases, $\Delta E = 0$	90
3. Zero Mobility in Phase II, $K_1^2 = 0$	91
4. All Regions Thermodynamically Equivalent, $\Delta E = E^1 = 0$.93	
5. General Case	94

STEADY STATE, INTERNAL COMPENSATION OF FLUXES, AND THERMODYNAMIC EQUILIBRIUM	95
KINETICS OF COUPLED NUCLEATION	103
Group i/ii. Interface Intermediate Between Two Bulk Phases	111
Group iii. Identical Bulk Phases, Different Interface.	116
Group iv. No Mobility in Phase II	119
DISCUSSION	122
REFERENCES TO PART II.	126
APPENDIX A 2. KINETIC CHARACTERISTICS OF COUPLED HETEROGENEOUS NUCLEATION AT HIGH MOBILITY ON THE INTERFACE	128
SUMMARY II	131
CONTENTS	133